

DETECTION OF HOMO/HETERO-DIMERIZATIONS BETWEEN ADENOSINE
A_{2A}, DOPAMINE D₂ AND NMDA RECEPTORS BY USE OF FRET AND BiFC
ASSAYS

A THESIS SUBMITTED TO
THE GRADUATE SCHOOL OF NATURAL AND APPLIED SCIENCES
OF
MIDDLE EAST TECHNICAL UNIVERSITY

BY

SİNEM ÇELEBİÖVEN

IN PARTIAL FULFILLMENT OF THE REQUIREMENTS
FOR
THE DEGREE OF MASTER OF SCIENCE
IN
BIOLOGY

SEPTEMBER 2014

Approval of the thesis

**DETECTION OF HOMO/HETERO-DIMERIZATIONS BETWEEN
ADENOSINE A_{2A}, DOPAMINE D₂ AND NMDA RECEPTORS BY USE OF
FRET AND BiFC ASSAYS**

submitted by **SİNEM ÇELEBİÖVEN** in partial fulfillment of the requirements for
the degree of **Master of Science in Biology Department, Middle East Technical
University** by,

Prof. Dr. Canan Özgen
Dean, Graduate School of **Natural and Applied Sciences**

Prof. Dr. Orhan Adalı
Head of Department, **Biology**

Assoc. Prof. Dr. Çağdaş Devrim Son
Supervisor, **Biology Dept., METU**

Examining Committee Members:

Assoc. Prof. Dr. Ayşegül Çetin Gözen
Biology Dept., METU

Assoc. Prof. Dr. Çağdaş Devrim Son
Biology Dept., METU

Assoc. Prof. Dr. Tülin Yanık
Biology Dept., METU

Assoc. Prof. Dr. Hakan Kayır
Medical Pharmacology Dept., GATA

Assist. Prof. Dr. Bala Gür Dedeoğlu
Biotechnology Dept., Ankara University

Date:
05.09.2014

I hereby declare that all information in this document has been obtained and presented in accordance with academic rules and ethical conduct. I also declare that, as required by these rules and conduct, I have fully cited and referenced all material and results that are not original to this work.

Name, Last name: SİNEM ÇELEBİÖVEN

Signature:

ABSTRACT

DETECTION OF HOMO/HETERO-DIMERIZATIONS BETWEEN ADENOSINE A_{2A}, DOPAMINE D₂ AND NMDA RECEPTORS BY USE OF FRET AND BiFC ASSAYS

Çelebiöven, Sinem

M.S., Department of Biology

Supervisor: Assoc. Prof. Dr. Çağdaş Devrim Son

September 2014, 143 pages

Recent studies showed that GPCRs on the cell surface can exist as homo- or hetero dimers and/or oligomers. To date, several G-protein coupled receptors have been revealed to interact either with other G-protein coupled receptors or other membrane proteins, including ion channels. Adenosine A_{2A}-Dopamine D₂ and Dopamine D₁-NMDA interactions are examples for well-studied heterodimerizations. All these receptors have critical functions in physiological processes. Adenosine A_{2A} receptor modulates neurotransmission, cardiovascular system and immune response; while Dopamine D₂ receptor controls the regulation of locomotion, food intake, learning, emotion and behavior. On the other hand, NMDAR mediates several signaling pathways necessary for synaptic plasticity, synaptic efficacy, neuronal morphology and memory formation by inducing long term potentiation. Dysfunctions in signaling mediated through these receptors have been shown in many neurological disorders, including Parkinson's disease, schizophrenia and Alzheimer's disease.

The purpose of this study is detection of physical interactions between A_{2A}R, D₂R and NMDARs using fluorescent based detection methods, specifically Bimolecular Fluorescence Complementation (BiFC) and Fluorescence Resonance Energy Transfer (FRET) assays. For this purpose, receptors were labelled with split-EGFP fragments, and full length EGFP and mCherry proteins from their C-tail; and by co-transfecting the labelled receptors to N2a cells with various combinations, homo- and heterodimerizations were analyzed with and without agonist treatment using laser scanning confocal microscope. Finally, the observed dimerizations were quantified using PixFRET, an imageJ plugin.

Moreover, further studies are planned to study oligomerization of these three receptors by combining BiFC and FRET techniques. Establishing this model will facilitate to understand the molecular mechanisms of these receptor interactions; and understanding these interactions in detail could help us design new treatment options. Additionally, the fluorescence based live cell model will be used to detect possible effects of potential drug candidates on the interactions of these receptors.

Keywords: Adenosine A_{2A}R, Dopamine D₂R, NMDAR, GPCR homo- and heterodimerization, BiFC, FRET

ÖZ

ADENOZİN A_{2A}, DOPAMİN D₂ VE NMDA RESEPTÖRLERİ ARASINDAKİ HOMO/HETERO-DİMER OLUŞUMLARININ BiFC VE FRET YÖNTEMLERİ İLE TESPİTİ

Çelebiöven, Sinem

Yüksek Lisans, Biyoloji Bölümü

Tez Yöneticisi: Doç. Dr. Çağdaş Devrim Son

Eylül 2014, 143 sayfa

Güncel çalışmalar, G-proteine kenetli reseptörlerin (GPKR) hücre zarı üzerinde homo- veya heterodimerler halinde bulunduğunu göstermiştir. Bugüne kadar, birçok GPKR'nin diğer GPKR'ler ile veya iyon kanalı gibi diğer membran proteinleri ile eşleştiği gösterilmiştir. Adenozin A_{2A} - Dopamin D₂ ve Dopamin D₁ - NMDA etkileşimleri iyi çalışılmış GPKR heterodimerizasyon çalışmalarına örnektir. Bu üç reseptör de fizyolojik fonksiyonlarda kritik rollere sahiptir. Adenozin A_{2A} reseptörü sinirsel iletim, kardiyovasküler sistem ve bağışıklık sisteminde önemli roller oynarken, Dopamin D₂ reseptörü hareket yeteneği, besin alımı, öğrenme, duygu ve davranış gibi fonksiyonların düzenlenmesini kontrol etmektedir. Diğer yandan, NMDA reseptörleri uzun süreli potansiyel artışı sağlayarak sinaptik pilastisite, sinaptik etkinlik, nöronal morfoloji ve hafıza oluşumu gibi önemli fonksiyonları düzenlemekte görev alır. Bu reseptörlerce yönetilen sinyalizasyonlardaki fonksiyon bozukluklarının Parkinson, şizofreni ve Alzheimer hastalıkları gibi birçok nörolojik rahatsızlıklar ile alakası olduğu yapılan çalışmalarda gösterilmiştir.

Bu çalışma, A_{2A} , D_2 ve NMDA reseptörleri arasındaki fiziksel etkileşimlerin, Bimoleküler Floresan Tamamlama ve Floresan Rezonans Enerji Transferi gibi floresan-temelli yöntemlerle tespit edilmesini amaçlamaktadır. Bu amaçla, hedef reseptörler bölünmüş-EGFP parçaları ve tüm EGFP ve mCherry floresan proteinleri ile işaretlenmiş ve işaretlenen reseptörler farklı kombinasyonlar ile N2a hücre hattında gözlemlenmiştir. Homo- ve heterodimerizasyon oluşumları agonistsiz ve agonistli koşullarda lazer taramalı konfokal mikroskop yardımı ile analiz edilmiştir. Tespit edilen dimerizasyonlar bir imageJ eklentisi olan PixFRET programı sayesinde niceliksel olarak belirlenmiştir.

Ayrıca, BiFC ve FRET tekniklerinin kombine edilmesi ile bu reseptörler arasındaki olası oligomer oluşumlarının çalışılması, bu çalışmanın devamı olarak planlanmıştır. Böyle bir modelin kurulması, bu reseptörler arasındaki etkileşimin moleküler mekanizmalarını anlamayı kolaylaştıracak ve bu mekanizmalar yeni tedavi opsiyonlarının tasarımı için kullanılabilir. Üstelik canlı hücrelerde kullanılabilen bu floresan tabanlı model, potansiyel ilaç adaylarının etkileşimler üzerindeki olası etkilerinin araştırılmasında kullanılabilir.

Anahtar kelimeler: Adenozin $A_{2A}R$, Dopamin D_2R , NMDAR, GPKR homo- ve heterodimerizasyonu, BiFC, FRET

To my family,

ACKNOWLEDGEMENTS

I would like to express my deepest appreciation to my supervisor Assoc. Prof. Dr. Çağdaş Devrim Son for his encouragement and recommendations throughout this study. I am also thankful for his endless moral support, patience and understanding that motivated me to work in the lab in peace.

I would also like to thank the members of my thesis examining committee; Assoc. Prof. Dr. Ayşegül Gözen, Assoc. Prof. Dr. Tülin Yanık, Assoc. Prof. Dr. Hakan Kayır and Assist. Prof. Dr. Bala Gür Dedeoğlu for their invaluable suggestions to complete this thesis better.

I am really grateful to all lab members of Son's lab; Beren Üstünkaya, Burcu Karakaya, Giray Bulut, İlke Süder, Merve Kasap, Orkun Cevheroğlu, Selin Akkuzu and Şeyda Pirinçci for their eternal motivation and help.

I also want to express my thanks to Zeynep Ergül Ülger for her kind assistance in and Bilkent UNAM for Confocal Microscopy facilities.

I am also deeply grateful to my precious friends Soner Yıldız, Ender Aykanlı, Gökçe Aköz, Çaka İnce, Bülent Ateş, Ahmet Yanbak, Murat Erdem, Müge Özgenoğlu, Anıl Demir and Volkan Tezer for their amusing contributions to my life and standing by me all the time. I never forget their supports and helps that encouraged me in my hard times.

My deepest appreciation goes to my valuable family; Belgin Çelebiöven, Neş et Çelebiöven, İsmail Cem Çelebiöven, Ayten Aytöre and Mualla Kardeş for their never ending support, continuous love and encouraging me throughout all my

education years. It is precious to know that they will always believe in me and support my decisions without hesitating.

Last but not the least, I would like to express my gratitude to my best friend Cevahir Karagöz for his real love, strong motivation, infinite patience, noteworthy helps and smart advices.

I greatly acknowledge TÜBİTAK 2210 Domestic Master Scholarship Program for supporting me financially.

This work is supported by Marie Curie Actions, International Reintegration Grant (IRG), TÜBİTAK with the project number 113Z639 and METU internal research funds with the project numbers BAP-08-11-2013-040 and BAP-08-11-2014-005.

TABLE OF CONTENTS

ABSTRACT	v
ÖZ	vii
ACKNOWLEDGEMENTS	x
TABLE OF CONTENTS	xii
LIST OF TABLES	xvi
LIST OF FIGURES	xvii
LIST OF ABBREVIATIONS	xx
CHAPTERS	
1 INTRODUCTION	1
1.1 G-Protein Coupled Receptors	1
1.1.1 Adenosine Signaling and Adenosine A _{2A} Receptors	4
1.1.2 Dopamine Signaling and Dopamine D ₂ Receptors	8
1.2 Ion Channels	11
1.2.1 N-Methyl D-Aspartate Receptors (NMDARs)	13
1.2.1.1 Molecular Structure of NMDARs	13
1.2.1.2 Trafficking of NMDARs	15
1.2.1.3 Signaling through NMDARs	17
1.3 Oligomerization of G-protein Coupled Receptors.....	19
1.3.1 Methods for the detection of GPCRs oligomerization	20
1.3.1.1 Fluorescence (Förster) Resonance Energy Transfer.....	21
1.3.1.2 Bimolecular Fluorescence Complementation Assay (BiFC).....	24
1.3.2 Homo/Hetero-dimerizations between Adenosine A _{2A} and Dopamine D ₂ receptors.....	27

1.3.3	Interactions between Dopamine and NMDA receptors	28
1.4	Aim of the study	29
2	MATERIALS AND METHODS	31
2.1	Materials	31
2.1.1	Neuro2a (N2a) Mouse Neuroblastoma Cell Line, Media and Conditions for Maintenance	31
2.1.2	Bacterial Strain, Culture Media and Conditions	33
2.1.3	Plasmids	33
2.1.4	Other chemicals and materials	34
2.2	Methods	35
2.2.1	Preparation of Competent <i>E. coli</i> Cells by CaCl ₂ Method.....	35
2.2.2	Transformation of Competent <i>E. Coli</i> cells	35
2.2.3	Plasmid Isolation from <i>E. Coli</i>	36
2.2.4	Restriction enzyme digestion	36
2.2.5	Ligation	37
2.2.6	Polymerase Chain Reaction (PCR)	37
2.2.7	Agarose Gel Electrophoresis.....	38
2.2.8	DNA extraction from Agarose Gel	39
2.2.9	Determination of DNA Amount	39
2.2.10	PCR Integration Method	39
2.2.11	Transfection of N2a cells with eukaryotic expression vectors	41
2.2.12	Imaging with Laser Scanning Confocal Microscope.....	42
2.2.13	Image Analysis with Pix-FRET	46
3	RESULTS AND DISCUSSION.....	49

3.1	Detection of homo/hetero-dimerizations between Adenosine A _{2A} and Dopamine D ₂ Receptors by use of BiFC assay	49
3.1.1	Labeling Adenosine A _{2A} and Dopamine D ₂ Receptor Genes with N-EGFP Tags Using PCR Integration Method	50
3.1.2	Labeling Adenosine A _{2A} and Dopamine D ₂ Receptor Genes with C-EGFP Tags Using PCR Integration Method	53
3.1.3	Reassembly of EGFP fragments in live cells	55
3.2	Detection of homo/hetero-dimerizations between Adenosine A _{2A} and Dopamine D ₂ Receptors by use of FRET	59
3.2.1	Validation of Adenosine A _{2A} and Dopamine D ₂ Receptors tagged with full length mCherry and EGFP	60
3.2.2	Homodimerization of Adenosine A _{2A} receptors	62
3.2.3	Homodimerization of Dopamine D ₂ Receptors	72
3.2.4	Heterodimerization of Adenosine A _{2A} and Dopamine D ₂ Receptors...	82
3.3	Detection of physical interactions between Adenosine A _{2A} and NMDA Receptors by use of FRET	89
4	CONCLUSION	96
	REFERENCES	99
	APPENDICES	
	A. COMPOSITIONS OF CELL CULTURE SOLUTIONS.....	117
	B. COMPOSITION AND PREPARATION OF BACTERIAL CULTURE MEDIUM.....	121
	C. COMPOSITIONS OF BUFFERS AND SOLUTIONS.....	123
	D. PLASMID MAPS.....	125
	E. PRIMERS.....	127

F. CODING SEQUENCES OF FUSION PROTEINS.....	129
G. FRET EFFICIENCY DATA.....	137

LIST OF TABLES

TABLES

Table 1.1 Summary of adenosine receptor subtypes, their mechanisms of action, main distributions and physiological consequences.....	6
Table 1.2 Summary of dopamine receptor subclasses (D1- and D2-like), their mechanisms of action, main distributions and therapeutic potentials.....	10
Table 2.1 Optimized PCR conditions to amplify fluorescent protein genes by adding 30 bp flanking ends.	38
Table 2.2 Optimized conditions for second PCR reaction of PCR integration method .	40
Table A. 1 Composition of D-MEM with high glucose	117
Table A. 2 Composition of 1X Phosphate Buffered Saline (PBS) solution	119
Table G. 1 FRET data of A _{2A} R- A _{2A} R homodimerization.....	137
Table G. 2 FRET data of D ₂ R- D ₂ R homodimerization.....	139
Table G. 3 FRET data of A _{2A} R-D ₂ R heterodimerization.....	141
Table G. 4 FRET data of A _{2A} R-NR1 heterodimerization	143

LIST OF FIGURES

FIGURES

Figure 1.1	An image representing the common structural architecture of GPCRs.....	2
Figure 1.2	GPCR signaling upon binding of a ligand and activation of G-proteins.....	3
Figure 1.3	Schematic representation of ATP/Adenosine signaling cascades	5
Figure 1.4	Schematic representation of membrane topology of a NMDAR subunit.....	14
Figure 1.5	Schematic diagrams representing the three essential conditions that must be met for efficient FRET to occur	22
Figure 1.6	Fluorescence spectrums of EGFP and mCherry	24
Figure 1.7	Representative image describing bimolecular fluorescence complementation assay	25
Figure 2.1	Representative scheme for PCR integration method (in order to tag a receptor gene with EGFP fluorescent protein).....	41
Figure 2.2	Track 1 configuration in laser scanning confocal microscope	43
Figure 2.3	Track 2 configuration in laser scanning confocal microscope	44
Figure 2.4	Track 3 configuration in laser scanning confocal microscope	45
Figure 3.1	Agarose gel electrophoresis image of PCR amplified N-EGFP fragments with Adenosine A _{2A} R flanking ends and Dopamine D ₂ R flanking ends.....	50
Figure 3.2	Agarose gel electrophoresis image of <i>NotI</i> & <i>HindIII</i> double-digestion screening of candidate A _{2A} and D ₂ receptors tagged with N-EGFP in pcDNA 3.1 (-) vectors.....	52
Figure 3.3	Agarose gel electrophoresis image of PCR amplified C-EGFP fragments with Adenosine A _{2A} R flanking ends and Dopamine D ₂ R flanking ends.....	53
Figure 3.4	Agarose gel electrophoresis image of <i>NotI</i> & <i>HindIII</i> double-digestion screening of candidate A _{2A} and D ₂ receptors tagged with C-EGFP in pcDNA 3.1 (-) vectors	54

Figure 3.5 N2a cells co-transfected with A _{2A} R+N-EGFP and A _{2A} R+C-EGFP fusion proteins.....	56
Figure 3.6 N2a cells co-transfected with D ₂ R+N-EGFP and D ₂ R+C-EGFP fusion proteins.....	57
Figure 3.7 N2a cells co-transfected with D ₂ R+N-EGFP and A _{2A} R+C-EGFP (first row) or A _{2A} R+N-EGFP and D ₂ R+C-EGFP (second row) fusion proteins.	58
Figure 3.8 Agarose gel electrophoresis image of digested pcDNA 3.1(-) vectors containing Adenosine A _{2A} receptor and Dopamine D ₂ receptor fused to EGFP/mCherry.....	61
Figure 3.9 N2a cells transfected only with A _{2A} R + EGFP.....	63
Figure 3.10 N2a cells transfected only with A _{2A} R + mCherry	64
Figure 3.11 Representative images (#1) of N2a cells transfected with A _{2A} R+EGFP and A _{2A} R+mCherry..	65
Figure 3.12 Representative images (#2) of N2a cells transfected with A _{2A} R+EGFP and A _{2A} R+mCherry.	66
Figure 3.13 Representative histogram image	67
Figure 3.14 Representative images of N2a cells transfected with A _{2A} R+EGFP and A _{2A} R+mCherry; and treated with CGS-21680.....	68
Figure 3.15 Graph of student's t-test results expressing effects of use of agonist CGS-21680 on homodimerization of Adenosine A _{2A} receptors	70
Figure 3.16 Mean distributions of efficiency ranges in N2a cells transfected with A _{2A} R+EGFP and A _{2A} R+mCherry genes.....	71
Figure 3.17 N2a cells transfected only with D ₂ R + EGFP.....	73
Figure 3.18 N2a cells transfected only with D ₂ R + mCherry	73
Figure 3.19 Representative images (#1) of N2a cells transfected with D ₂ R+EGFP and D ₂ R+mCherry	75
Figure 3.20 Representative images (#2) of N2a cells transfected with D ₂ R+EGFP and D ₂ R+mCherry	76
Figure 3.21 Representative images of N2a cells transfected with A _{2A} R+EGFP and A _{2A} R+mCherry; and treated with quinpirole	78

Figure 3.22 Graph of student's t-test results expressing effects of use of agonist quinpirole on homodimerization of Dopamine D ₂ receptors	79
Figure 3.23 Mean distributions of efficiency ranges in N2a cells co-transfected with D ₂ R+EGFP and D ₂ R +mCherry genes	80
Figure 3.24 Representative images (#1) of N2a cells co-transfected with A _{2A} R+EGFP and D ₂ R+mCherry	83
Figure 3.25 Representative images (#2) of N2a cells co-transfected with A _{2A} R+EGFP and D ₂ R+mCherry	84
Figure 3.26 Representative images of N2a cells co-transfected with A _{2A} R+EGFP and D ₂ R+mCherry; and co-treated with CGS-21680 and quinpirole.....	86
Figure 3.27 Graph of student's t-test results demonstrating combined effects of CGS-21680 and quinpirole on heterodimerization of A _{2A} and D ₂ receptors	87
Figure 3.28 Mean distributions of efficiency ranges in N2a cells co-transfected with A _{2A} R+EGFP and D ₂ R+mCherry genes.....	88
Figure 3.29 Agarose gel electrophoresis image of digested pcDNA 3.1(-) vectors containing NR1 subunit fused to EGFP/mCherry.....	90
Figure 3.30 Representative images (#1) of N2a cells transfected with A _{2A} R+EGFP, NR1+mCherry and NR2B.....	92
Figure 3.31 Representative images (#2) of N2a cells transfected with A _{2A} R+EGFP, NR1+mCherry and NR2B.....	93
Figure 3.32 Mean distributions of efficiency ranges in N2a cells transfected with A _{2A} R+EGFP, NR1+mCherry and NR2B genes.	94
Figure D. 1 Map of pcDNA 3.1 (-) vector	125

LIST OF ABBREVIATIONS

A ₁ R	Adenosine A ₁ Receptor
A _{2A} R	Adenosine A _{2A} Receptor
AC	Adenylyl Cyclase
ADHD	Attention Deficit Hyperactive Disorder
ADP	Adenosine Diphosphate
AGE	Agarose gel electrophoresis
AMP	Adenosine Monophosphate
ATP	Adenosine Triphosphate
bp	base pair
BiFC	Bimolecular Fluorescence Complementation
BRET	Bioluminescence Resonance Energy Transfer
BSA	Bovine Serum Albumin
cAMP	cyclic AMP
CaCl ₂	Calcium chloride
CFP	Cyan Fluorescent Protein
cDNA	Complementary Deoxyribonucleic Acid
CNS	Central Nervous System
DAG	Diacylglycerol
D ₂ R	Dopamine D ₂ Receptor
D-MEM	Dulbecco's Modified Eagle Medium
DMSO	Dimethyl sulfoxide
DNA	Deoxyribonucleic Acid
EDTA	Ethylenediamine tetraacetic acid
EGFP	Enhanced Green Fluorescent Protein

ER	Endoplasmic Reticulum
ERK	Extracellular signal regulated kinase
EtBr	Ethidium bromide
FRET	Fluorescence/Förster Resonance Energy Transfer
G _i	Inhibitory G α subunit
G _{olf}	Olfactory G α subunit
G _s	Stimulatory G α subunit
GABA	γ -amino Butyric Acid
GDP	Guanosine Diphosphate
GFP	Green Fluorescent Protein
GPCR	G-Protein Coupled Receptor
GTP	Guanosine Triphosphate
IP3	Inositol 1,4,5-triphosphate
JNK	Jun amino-terminal kinase
kb	Kilobase pair
LB	Luria Bertani
LTD	Long term depression
LTP	Long term potentiation
MAP	Mitogen Activated Protein
mCherry	monomericCherry
MgCl ₂	Magnesium chloride
mGluR	Metabotropic Glutamate Receptor
mRNA	Messenger Ribonucleic Acid
N2a	Neuro2a
NMDAR	N-Methyl D-Aspartate Receptor
PBS	Phosphate Buffered Saline
PCR	Polymerase Chain Reaction
PKA	Protein kinase A

PLC	Phospholipase C
PLD	Phospholipase D
RE	Restriction Enzyme
rpm	Revolution per Minute
SAPK	Stress activated protein kinase
SBT	Spectral bleed-through
TBE	Tris Borate EDTA
TGN	<i>trans</i> -Golgi network
UV	Ultraviolet
YFP	Yellow Fluorescent Protein

CHAPTER 1

INTRODUCTION

1.1 G-Protein Coupled Receptors

G-Protein coupled receptors (GPCRs), also known as seven-transmembrane (7-TM) domain receptors, are the largest and most diverse group of membrane proteins in eukaryotes (Kobilka, 2007; Latek *et al.*, 2012). These receptors sense external cues outside the cell such as hormones, neurotransmitters and drugs, and cause cellular responses by activating signal transduction pathways within the cell (Kobilka, 2007; Lin, 2013).

It has been reported that around 1000 genes are responsible to encode G-protein coupled receptors in the human genome (Takeda *et al.*, 2002). Despite differences in their primary sequences, GPCRs share a common structural architecture basically including seven hydrophobic transmembrane segments with an extracellular amino terminus and an intracellular carboxyl terminus (Figure 1.1) (Kobilka, 2007; Venkatakrisnan *et al.*, 2013).

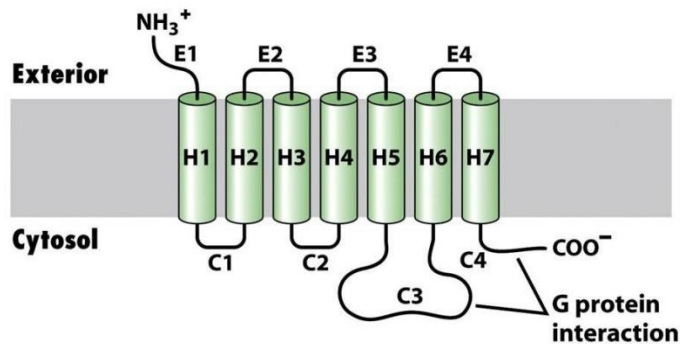


Figure 1.1 An image representing the common structural architecture of GPCRs (taken from © 2008 W. H. Freeman and Company, *Molecular Cell Biology*, 6th edition).

This structural similarity of GPCRs stands in contrast to the structural diversity of the natural GPCR ligands. GPCRs mediate responses to neurotransmitters, biological amines, chemokines, amino acids, peptides, and nucleic acids, as well as the senses of sight, smell and taste (Bouvier, 2001; Deupi & Kobilka, 2007). Upon external binding of these ligands, GPCRs help regulate a variety of cellular processes, such as neurotransmission, inflammation, differentiation, secretion and cell growth.

As their name implies, GPCRs transmit signals by interacting with heterotrimeric G-proteins. Binding of a ligand causes a conformational change in the GPCRs; and thus GPCRs can interact with a nearby G-protein, having three different subunits, α , β and γ (Kobilka, 2007). In an inactive form, G_α subunit binds to guanosine diphosphate (GDP). Upon binding of a ligand to GPCR, the receptor activates the bound G-protein by replacing GTP in place of GDP. As a result, G_α subunit dissociates from $G\beta\gamma$ subunit and activated G-proteins transmit signals by interacting with other membrane proteins involved in signal transduction or various enzymes producing secondary messengers such as cAMP, diacylglycerol (DAG), and inositol 1, 4, 5-

triphosphate (IP3). Some G-proteins activate these targets while the others inhibit them (Crespo *et al.*, 1994; Kobilka, 2007; Lambright *et al.*, 1996).

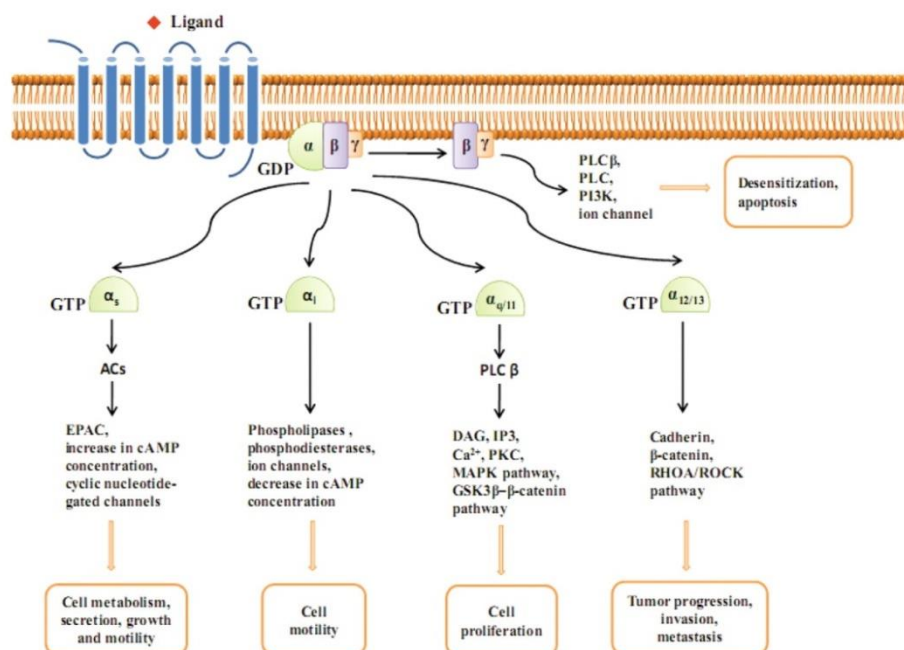


Figure 1.2 GPCR signaling upon binding of a ligand and activation of G-proteins (taken from (Wu *et al.*, 2012)).

Due to the vital roles in human metabolism, GPCRs have become a significant target in modern medicine. Researchers estimate that more than 50% of marketed drugs act by binding to GPCRs (Hipser *et al.*, 2010). These drugs include various agonists and antagonists of GPCRs used in many diseases such as heart failure, asthma, hypertension, diabetes, allergies, migraine and neurological disorders (Bouvier, 2001; Schöneberg *et al.*, 2004).

1.1.1 Adenosine Signaling and Adenosine A_{2A} Receptors

Adenosine is a purine nucleoside playing a central role as a structural element of nucleic acids and in biochemical processes, such as energy transfer (Eltzschig, 2013). It also functions as extracellular signaling molecule mediating in cardiovascular system (Baines, Cohen, & Downey, 1999), central nervous system (B B Fredholm, 1997; Haas & Selbach, 2000; Svenningsson *et al.*, 1999), gastrointestinal tract (Roman & Fitz, 1999), immune system (Cronstein, 1994), as well as in asthma (Forsythe & Ennis, 1999), and cell growth and apoptosis (Ohana *et al.*, 2001), etc.

Adenosine signaling is tightly regulated by extracellular or intracellular adenosine levels and by the action of Adenosine receptors. During disease and stress conditions, such as hypoxia, ischemia, trauma, seizures or inflammation, extracellular adenosine arises from the breakdown of nucleotide adenosine triphosphate (ATP) or release of ATP from cytosol (Eltzschig *et al.*, 2006; Faigle *et al.*, 2008). ATP is converted to adenosine monophosphate (AMP) via ectonucleoside triphosphate diphosphohydrolase 1 (CD39) (Reutershan *et al.*, 2009). AMP is then cleaved by ecto-5'-nucleotidase CD73 to form adenosine (Figure 1.3) (Hart *et al.*, 2011).

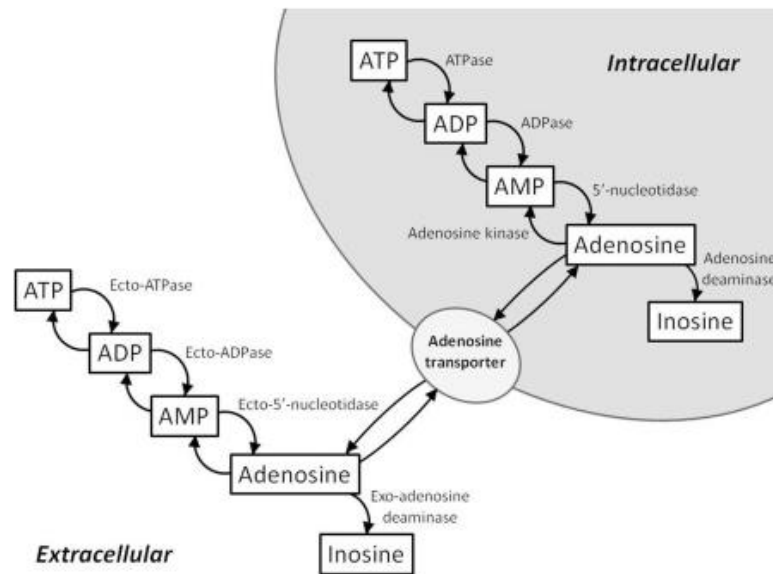


Figure 1.3 Schematic representation of ATP/Adenosine signaling cascades (taken from (Chikahisa & Séi, 2011)).

When dramatic increase in extracellular adenosine concentration occurs, activated adenosine receptors become responsible for adenosine's biological activities by triggering signaling pathways within the cells. Adenosine taken through the receptors is converted to inosine via adenosine deaminase or to AMP via adenosine kinase (Schulte, 2002). Thus, extracellular adenosine signaling is regulated on expression levels of adenosine receptors and activity of enzymes playing roles in ATP/Adenosine cascades (Löffler *et al.*, 2007).

The effects of adenosine on cells are mediated through four distinct adenosine receptor subtypes, named as A_1 , A_{2A} , A_{2B} , A_3 , all of which belong to the family of GPCRs (Olah & Stiles, 1995). The most abundant ones in the central nervous system are A_1 and A_{2A} types (Auchampach & Bolli, 1999). Adenosine A_1 receptors (A_1R) slow down metabolic activity in the brain due to inhibitory properties. A_1R is coupled to G_i , a $G\alpha$ subunit with an inhibitory effect, and thus inhibits adenylyl cyclase activity. It also triggers phospholipase C (PLC) activity and potassium (K^+) channels, while inhibits calcium (Ca^{2+}) channels (Ribeiro, 2005). Unlike A_1R ,

Adenosine A_{2A} receptors are coupled to stimulatory G_s proteins to increase adenylyl cyclase activity. Although A_{2B} receptors are also coupled to G_s proteins and have similar functions as A_{2A}R, A_{2B}R is distinguished by its lower affinity for adenosine (Polosa, 2002). Adenosine A₃ receptors are also coupled to G_i proteins and inhibit adenylyl cyclase activity while stimulating PLC (Dunwiddie & Masino, 2001). The detailed information and comparison among adenosine receptor subtypes is given in Table 1.1.

Table 1.1 Summary of adenosine receptor subtypes, their mechanisms of action, main distributions and physiological consequences (adapted from Schulte 2002)

Receptor	G-protein	Mechanism	Distribution	Effects
A ₁ (ADORA1)	G _{i/o}	Decreased cAMP Increased IP ₃ /DAG (PLC) Increased Arachidonate (PLA ₂) Increased choline (PLD)	Cerebral cortex, cerebellum, brain stem, spinal cord	Decreased heart rate Reduced synaptic vesicle release
		Increased activity of K ⁺ channels	Atrial cells, neurons	Regulation of myocardial oxygen consumption and coronary blood flow
		Decreased activity of Q, P, N-type Ca ²⁺ channels	Hippocampus	
A _{2A} (ADORA2A)	G _s	Increased cAMP	General (neurons)	Coronary artery vasodilation and myocardial oxygen consumption
	G _{olf}	Increased cAMP	Striatum	Decreased dopaminergic activity
A _{2B} (ADORA2B)	G _s	Increased cAMP	Striatum	Axon elongation Bronchospasm

A ₃ (ADORA3)	G _{i/o}	Decreased cAMP Increased IP ₃ /DAG (PLC) Increased choline (PLD)	Cerebellum	Cardiac muscle relaxation Smooth muscle contraction
		Increased activity of K ⁺ channels	Cardiac cells	Cardio protective in cardiac ischemia
		Increased activity of Cl ⁻ channels	Epithelial cells	Inhibition of neutrophil degranulation

The Adenosine A_{2A} receptor (A_{2A}R) is one of the major mediators of adenosine signaling in nervous system (Dunwiddie & Masino, 2001). These receptors are mainly expressed in striatum (Bertil B Fredholm *et al.*, 2005), blood vessels (Shi *et al.*, 2008), microglia and astrocytes (Schwarzschild *et al.*, 2006). A_{2A}R is coupled to G_s or G_{oif} to stimulate adenylyl cyclase activity and thus increase intracellular cAMP levels (Bertil B Fredholm *et al.*, 2005). In addition to interactions with G-proteins, A_{2A}R can also signal through a pathway which is independent of G-proteins; such as mitogen-activated protein kinase (MAPK) cascade (Seidel *et al.*, 1999). They modulate many physiological processes, such as regulation of myocardial oxygen consumption and vasodilation of coronary arteries (Cunha *et al.*, 2008). A_{2A}R signaling in micro vessels has a protective role during ischemia or seizures by stimulating cerebral vasodilation (Shin, Park, & Hong, 2000). In astrocytes, A_{2A}R signaling triggers proliferation of cells during acute injury. Moreover, activation of A_{2A}R induces release of neural growth factor in microglial cell (Benarroch, 2008). In addition, A_{2A}R protects tissues from collateral inflammatory damage by negatively regulating overactive immune cells (Ohta & Sitkovsky, 2001). A_{2A}R has also significant roles in the regulation of glutamate and dopamine release, thus affecting

the other signaling cascades too. All of these cellular processes affected by this subtype of adenosine receptor make it a potential therapeutic target for the treatment of insomnia, pain, depression, drug addiction and some neurological disorders, such as Parkinson's disease, Alzheimer's disease and schizophrenia (Brown & Short, 2008; Cunha *et al.*, 2008; S. Ferré *et al.*, 2007; Morelli *et al.*, 2007).

A number of selective A_{2A}R ligands have been identified for different therapeutic applications; for example, several A_{2A}R antagonists have been developed for the treatment of Parkinson's disease (Jenner, 2003; Pinna *et al.*, 2005). The most widely used antagonists of A_{2A}R include istradefylline (KW-6002), SCH-58261, MSX-3, Preladenant, ST-1535, Vipadenant and caffeine (Ongini *et al.*, 2001; Pinna *et al.*, 2005). As A_{2A}R agonists, CGS-21680, ATL-146e, DPMA, Regadenoson, UK-432,097 and Limonene are well known ones (Cristalli *et al.*, 2003; Diniz *et al.*, 2008).

1.1.2 Dopamine Signaling and Dopamine D₂ Receptors

Dopamine is a neurotransmitter of the catecholamine family playing a key role in the regulation of various physiological processes of human brain; such as reward, locomotion, food intake, learning, emotion and behavior (Schultz, 2007). This catecholamine also plays roles in the periphery to regulate cardiovascular function, catecholamine release, hormone secretion and gastrointestinal motility (Missale *et al.*, 1998). Thus, abnormalities in dopaminergic neurotransmission are implicated in many neurological or psychiatric disorders including Parkinson's disease, Alzheimer's disease, schizophrenia, hyperactivity, depression, attention deficit and drug addiction (Neve, Seamans, & Trantham-Davidson, 2004; Pivonello *et al.*, 2007). Due to such significant functions, dopamine receptors are targets of several drugs designed to treat these disorders (Emilien *et al.*, 1999).

The biological effects of dopamine are mediated through five subtypes of dopamine receptors, all of which belongs to the superfamily of GPCRs. Dopamine receptors are subdivided into two subclasses: D1-like (D1 & D5) and D2-like (D2, D3 & D4) receptors (Missale *et al.*, 1998). Among these subtypes, D1 and D2 receptors are the most abundant ones in central nervous system. The most studied dopamine signaling pathway is the regulation of cyclic AMP production and D1-like and D2-like dopamine receptors are diverging due to their opposite effects on this pathway. D1-like receptors are coupled to G_s or G_{olf} proteins to stimulate activation of adenylyl cyclase and thus activation of cAMP production. Increased cAMP level results in the activation of protein kinase A (PKA) which phosphorylates many proteins responsible to regulate cellular metabolism. On the other hand, D2-like receptors inhibit adenylyl cyclase activity by interacting with $G_{i/o}$ proteins and thus decrease intracellular cAMP level (Neve *et al.*, 2004). In addition to cAMP pathway, dopamine receptors have been shown to modulate Akt-GSK3 and PAR4 signaling pathways (Sang *et al.*, 2005). The D1- and D2- like dopamine receptors are also different in terms of their genetic structures. The D1-like receptors do not contain any intron in their coding sequences, while genes encoding D2-like receptors have several introns and that is why D2-like receptors have different splice variants (Beaulieu & Gainetdinov, 2011). The detailed information about dopamine receptor subclasses is given in Table 1.2.

Table 1.2 Summary of dopamine receptor subclasses (D1- and D2-like), their mechanisms of action, main distributions and therapeutic potentials (taken from Crocker 1994)

Receptor subfamily	Location	Action	Therapeutic potential
Central			
D1 and D2	substantia nigra and striatum	motor control	agonists - Parkinson's disease
D1 and D2	limbic cortex and associated structures	information processing	antagonists - schizophrenia
D2	anterior pituitary	inhibits prolactin release	agonists - hyperprolactinaemia
Peripheral			
D1	blood vessels	vasodilatation	agonists - congestive
D1	proximal tubule cells	natriuresis	heart failure and
D2	sympathetic nerve terminals	decreases release	hypertension

The dopamine D₂ receptor (D₂R) is one of the most expressed subtypes, mediating many important effects of dopamine signaling in both central and peripheral nervous system (Missale *et al.*, 1998). D₂R is mainly found in the nigral and striatal region of basal ganglia, olfactory bulb, retina and prolactin cells of anterior pituitary gland (Sidhu & Niznik, 2000). D₂R exists as two alternatively spliced isoforms differing in the insertion of 29 amino acids in its third intracellular loop. The short isoform is called D_{2S} and the long variant is called D_{2L} (Dal Toso *et al.*, 1989). Both isoforms are coupled to inhibitory G_{i/o} proteins and therefore, inhibit adenylyl cyclase activity. However, no obvious difference in their functional properties has been shown up to now. Both variants share the similar function, distribution and pharmacological profile (Dal Toso *et al.*, 1989; Giros *et al.*, 1989). The only difference caused by alternative splicing is that D_{2S} receptor displays a higher affinity than D_{2L} (Dal Toso

et al., 1989). D₂R signaling through inhibition of adenylyl cyclase activity results in the reduction of PKA activity, thus leading to inhibition of Na⁺, K⁺, ATPase in neostriatal neurons (Nishi *et al.*, 1999) and suppression of tyrosine hydroxylase activity. In addition to adenylyl cyclase activity, the interactions of D₂ receptors with G_{i/o} proteins also regulate some other signaling pathways including phospholipases, ion channels, Map kinases and Na⁺/H⁺ exchanger. D₂R stimulation activates PLC-1, a kind of phospholipase C, resulting in inositol triphosphate-induced calcium mobilization and activation of Ca²⁺-dependent proteins (Kanterman *et al.*, 1991). Moreover, D₂R stimulation activates K⁺ channels to decrease cell excitability, while inhibits L, N and Q-type Ca²⁺ channels and NMDA channels (Lledo *et al.*, 1992; Okada, Miyamoto, & Toda, 2003; Seabrook *et al.*, 1994). D₂R signaling also stimulates MAP kinase pathways, including extracellular signal regulated kinase (ERK) and stress activated protein kinase/Jun amino-terminal kinase (SAPK/JNK) (Choi *et al.*, 1999; Luo *et al.*, 1998).

1.2 Ion Channels

Several types of excitable cells, including neurons and muscle cells, are known with their abilities to generate electrical signals. They convert chemical or mechanical messages to electrical signals by use of ion channel that are usually multimeric proteins located in the plasma membrane. These proteins form hydrophilic pores across the membrane and permits rapid ion movement through the pores by mediating passive transport. Ion concentration gradient across the membrane creates an electrical potential across the membrane and lets ion channels open to allow passage of specific ions until balancing the concentrations of ions in cytoplasm and extracellular environment (Purves *et al.*, 2001). Ion channels are usually specific to only a single type of ion, primarily Na⁺, K⁺, Ca²⁺ and Cl⁻. Amino acids lining the

pores of proteins and physical width of the channels determine which ions can pass through the channels (Alberts *et al.*, 2002).

Ion channels are classified in terms of their gating mechanisms. Voltage-gated ion channels conduct ions at high rates regulated by the voltage gradient across the membrane. The well-known examples to voltage gated channels are Na⁺, K⁺, Ca²⁺ or Cl⁻ ion channels. This class of channels functions in the excitation of neurons and muscle contraction by providing quick depolarization upon voltage change (Bezaniilla, 2005). The other class, ligand-gated ion channels, open and conduct ions in response to specific ligand molecules. Once cytoplasmic messengers or extracellular neurotransmitters bind to these proteins, conformational change in the structure of channel opens the gate and ion passage occurs across the membrane (Harmar *et al.*, 2009). Nicotinic Acetylcholine receptor, ionotropic glutamate-gated receptors, ATP-gated P2X receptors, γ -aminobutyric acid-gated GABA receptors are examples to the most studied ligand-gated ion channels (Purves *et al.*, 2001). There are also other types of ion channels including light-gated channels, such as channelrhodopsin (Wietek *et al.*, 2014), mechanosensitive channels opening in response to pressure (Poole, Moroni, & Lewin, 2014) and temperature gated channels, such as TRPV1 or TRPM8 (Vriens, Nilius, & Voets, 2014).

Ion channels are important in the regulation of several biological processes, including electrical activity of neurons, regulation of membrane potential, neuronal responses and cellular secretion. These proteins have critical roles in various signaling pathways by generating secondary messengers or by functioning as effectors and responding to such messengers (Berridge, 2012). Contraction of heart, skeletal and smooth muscle, regulation of ion concentration and acidification of intracellular organelles, regulation of cell volume, epithelial transport of nutrients and T-cell activation are other examples of physiological processes that ion channels significantly contribute. All of these functions make the ion channel an important target for drug designers (Conte Camerino, Tricarico, & Desaphy, 2007).

1.2.1 N-Methyl D-Aspartate Receptors (NMDARs)

N-Methyl D-Aspartate receptors (NMDARs) are members of ionotropic glutamate receptor family of ion channels, which also includes AMPA and kainate receptors (Prybylowski & Wenthold, 2004). NMDARs play a critical role at excitatory synapses in the central nervous system. These channels are permeable to Na⁺, K⁺, and Ca²⁺ ions. Ca²⁺ influx through NMDAR mediates several signaling pathways necessary for synaptic plasticity, synaptic efficacy, neuronal morphology and memory formation by inducing long term potentiation (Köhr, 2006; Sanz-Clemente, Nicoll, & Roche, 2012). Moreover, NMDAR dysfunction has been shown in many neurological disorders. NMDAR hypo-function contributes to schizophrenia, attention deficit hyperactivity disorder (ADHD) and chronic depression; while NMDAR hyper-function may result in stroke, Alzheimer's and Huntington's disease (Cull-Candy, Brickley, & Farrant, 2001; Lynch & Guttman, 2002).

1.2.1.1 Molecular Structure of NMDARs

The functional NMDAR is a tetrameric protein comprised of four subunits. These subunits are expressed by three gene families: NR1, NR2 and NR3. To be a functional channel, NMDAR must contain two NR1 subunits combined with two NR2 or NR3 subunits. All these subunits have a common membrane topology as shown in Figure 1.4. This shared topology is defined with three transmembrane segments (M1, M3 and M4), a re-entrant pore loop (M2), an extracellular amino-terminal domain and an intracellular C-terminus region (Wenthold *et al.*, 2008).

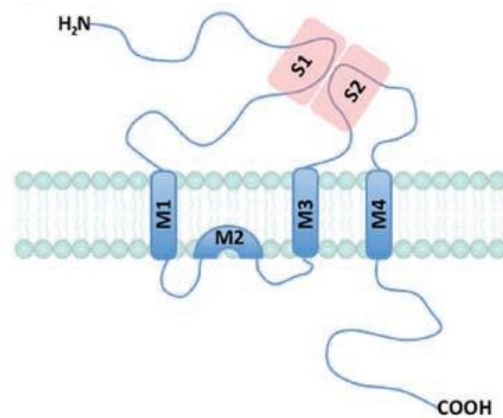


Figure 1.4 Schematic representation of membrane topology of a NMDAR subunit (adapted from Sanz-Clemente, Nicoll, and Roche 2012)

The amino terminal domain is involved in subunit assembly and receptor sensitivity (Durand, Bennett, & Zukin, 1993; McIlhinney *et al.*, 2003). On the other hand, C-terminal region interacts with various cytosolic proteins or molecules, is implicated in the trafficking of subunits and contains multiple phosphorylation sites (Pérez-Otaño & Ehlers, 2004; Salter & Kalia, 2004). The extracellular S1 and S2 regions (agonist binding domains after N-terminal domain and between M3 and M4 segments, respectively) contain glycine-binding sites for NR1 and NR3, or glutamate-binding sites for NR2 subunits (Awobuluyi *et al.*, 2007; Laube *et al.*, 1997). The transmembrane segments (M1, M3 and M4) and the re-entrant M2 loop form the channel pore. The M2 loop contains a critical asparagine residue determining calcium permeability of the channel and mediating magnesium blockade (Mayer & Armstrong, 2004).

Several distinct NMDAR subtypes have been identified in the central nervous system. Despite their structural similarities, NMDAR subtypes are different in channel conductance, kinetic properties, sensitivity to ligands, and synaptic localization (Law *et al.*, 2003). Previous studies have shown that NR1 subunit exists in eight different splice variants due to the alternative splicing at N-terminus (N1

cassette) and C-terminus (C1 and C2 cassettes) (Carroll & Zukin, 2002). The N1 cassette regulates the sensitivity of channel to protons (Traynelis, Hartley, & Heinemann, 1995), whereas C terminal cassettes affect the protein interactions (Wenthold *et al.*, 2003). Splicing in the C-terminus causes the expression of four different cassettes, named as C0, C1, C2 and C2' (Prybylowski & Wenthold, 2004). C0 is present in all isoforms, while the other cassettes are present in different combinations among different isoforms. With these different combinations of C terminal cassettes, isoforms of NR1 subunits have different regional, developmental and expression profiles (Zukin & Bennett, 1995). NR1-1a is the most abundantly expressed isoform, containing C1 and C2 cassettes. On the other hand, there are four genes encoding NR2 subunits; NR2A, NR2B, NR2C and NR2D. NR2 subunits contain glutamate binding sites and regulate most of the NMDAR responses in the central nervous system including proton sensitivity, channel conductance, deactivation kinetics and interactions with other proteins (Köhr, 2006; Stephenson, 2001). NR2A and NR2B are the most abundantly found forms in the mammalian forebrain (Cull-Candy *et al.*, 2001). NR2B expression predominates in the early developmental stage. During development, NR2A expression increases and predominates the synaptic pool in adults (Stephenson, 2001). This kind of expression profile has a significant effect in the decrease of synaptic plasticity (Wenthold *et al.*, 2003). Subunit composition also determines subcellular localization. NR2A-containing NMDA channels are abundant at synapses, while NR2B-containing channels are enriched at extrasynaptic regions (Wenthold *et al.*, 2003).

1.2.1.2 Trafficking of NMDARs

Like most of the other membrane proteins, NMDAR subunits are synthesized in ribosomes located in the membrane of endoplasmic reticulum (ER). Generally, after their translation, membrane proteins are subjected to different kinds of quality

control mechanisms in the ER to prevent export of imperfect proteins (D. N. Hebert & Molinari, 2007). For NMDA channels, the NR1, NR2 and NR3 subunits come together in various combinations to form tetramers and the assembly of subunits results in the masking of ER retention signals. In other words, these NMDAR subunits are retained in the ER until they assemble (Wenthold *et al.*, 2008).

NR2 (NR2A and NR2B) and NR3 subunits do not reach the plasma membrane and thus cannot form a functional receptor when expressed alone. NR1 subunits also do not form a functional channel on the membrane without assembling with NR2 or NR3 subunits (Monyer *et al.*, 1992). NR1 C-terminus contains four distinct kinds of cassettes, resulted by the alternative splicing in C-tail. The most abundant isoform, NR1-1, contains C0, C1 and C2 in its C-tail. This variant is not exported from the ER when expressed without NR2 or NR3 subunits. An RXR motif in the C1 cassette of NR1-1 is responsible from the ER retention of unassembled subunits (Standley *et al.*, 2000). The assembly with NR2 subunit may mask this ER retention signal on C1 cassette; however, the exact mechanism underlying NR1/NR2 assembly and export from the ER remains largely unexplored. On the other hand, the isoforms containing C2' cassette in their C-terminus represent different mechanism. For example, NR1-3 isoforms containing C1 and C2' cassettes are directly trafficked to the membrane. It has been shown that PDZ-binding domain, STVV, found in C2' cassette is responsible from the negation of RXR retention signal on C1 cassette. This retention motif may be masked by the PDZ proteins interacting with C2' cassette (Scott *et al.*, 2001). Although some other NR1 isoforms (eg. NR1-2 and NR1-4) are directed to membrane without NR2 or NR3 subunits, they are rapidly internalized and degraded since homomeric NR1 has not been detected on the membranes of neurons (Carroll & Zukin, 2002). Similarly, NR2 subunits are remained in the ER without NR1 subunits and this retention also appears to depend on retention signals on the C-terminus of NR2 subunits. However, the details about these signals and masking of these signals are not clear yet (H. Xia, Hornby, & Malenka, 2001). In brief, the functional significance of multiple C-terminal configurations of subunits and their

different mechanism in the ER retention and trafficking to the membrane remain largely unclear.

Presumably, sustained conformational changes during tetramer formation may mask the retention signals or enhance exit signals from the ER (Horak, Chang, & Wenthold, 2008). For the assembly of NMDAR subunits, the mechanism of tetramer formation is also unclear. According to suggestions, two NR1 may make a homodimer which then interacts with another dimer containing NR2 and/or NR3 subunits (Schorge & Colquhoun, 2003). Another study suggests that NR2 or NR3 dimerize with NR1 and two heterodimers assemble to form a tetrameric NMDA channel (Farina *et al.*, 2011).

After they are released from the ER, NMDARs enter the Golgi apparatus and then processed in the *trans*-Golgi network (TGN). Within this network, proteins are packaged into vesicular carriers and transported to the plasma membrane within these vesicles (Wenthold *et al.*, 2008).

1.2.1.3 Signaling through NMDARs

Glutamatergic signaling through NMDA receptors modulate various responses in central nervous system, including neuronal development, synaptic plasticity, memory and learning (Benquet, Gee, & Gerber, 2002). During excitatory neurotransmission, presynaptic release of glutamate activates two classes of glutamate receptors: non-NMDA (AMPA/kainate receptors) and NMDA receptors. Non-NMDA receptors provide rapid depolarization during synaptic transmission, while NMDA receptors modulate duration of synaptic current (Zito & Scheuss, 2010).

NMDARs are both ligand and voltage gated ion channels. Activation of NMDAR requires two neurotransmitters; glutamate and glycine or D-serine. The voltage dependent activation of this protein comes from the removal of channel block by Mg^{2+} . When excitation by synaptic inputs causes sufficient depolarization, the Mg^{2+} block is removed and upon binding of glutamate and glycine, NMDA pores open and result in influx of Na^+ and Ca^{2+} ions and efflux of K^+ ions (Edmonds, Gibb, & Colquhoun, 1995; Paoletti & Neyton, 2007). Especially, Ca^{2+} flux is significant in the modulation of synaptic plasticity, learning and memory formation (Furukawa *et al.*, 2005). Entry of calcium into the postsynapse allows coupling of electrical synaptic activity to biochemical signaling via activation of Ca^{2+} -dependent enzymes and downstream signaling pathways. Therefore, calcium influx in this way results in long term changes in synaptic strength and connectivity (Zito & Scheuss, 2010). Moreover, NR2 subunits have been shown to get involved in the formations of long-term potentiation (LTP) and long term depression (LTD). NR2A is mainly associated with LTP, while NR2B mainly with LTD (L. Liu *et al.*, 2004; Woo *et al.*, 2005).

Mechanisms of NMDAR regulations are critical for several diseases. Firstly, excessive Ca^{2+} influx through NMDA channels triggers excitotoxic cell death (Lynch & Guttman, 2002). The other channels can also trigger excessive Ca^{2+} influx; however they do not cause cell deaths. Thus, Ca^{2+} influx through NMDARs may regulate specific downstream signaling cascades resulting in cell death (Tymianski *et al.*, 1993). Secondly, NMDAR dysfunction may lead to loss of synaptic function; thus triggering many neurological or psychiatric disorders including Huntington's, Alzheimer's, Parkinson's diseases, schizophrenia, depression and bipolar disorder (Wenthold *et al.*, 2008).

1.3 Oligomerization of G-protein Coupled Receptors

GPCRs exist in various oligomeric forms, consisting of dimers, trimers, tetramers and higher complexes. A specific type of GPCR can form a homo-oligomer, or different GPCRs can interact to form hetero-oligomers (Palczewski, 2010). The properties of GPCR oligomers can differ from those of monomers in many ways, such as altered ligand binding sites, G-protein coupling, intracellular trafficking, tendency to internalization or sensitization profile (Fuxe *et al.*, 2012). The receptor complexes formed by muscarinic M3 and α_{2C} -adrenergic receptor provided the first evidence for GPCR dimerization (Maggio, Vogel, & Wess, 1993). Moreover, the studies on the dimerizations between GABA_B-R1 and GABA_BR2, and δ - and κ -opioid receptors have showed the significance of GPCR oligomerization in receptor signaling and ligand binding (Bowery & Enna, 2000; Jordan & Devi, 1999).

GPCR oligomers play a key function in signal triggering and orchestrating the molecular events significant in plasticity-associated changes (Gandia *et al.*, 2008a). There are many other suggestions to explain the role of GPCR oligomerization. Firstly, GPCRs may be activated by their ligands when they are in a dimer form. For example, metabotropic glutamate (mGlu) receptor has been shown to become fully activated when two agonists bind to both protomers in the dimer. However, its monomer is partially active with a single agonist bound to it (Kniazeff *et al.*, 2004). Secondly, some other studies indicate that GPCRs dimerize for their biosynthesis and trafficking to the membrane. They start to dimerize in the ER early after their biosynthesis which means that they do not need to be activated by their ligands to dimerize (Bulenger, Marullo, & Bouvier, 2005). For instance, oxytocin and vasopressin V1a receptors have been shown to dimerize during their biosynthesis in the ER (Terrillon *et al.*, 2003); and oligomerization of C-C chemokine type 5 receptors (CCR5) is not affected by the treatment with agonist (Issafras *et al.*, 2002). Mutation studies also demonstrated that non-dimerized GPCRs are mostly retained in

the ER; thus GPCR dimerization is critical for the trafficking of receptors to the cell membrane (Terrillon & Bouvier, 2004). In short, GPCR oligomerization is thought to be involved in signaling, passing quality control points during synthesis in ER, maturation and trafficking to the cell surface (Bulenger *et al.*, 2005).

1.3.1 Methods for the detection of GPCRs oligomerization

Several different approaches, based on protein-protein interactions, have been applied to study oligomerization of GPCRs. Coimmunoprecipitation, various adaptations of resonance energy transfer techniques and functional complementation studies are commonly used methods for such interaction studies. All of these techniques have provided many evidences indicating GPCRs function as dimers or oligomers in the membrane (Milligan & Bouvier, 2005).

In the early eighties, indirect functional evidences suggested that GPCRs function as dimers on the plasma membrane. In the early nineties, coimmunoprecipitation studies revealed the first direct evidences for the interaction of GPCRs (Cabello *et al.*, 2009). First GPCR dimer detected by coimmunoprecipitation was a homodimer of β_2 adrenoreceptors in Sf9 insect cells (T. E. Hebert *et al.*, 1996). Although many other dimers were detected by use of coimmunoprecipitation, the technique has some disadvantages in biophysical level. Firstly, the receptors may not be detected in actual physical contact. They have to be extracted and purified from their native environments. The hydrophobicity of the membrane domains of receptors may also lead to detect nonspecific aggregations in addition to actual oligomers. Secondly, obtaining fully soluble membrane fractions and eliminating the whole insoluble fragments are quite labor-intensive. Moreover, harsh and stringent solubilization conditions may destroy the association between receptors (Dziedzicka-Wasylewska *et al.*, 2006). Due to these artifacts of biochemical approaches, fluorescence-based

methods have played a key role in the characterization of GPCR oligomers in recent years (Navarro *et al.*, 2008). Bioluminescence resonance energy transfer (BRET) and fluorescence resonance energy transfer (FRET) methods allowed the demonstration of GPCR dimerization in living cells (Agnati *et al.*, 2003; Bouvier, 2001). Another powerful technique, combination of resonance energy transfer with bimolecular fluorescence complementation assay (BiFC), has been described recently to detect GPCR heteromers containing more than two receptors (Guo *et al.*, 2008; Navarro *et al.*, 2008).

1.3.1.1 Fluorescence (Förster) Resonance Energy Transfer

Protein-protein interactions are a major target for pharmacologic studies since these interactions have critical roles in various cellular processes. Fluorescence (Förster) resonance energy transfer (FRET) is one of the most widely used techniques to detect protein-protein interactions, protein-DNA interactions and conformational changes of molecules in living cells. FRET is based on the non-radiative energy transfer from an excited fluorophore (donor) to another fluorophore (acceptor). The energy is transferred non-radiatively by means of intermolecular long-range dipole-dipole coupling. FRET only occurs when the fluorophores are in very close proximity, at most 100 Å (Milligan & Bouvier, 2005). The other essential requirements for FRET to occur is that emission spectrum of the donor molecule and excitation spectrum of the acceptor molecule must overlap adequately and both the quantum yield of donor and the absorption coefficient of acceptor must be high enough (Clegg, 1995). Moreover, donor and acceptor molecules must be oriented properly for the dipole-dipole interaction to occur. The transfer of energy leads to a reduction in the donor's fluorescence intensity and excited state lifetime while acceptor's emission intensity increases (Periasamy, 2001). The conditions required for an efficient FRET is summarized in Figure 1.5.

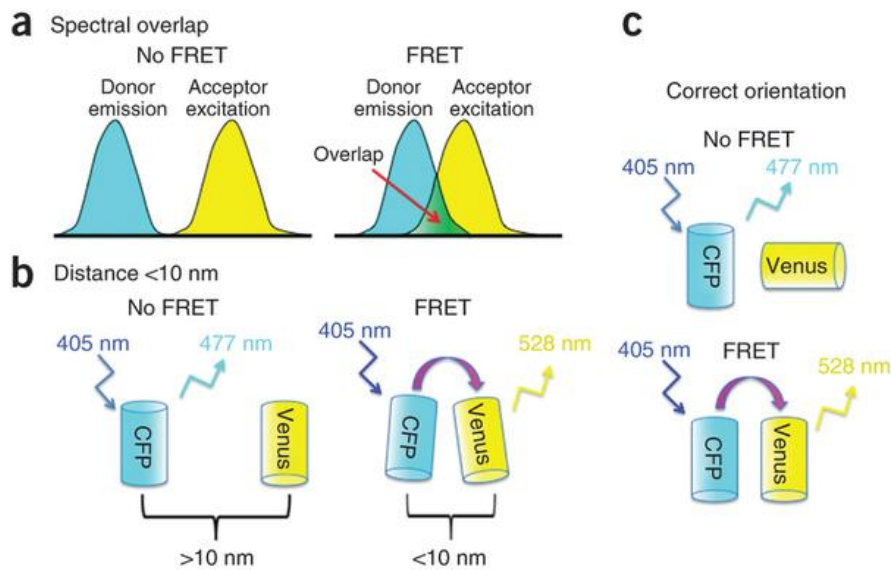


Figure 1.5 Schematic diagrams representing the three essential conditions that must be met for efficient FRET to occur (adapted from (Broussard *et al.*, 2013))

Detection of FRET can be used to quantify the distance between donor and acceptor molecules and to detect when/where the proteins interact. Förster (1946) demonstrated that the efficiency of FRET (E) decreases with the 6th power of the distance between donor and acceptor and formulated as shown below.

$$E = R_0^6 / (R_0^6 + r^6)$$

R_0 : Förster distance, the distance where energy transfer is 50% efficient. It depends on the spectral properties of donor and acceptor molecules.

r : actual distance between donor and acceptor

Major advantage of applying FRET for interaction studies is the detection of protein dimers or oligomers in intact living cells. In living cells, subcellular localization of protein interactions and molecular distance between interacting proteins can be

detected, which are difficult to study with other methods. Furthermore, high sensitivity of technique allows studying with small quantities of samples in small volumes. Additionally, it is quite applicable to investigate interactions between membrane proteins unlike many other methods (Herrick-Davis, Grinde, & Mazurkiewicz, 2004). However, the technique also has some limitations. Firstly, the chromophores must be attached to precise sites of macromolecules. Otherwise, absence of FRET may not be definitive or presence of FRET may be misleading. In addition, FRET only works if fluorophores are in correct orientation. During FRET experiments, noise signals may be produced due to direct excitation of the acceptor at the wavelength used to excite donor molecule; thus free fluorophores may mask the energy transfer and interfere to FRET measurements (R N Day, Periasamy, & Schaufele, 2001; Szöllosi *et al.*, 2006).

With the isolation of Green Fluorescent Protein (GFP) from the jelly fish *Victoria aequorea* (Shimomura, Johnson, & Saiga, 1962), it has served as a versatile tool to study gene expression, protein folding and trafficking (Tsien, 1998). In recent years, GFP and red derivatives of this protein were chosen to be better FRET pairs (Cornea *et al.*, 2001). One of the best acceptor proteins is now considered as mCherry (a red fluorescent derivative of a protein isolated from *Discosoma sp.*), to be used in FRET experiments with EGFP (enhanced GFP, a GFP variant with two amino acid substitution) because emission spectrum of the donor EGFP and excitation spectrum of the acceptor mCherry give a suitable overlap for FRET to occur efficiently. Additionally, their excitation spectrums present a low level of crosstalk that is crucial to eliminate noise arose from direct excitation of mCherry at the wavelength of donor excitation (Albertazzi *et al.*, 2009).

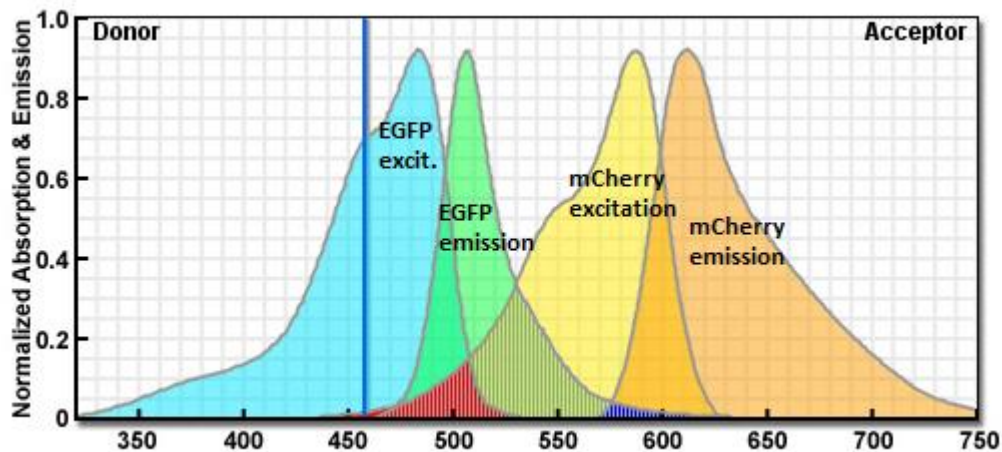


Figure 1.6 Fluorescence spectrums of EGFP and mCherry (obtained from FRET for Fluorescence Proteins JAVA Tutorial, provided by MicroscopyU of Nikon®)

As shown in Figure 1.6, excitation spectrums of EGFP and mCherry proteins give a little crosstalk, shown as red area. Exciting the donor EGFP at 458 nm (blue vertical line on the figure) cannot directly excite mCherry. Their emission spectrums also present very little overlap, shown as blue shaded area. Moreover, emission spectrum of EGFP and excitation spectrum of mCherry have a large overlapping area making this pair quite suitable for FRET experiments.

1.3.1.2 Bimolecular Fluorescence Complementation Assay (BiFC)

Complementation between protein fragments was first demonstrated for proteolytic fragments of ribonuclease (Richards, 1958), and then many other proteins have been subsequently shown to be complemented from their fragments. Complementation between fragments of these proteins provides to visualize protein-protein interactions in a variety of model organisms. However, visualization of the subcellular

localization of protein complexes needs high spatial resolution which can be provided by using bimolecular fluorescence complementation assay (Kerppola, 2008).

BiFC assay is based on the structural complementation of non-functional fragments of a fluorescent protein, named as N-terminal and C-terminal fragments. Proteins which are postulated to interact are fused to fragments of a fluorescent protein in gene level. After expressed in live cells, interaction of these target proteins brings the N-terminal and C-terminal fragments of fluorescent protein in a close proximity. With the complementation of N- and C-terminal fragments, fluorescence property is recovered and therefore, obtained fluorescence signal can be directly evaluated as interaction between target proteins (Kerppola, 2006). The logic of the assay is represented schematically in Figure 1.7.

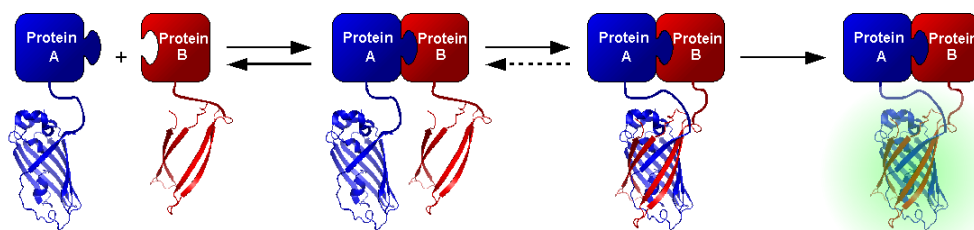


Figure 1.7 Representative image describing bimolecular fluorescence complementation assay. In the image, interaction of protein A and protein B allows complementation of N-EGFP (blue) and C-EGFP (red) fragments to reform native three-dimensional structure of EGFP that emits its fluorescent signal upon excitation (from http://de.wikipedia.org/wiki/Bimolekulare_Fluoreszenzkomplementation)

In this study EGFP is splitted and used in BiFC experiments. EGFP (enhanced green fluorescence protein) is a GFP variant that has only two amino acid substitutions; F64L and S65T (Richard N Day & Davidson, 2009). These two amino acid

substitutions improve folding efficiency and brightness of protein that make the EGFP better for BiFC analysis (Kerppola, 2009). To produce non-fluorescent fragments from EGFP, it is splitted after its 157th amino acid (Ozawa *et al.*, 2001).

BiFC assay enables direct visualization of protein interactions in living cells, eliminating potential artifacts associated with cell lysis or fixation (Kerppola, 2006). Subcellular localization of interactions can also be determined even with a simple inverted fluorescence microscope (Hu, Chinenov, & Kerppola, 2002). Recent studies have also suggested that BiFC assay can be used to study topology of membrane proteins and to screen effects of small molecules on protein complexes (MacDonald *et al.*, 2006; Zamyatnin *et al.*, 2006). Like most of the other techniques, BiFC assay has some drawbacks in addition to its advantages. Firstly, slow maturation of fluorescent complex limits real-time detection of rapid changes in protein interactions (Demidov *et al.*, 2006). Secondly, linkage of fluorescent protein fragments may affect the folding or structure of the target proteins, leading to prevent proteins from interacting. Additionally, although the target proteins interact in living cells, the fragments of fluorescent protein may not be complementing due to improper orientation according to each other. Therefore, absence of fluorescent signal may be a false negative and doesn't certainly mean that the interaction doesn't occur (Kerppola, 2006). Lastly, interaction-based fluorescent signal intensity decreases with the interaction of proteins both fused to same fragment, N-fragment or C-fragment.

1.3.2 Homo/Hetero-dimerizations between Adenosine A_{2A} and Dopamine D₂ receptors

Dimerization has been proposed to occur between adenosine receptors, leading to homo- or heterodimers (Franco *et al.*, 2006). More specifically, existence of A_{2A}R homodimers at the cell surface was demonstrated by several approaches including coimmunoprecipitation and non-invasive light resonance energy transfer based methods. Moreover, it has been suggested that these homo-dimers, not the monomers, are the functional forms of receptors present on the plasma membrane (Canals *et al.*, 2004). Similarly, it is now widely accepted that dopamine D₁, D₂, and D₃ receptors also form functional homodimers in transfected cell lines (Dziedzicka-Wasylewska *et al.*, 2006) and D₂ receptors exist as dimers in human and rat brain tissues (Zawarynski *et al.*, 1998).

Both of the adenosine A_{2A} and dopamine D₂ receptors localize densely in striatopallidal γ -aminobutyric acid (GABA) containing neurons (Sergi Ferré *et al.*, 2004) and critical in the function of basal ganglia. A_{2A}R-D₂R dimer was one of the first reported heteromers. First evidences of antagonistic interaction between A_{2A}R and D₂R were given by electrophysiology experiments showing that stimulation of A_{2A}R has an excitatory effect on striatopallidal neurons; whereas D₂R stimulation displays an inhibitory response on these neurons (Ferre *et al.*, 1991). Later on, physical interactions between these receptors has been supported by using different approaches, including coimmunoprecipitation and colocalization assays (Hillion *et al.*, 2002), FRET and BRET techniques (Canals *et al.*, 2003). At the biochemical level, two kinds of antagonistic interactions between A_{2A}R-D₂R heterodimer were observed. First, activation of A_{2A}R decreases the affinity of D₂R for its agonists (Ferre *et al.*, 1991). Second, stimulation of D₂R inhibits A_{2A}R-driven cAMP accumulation within neurons (Hillion *et al.*, 2002). Therefore, this kind of antagonistic interaction between A_{2A}R-D₂R heterodimer was thought to be critical to

study new therapeutic approaches for Parkinson's disease, Alzheimer's disease, schizophrenia and drug addiction (Sergi Ferré *et al.*, 2004).

1.3.3 Interactions between Dopamine and NMDA receptors

In recent years, the interaction between glutamate and dopamine receptors in the basal ganglia has been suggested to be important for motor activity, emotion and cognition. Although the mechanism of such interactions is not yet well understood, impairments in interaction have been shown to affect several neurological disorders (Mora, Segovia, & del Arco, 2008). Early neurochemical and electrophysiological studies have shown the interaction between glutamatergic and dopaminergic systems (Carlos Cepeda & Levine, 1998; Morari *et al.*, 1998). In particular, ongoing studies have suggested functional interactions between dopamine D₁ receptors and NMDA channels (Greengard, 2001). It has been shown that D₁ receptors increase NMDA receptor-mediated responses by phosphorylation of NR1 subunit via a PKA-dependent pathway triggered by D₁ receptors. Later on, biochemical and fluorescence based studies revealed that D₁ receptor physically interacts with NMDA receptor through its carboxyl tail with two distinct subunit of NMDA receptor, namely NR1 and NR2A (Fiorentini & Missale, 2004; Lee *et al.*, 2002). Moreover, D₂ receptor has also been reported to interact with NMDA receptor through its NR2B subunit (X. Y. Liu *et al.*, 2006). Unlike D₁R, D₂R stimulation decreases NMDA currents, but the mechanism of interaction and functional relevance is still debated. According to one theory, activation of D₂R affects K⁺ and Na⁺ permeabilities that hyperpolarize cells and prevent removal of Mg²⁺ block over NMDA channels (C Cepeda, Buchwald, & Levine, 1993). Alternatively, D₂R stimulation may result in the dephosphorylation of NR1 subunit; thus reducing NMDA receptor-mediated responses (Snyder *et al.*, 1998).

These interactions bear critical consequences for the cells since NMDA is an ion channel and regulates Ca^{2+} transport. All of these molecular mechanisms of actions and functions make dopamine receptors and NMDA channels potential drug targets and underlying causes of neurological disorders.

1.4 Aim of the study

Adenosine A_{2A} , Dopamine D_2 and NMDA receptors significantly function in neurophysiological events and are targeted by neuropsychiatric drugs. Therefore, revealing the mechanisms of their physical interactions has become crucial to explain physiology and pharmacology of these receptors in more detail. Concordantly, we aimed to detect homo- and heterodimerizations of these three receptors in different combinations using fluorescent based detection methods. In this study, Bimolecular Fluorescence Complementation (BiFC) and Fluorescent Resonance Energy Transfer (FRET) assays, which are rapid and easy screening techniques, are favored to detect possible dimerizations between these receptors real-time in live cell cultures. For this purpose, firstly, labeling studies were completed to tag receptor genes with fluorescent proteins (EGFP and mCherry) or split-EGFP fragments. Afterwards, tagged receptors were co-transfected to N2a cells with different combinations; and dimerizations were analyzed and quantified under laser scanning confocal microscope. Moreover, optimization of both techniques provides tools for monitoring possible homo- or heterooligomeric (interaction of more than two proteins) protein complexes comprising $A_{2A}R$, D_2R and NMDARs. Thus, our further aim is to introduce a novel approach for revealing protein-protein interactions to literature by combining BiFC and FRET methods.

Completing of this project presents a system for testing possible drugs at the first step in cell culture to ease drug discovery studies. Potential drug candidates following in culture tests can be administered and tested in animal models used for neurological disorders in order to understand their potential activities.

CHAPTER 2

MATERIALS AND METHODS

2.1 Materials

2.1.1 Neuro2a (N2a) Mouse Neuroblastoma Cell Line, Media and Conditions for Maintenance

In order to visualize the receptors tagged with fluorescent proteins in live cells, constructs were transiently transfected into Neuro2a cells; supplied by ATCC and thoughtfully gifted by Assoc. Prof. Dr. Tülin Yanık, from METU Biological Sciences, Ankara, Turkey.

For the maintenance of N2a cell line, cells were grown in the growth medium for 3 / 4 days to reach around 90 % confluence. During their growth, the cells were incubated in Heraeus[®] Hera Cell 150 Tri-Gas Cell Culture incubator, at 37 °C with 5 % CO₂. All cell culture studies were performed in a laminar flow cabinet with a high-efficiency particulate absorption (hepa) filter.

The growth medium of N2a cells was prepared by mixing Dulbecco's Modified Eagle Medium (D-MEM) high glucose with L-glutamine (Invitrogen, Cat#41966029), OptiMEM[®]I Reduced Serum Medium with L-glutamine (Invitrogen, Cat#31985047), Fetal Bovine Serum (Invitrogen, Cat#26140-079) and Penicillin/Streptomycin solution (Invitrogen, Cat#15140-122); in a ratio of 44,5 % , 44,5 % , 10 % and 1 % respectively. The prepared medium was then filtered by use

of Millipore Stericup[®] Filter Unit to sterilize it. Complete formulation of D-MEM, high glucose with L-glutamine is available in Appendix A.

To keep N2a cell line alive, cells were passaged every after 3 / 4 days when they are 90 % confluent. During cell-passage procedure, the growth medium was removed and Phosphate Buffered Saline (PBS) solution was used to wash cells; so that waste materials and dead cells could be removed (Composition of PBS solution is written in Appendix A). After washing with PBS, cells were incubated in 1 ml of Express Stable Trypsin Like Enzyme with Phenol Red (Invitrogen, Cat#12605-028) for 5 minutes in order to detach them from the surface of cell culture flask. Lifted cells are then mixed with 9 ml of fresh growth medium; and 10 % of the cells were transferred into a new flask containing fresh medium.

To stock the cells, freezing medium involving 35 % DMEM, 35 % OptiMEM[®], 20 % glycerol and 10 % FBS was used. Around 10^7 cells were centrifuged at 1000 rpm for 5 minutes and the cell precipitate was resuspended in 1 ml of freezing medium. After transferring them to a screw-cap cryovial, cells were stored in -80°C . The next day, they were moved into nitrogen tank for long storage. In order to revive the cells, stored cryovials were incubated at 37°C and the thawed cells were transferred to falcon tube containing 9 ml of fresh growth medium. After centrifuging at 1000 rpm for 5 minutes, precipitated cells were resuspended in 1 ml growth medium and transferred to cell culture flask.

2.1.2 Bacterial Strain, Culture Media and Conditions

Escherichia coli TOP10 and *Escherichia coli* DH5 α strains were used in gene cloning studies to amplify plasmids. The cells were cultivated in Luria Bertani (LB) Medium; liquid or solid. The components (written in Appendix B) of the medium were dissolved in distilled water, and the medium was sterilized at 121 °C for 20 minutes after arrangement of pH to 7.0. Solid cultures were incubated at 37 °C for 12-16 hours in an incubator; while liquid cultures were grown in the same conditions within the rotary shaker incubator at 200 rpm. To select the colonies containing desired plasmids, 100 μ g/mL of ampicillin was added to LB medium.

For the storage of bacterial samples, an aliquot of culture in a liquid LB medium was mixed with 50 % glycerol with the ratio of 1:1; and placed at -80 °C.

2.1.3 Plasmids

cDNA clones of A_{2A} receptor (Accession Number: NM_000675) and D₂ receptor (Accession Number: NM_000795) were purchased from PlasmID, Harvard Medical School (MA, USA) and obtained in pDNR-Dual and pDONR221 vectors, respectively. Enhanced Green Fluorescent Protein (EGFP) (Accession Number: AAB02574) and mCherry (Accession Number: ACO48282) cDNA clones were kindly gifted by Prof. Dr. Henry Lester, California Institute of Technology (CA, USA) and obtained in pEGFP-N1 and pCS2-mCherry vectors, respectively. All receptors and fluorescent proteins were cloned into pcDNA 3.1 (-), mammalian expression vector with CMV promoter (see Appendix D), which was kindly gifted by Assoc. Prof. Dr. Ayşe Elif Erson Bensen, Middle East Technical University, Turkey.

2.1.4 Other chemicals and materials

The chemicals required in this study were supplied from Sigma Chemical Company (NY, USA) and Applichem (Darmstadt, Germany). DNA Polymerases used in PCR protocols, Plasmid Isolation and PCR purification kits were purchased from Fermentas (Ontario, Canada). For gel elution, kit was obtained from QIAGEN (Düsseldorf, Germany). All of the restriction enzymes and T4 DNA ligase were purchased from New England Biolabs (Hertfordshire, UK).

Primer sets designed to label receptors were synthesized by Alpha DNA (Quebec, Canada) or Integrated DNA Technologies (Iowa, USA).

Components of the media and required reagents, including transfection kit, were supplied from GIBCO®, Invitrogen (CA, USA). Glass bottom dishes used in live-cell imaging studies were purchased from In Vitro Scientific (CA, USA).

Live cell imaging studies were carried out by use of Zeiss 510 laser scanning microscope (UNAM, Bilkent University).

2.2 Methods

2.2.1 Preparation of Competent *E. coli* Cells by CaCl₂ Method

A single colony of *Escherichia coli* (TOP10 strain) cells was taken from streak plate and inoculated into 5 ml of liquid LB medium and incubated for 12-16 hours at 37 °C and 200 rpm in the shaker incubator. This 5 ml inoculum was transferred into 250 ml Erlenmeyer flask containing 50 ml fresh liquid LB medium; and incubated for 2-3 hours in the same conditions until the optical density of bacterial culture at 600 nm (OD₆₀₀) reaches to around 0.5. After required density was obtained, Erlenmeyer flask was chilled on ice for 15 minutes. The whole bacterial culture was then transferred to a 50 ml falcon tube and centrifuged at 4000 rpm for 10 minutes at 4 °C. After removing supernatant, settled cells were resuspended with 15 ml 0.1M CaCl₂ solution. After chilling on ice for 15 minutes, it was centrifuged again at 4000 rpm for 10 minutes. Supernatant was decanted and remaining pellet was dissolved in 4 ml of 0.1 M CaCl₂ + 15 % glycerol solution (15% of the solution was glycerol). The suspended cells were aliquoted as 100 µl in 1.5 ml Eppendorf tubes. Finally, these tubes containing competent cells were frozen in liquid nitrogen and stored at -80 °C.

2.2.2 Transformation of Competent *E. Coli* cells

Competent *E. Coli* cells were chilled on ice for 15 minutes after taken from -80 °C freezer. 50-100 ng of plasmid or 10 µl of ligation / PCR product was added into thawed competent bacterial cells. After adding DNA, cells were chilled on ice for 30 minutes. Cells were then incubated at 42 °C for 90 seconds to apply heat shock; and immediately after heat shock process they were chilled on ice for 5 minutes. In the

next step, 900 μ l of preheated LB broth was added and cells were incubated at 37 °C for an hour. Afterwards, cells were centrifuged at 6000 rpm for 4 minutes and 800 μ l of supernatant was discarded. The pellet was resuspended in the remaining supernatant. Then, suspension was spreaded on LB agar plate containing ampicillin. Finally, plates were incubated at 37 °C for ~16 hours.

2.2.3 Plasmid Isolation from *E. Coli*

A single colony was picked from LB agar plate and inoculated into 4 ml liquid LB medium containing ampicillin (100 mg/ml). After growing cells by shaking at 200 rpm for ~16 hours at 37 °C, plasmid DNA was isolated from bacterial culture by use of Thermo Scientific® GeneJET Plasmid Miniprep Kit, according to manufacturer's instructions.

2.2.4 Restriction enzyme digestion

1-2 μ g of DNA was digested with 1 unit of the restriction enzyme within the proper NEB buffer (Appendix C); and total volume of the reaction was completed to 20 μ l with nuclease free water. If it is suggested, 1X BSA was also added to the reaction mixture. All restriction enzymes used in this study were supplied from New England Biolabs Inc. (NEB); thus, all digestion reactions were prepared according to NEB's instructions. At the end, reaction mixture was incubated at 37 °C for 2-3 hours.

2.2.5 Ligation

After digested DNA was run on the gel, digested constructs (inserts) and vectors were eluted from the gel. Isolated inserts and vectors were used for ligation reaction containing 1 unit of T4 DNA ligase (NEB, Cat#0202T), 1X T4 DNA ligase buffer (Appendix C) and nuclease free water to complete the reaction volume to 20 μ l. Amounts of the inserts and vectors were decided by considering their sizes and taking the molar ratio of vector to insert as 1:5. Finally, the reaction mixture was incubated at room temperature for at least 1 hour.

2.2.6 Polymerase Chain Reaction (PCR)

To amplify EGFP and mCherry genes with 30 bp overhangs in order to use them in the PCR integration step, PCR protocol was optimized and applied PCR protocol is shown in Table 2.1

Table 2.1 Optimized PCR conditions to amplify fluorescent protein genes by adding 30 bp flanking ends.

Reagent		Amount
Template (EGFP/mCherry in pcDNA)		100-150 ng
5X Phire Reaction Buffer		10 μ l
Phire Hot Start II DNA Polymerase		1 μ l
dNTPs (25 mM)		1 μ l
Forward Primer (20 pmol)		1 μ l
Reverse Primer (20 pmol)		1 μ l
DMSO		1 μ l
MgCl ₂		1 μ l
Nuclease-free Water		Completed to 50 μ l
Pre-denaturation	98°C	30 sec
Denaturation	98°C	5 sec
Annealing	55°C	5 sec
Extension	72°C	15 sec
Final extension	72°C	1 min

} 35 cycles

2.2.7 Agarose Gel Electrophoresis

In order to confirm the amplification by PCR or digestion reactions, sizes of DNA fragments are controlled by use of agarose gel electrophoresis. In this study, 1 % agarose gel was preferred to check DNA smaller than 1 kb; and 0.8 % agarose gel was prepared to check DNA longer than 1 kb. For the preparation of gel, the pre-weighed agarose was dissolved in 1X TBE (Appendix C) by heating within the microwave oven. After cooling it, EtBr was added into the gel so that DNA

fragments become visible under UV light. Then it was poured into the tray and combs were placed to generate proper wells. After solidified, GeneRuler DNA Ladders (Fermentas) and DNA sample mixed with 6X DNA loading dye (Fermentas®, Cat#R0611, see Appendix C) were loaded into each well. Finally, the gel was run in 1X TBE buffer at 80-100 V for around 40 minutes.

2.2.8 DNA extraction from Agarose Gel

After controlling PCR or digestion products with agarose gel electrophoresis, confirmed DNA fragments were extracted from the gel by use of QIAGEN® Gel Extraction Kit (Cat# 28704) according to provided manual of the kit.

2.2.9 Determination of DNA Amount

After plasmid isolation or gel extraction protocols, the obtained DNA concentration was quantified with NanoDrop 2000 spectrophotometer from Thermo Scientific® according to user's manual.

2.2.10 PCR Integration Method

The receptor genes were tagged with EGFP and mCherry fluorescent proteins from their C-termini by using PCR integration method. The method involves two sequential PCR reactions. The first PCR reaction was conducted as indicated in Table 2.1. In this first PCR reaction, fluorescent protein genes were amplified with

30 bp long overhangs, corresponding to target integration site within the plasmid containing receptor gene. In our case, to label the receptor genes from their C-termini, 5' of the forward primer includes an overhang homologous to the last 30 bp of the receptor gene without the stop codon. Similarly, the 5' of the reverse primer includes an overhang homologous to the 30 bp of the vector sequence that directly follows the receptor gene. After that, the first PCR product is used as double stranded DNA primer; and the vector containing the desired receptor gene is included as a template in the second PCR reaction. For an optimal integration reaction, template (plasmid with receptor) to insert (first PCR product) ratio should be 1:5. The whole reaction conditions are given in Table 2.2.

Table 2.2 Optimized conditions for second PCR reaction of PCR integration method

Reagent		Amount
5X Phire Reaction Buffer		10 μ l
Phire Hot Start II DNA Polymerase		1 μ l
dNTPs (25 mM)		1 μ l
DMSO		1 μ l
Template (A2AR / D2R in pcDNA)		100 ng
1 st PCR product		500 ng
Nuclease-free Water		Completed to 50 μ l

Pre-denaturation	95°C	30 sec	} 18 cycles
Denaturation	95°C	30 sec	
Annealing	51°C	1 min	
Extension	68°C	2 min/kb	
Final extension	68°C	5 min	

At the end of this second PCR reaction, a vector containing receptor gene tagged with fluorescent protein gene was constructed. To make the strategy more clear a representative scheme of the method is given in Figure 2.1.

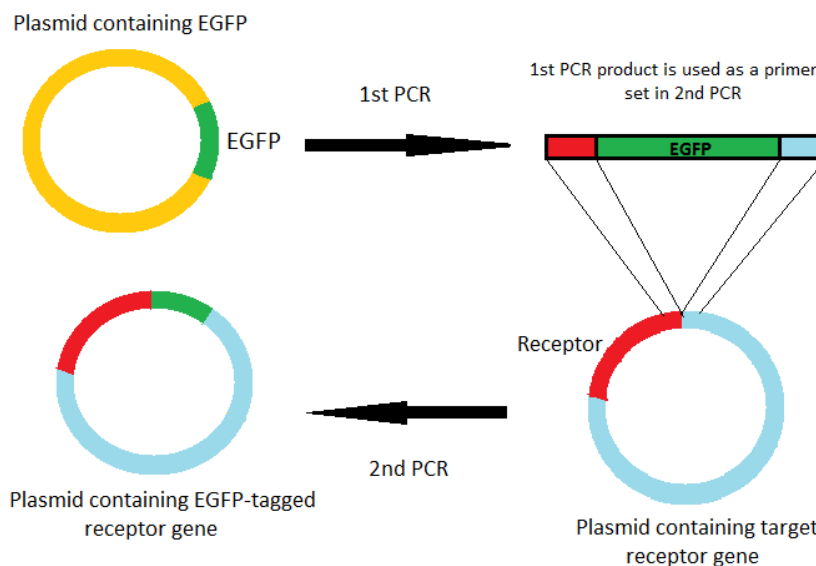


Figure 2.1 Representative scheme for PCR integration method (in order to tag a receptor gene with EGFP fluorescent protein)

2.2.11 Transfection of N2a cells with eukaryotic expression vectors

In order to express and visualize tagged receptors, live N2a cells were transfected with expression vectors containing receptor gene fused to fluorescent protein gene by use of Lipofectamine_{TM} LTX with Plus_{TM} reagents (from Invitrogen®). The day before the transfection, 50.000 cells were seeded on a glass bottom dish and grown for 24 hours in their normal growth media. The next day, 500 ng of the desired plasmid was diluted in 100 μ l of OptiMEM[®] I. Right after, 4 μ l of Plus_{TM} reagent was added and this mixture was incubated at room temperature for 15 minutes. At

the end of this incubation, 4 μ l of Lipofectamine LTX diluted in 100 μ l of OptiMEM[®] I was added into the first mixture containing DNA samples. This final mixture was also incubated at room temperature for 20 minutes. In the meantime, the medium on the cells seeded before was taken and cells were washed with 1 ml of sterile 1X PBS solution. Then the rinsed cells were covered with 1 ml of OptiMEM[®] I. When the incubation time of transfection mixture was up, the mixture was added into dishes. The cells were incubated for 3 hours in the 5 % CO₂ incubator at 37 °C. After 3 hours, 2 ml of normal growth medium was directly added on the cells and cells were let to grow for 48 hours, before imaging them.

2.2.12 Imaging with Laser Scanning Confocal Microscope

After cells were transfected with desired plasmids and grown for 2 days, the expressed receptors were visualized under Zeiss LSM 510 confocal microscope with an objective Plan-Apochromat 63x/1.40 Oil DIC M27. While fluorescent signals in live cells were detected, LP 650 and LP 585 filters for mCherry signals; and BP 505-550 filters for EGFP signals were used with this confocal microscope.

To visualize green signal, EGFP channel (Track 2) was used in which cells were excited at 458 nm and the emission was collected in the 505-580 nm range. On the other hand to visualize red signal, mCherry channel (Track 3) was used in which cells were excited at 543 nm and emission was collected over 585 nm. Finally, FRET images were collected from Track 1, which uses 458 nm to excite EGFP and detects emission over 585 nm coming from mCherry. Configuration settings are detailed below.

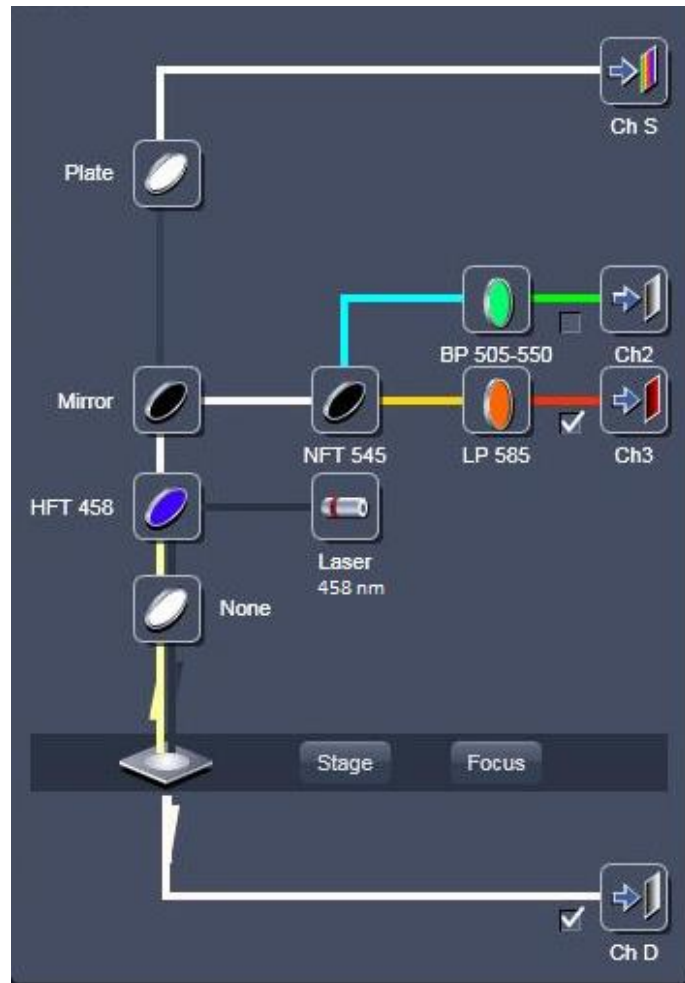


Figure 2.2 Track 1 configuration in laser scanning confocal microscope to detect FRET after exciting the cells at 458 nm

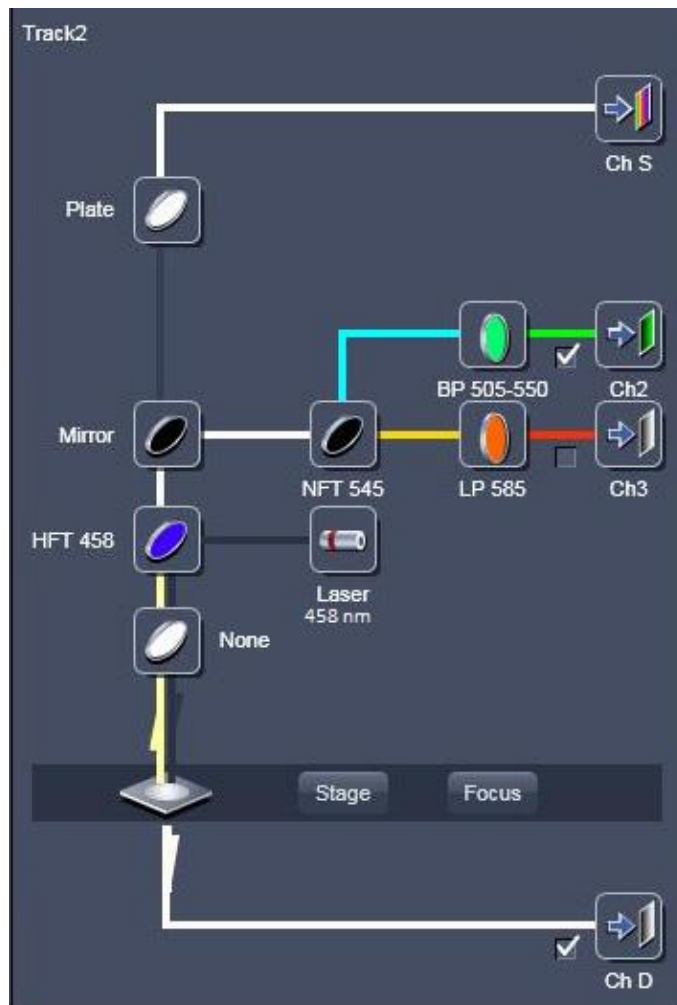


Figure 2.3 Track 2 configuration in laser scanning confocal microscope to detect donor bleed-through (EGFP signal) after exciting the cell at 458 nm

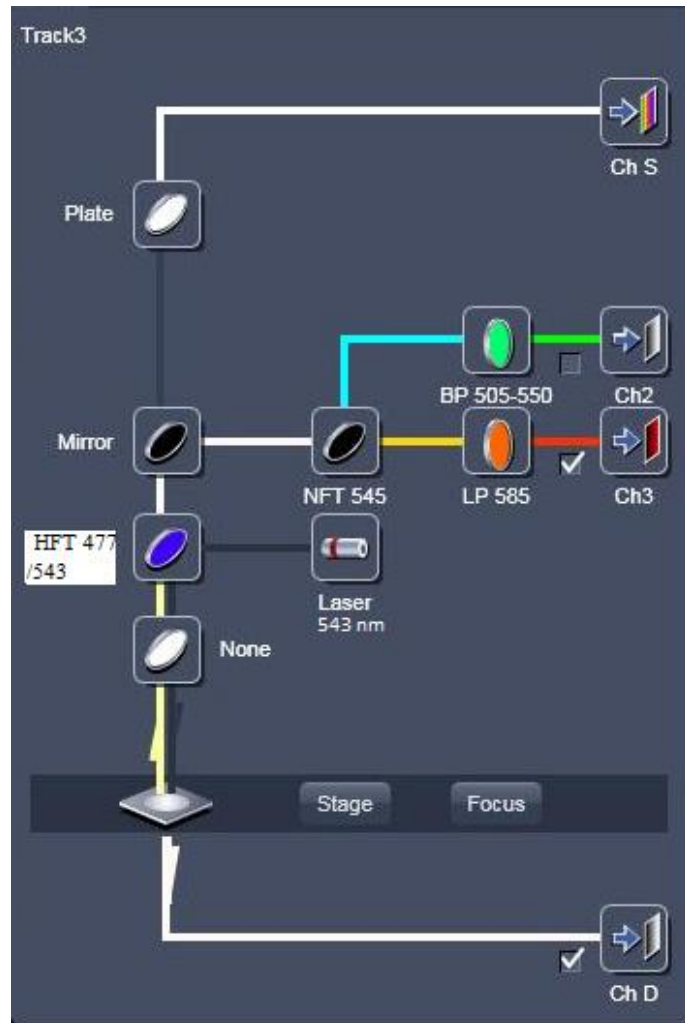


Figure 2.4 Track 3 configuration in laser scanning confocal microscope to detect acceptor bleed through (mCherry signal) after exciting the cell at 543 nm

2.2.13 Image Analysis with Pix-FRET

One important point for the calculation of sensitized emission FRET is the correction of spectral bleed-throughs (SBT). For an efficient FRET analysis, one has to calculate SBTs by considering ratios between the fluorescence intensities in the FRET plates and that in the donor or acceptor plates. While FRET plates contain both donor and acceptor molecules, donor and acceptor plates contain only the donor and acceptor molecules, respectively. Another crucial point in FRET analysis is demonstrating the localization of FRET within the live cells. A freely available ImageJ plug-in, called PixFRET, was developed to generate images of sensitized-emission FRET and to visualize the location of FRET (Feige *et al.*, 2005). The program computes the FRET by analyzing the image pixel by pixel in a three channel setting, based on the formulas and the methodologies described by Gordon *et al.* (1998) and Xia and Liu (2001).

Spectral bleed-through (or crossover / crosstalk) is a fundamental problem while using more than one fluorophore in both widefield and laser scanning confocal fluorescence microscopy. In FRET analysis, signals coming from excitation of the acceptor at the wavelength of donor excitation, or emission of donor molecule in the acceptor channel are considered as SBTs. Pix-FRET contains an algorithm that eliminates false FRET signals due to SBTs, and for such algorithm three sets of experiments must be prepared.

The first set is transfected only with donor-labeled proteins since it is for the calculation of donor bleed-through. Two different images are taken from this set by use of following setups:

- Excitation of donor while collecting emission from acceptor
- Excitation of donor while collecting emission from donor

The second set is transfected only with acceptor-labeled proteins since it is for the calculation of acceptor bleed-through. Two images are obtained from this set by use of the following setups:

- Excitation of donor while collecting emission from acceptor
- Excitation of acceptor while collecting emission from acceptor

The last set is transfected with both donor- and acceptor-labeled proteins to demonstrate FRET. Three images are taken from this set by using following setups:

- Excitation of donor while collecting emission from acceptor
- Excitation of donor while collecting emission from donor
- Excitation of acceptor while collecting emission from acceptor

Using these images, PixFRET normalizes the bleed-throughs and calculates the FRET efficiency.

CHAPTER 3

RESULTS AND DISCUSSION

3.1 Detection of homo/hetero-dimerizations between Adenosine A_{2A} and Dopamine D₂ Receptors by use of BiFC assay

The concept of Bimolecular Fluorescence Complementation Assay to detect protein-protein interactions in this study is based on reconstitution of split-EGFP (enhanced green fluorescent protein) tags. It has been reported that split-EGFP reconstitution shows the strongest fluorescence intensity upon protein interaction when the EGFP protein is dissected at the position between 157th and 158th amino acids (Ozawa *et al.*, 2001). The EGFP portion from 1st to 157th amino acid is indicated as N-EGFP tag and the remaining portion from 158th to 240th amino acid is named as C-EGFP tag in this study.

Studies using FRET and/or BRET methods have detected the homo- or heterodimerizations of C-terminally tagged A_{2A} and D₂ receptors (Canals *et al.*, 2003; Gandia *et al.*, 2008a). Depending on these studies, Adenosine A_{2A} and Dopamine D₂ receptor genes were tagged with split EGFP tags right after their C-termini in this research.

3.1.1 Labeling Adenosine A_{2A} and Dopamine D₂ Receptor Genes with N-EGFP Tags Using PCR Integration Method

For the construction of fusion proteins, PCR integration method was applied as illustrated in Figure 2.1. In the first PCR reaction, N-EGFP coding sequence was amplified with 30 bp overhangs corresponding to insertion positions. Primers are given in Appendix E. To amplify N-EGFP portion, pcDNA 3.1(-) vector containing EGFP gene (Accession Number: AAB02574) was used as a template of the reaction. The 1st PCR products were then run on 1% agarose gel as seen in Figure 3.1.

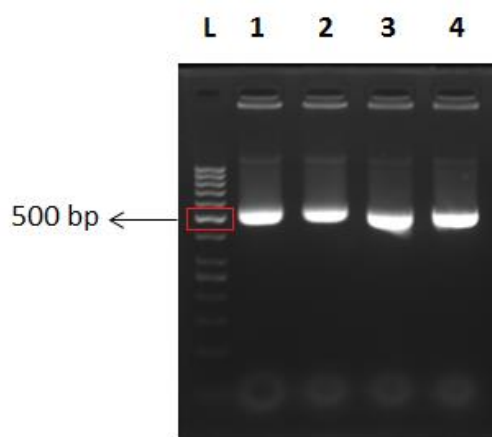


Figure 3.1 Agarose gel electrophoresis image of PCR amplified N-EGFP fragments with Adenosine A_{2A}R flanking ends (lane 1&2) and Dopamine D₂R flanking ends (lane 3&4). Fermentas[®] GeneRuler[™] 50 bp DNA Ladder was used.

As expected, amplified N-EGFP tags gave the bands around 500 bp (N-EGFP tag is 471 bp; overhangs are 30 bp long). These 1st PCR products were then extracted from the gel. Later on, these purified N-EGFP tags were used as a primer set in the 2nd PCR reaction while pcDNA 3.1(-) vectors containing Adenosine A_{2A} or Dopamine

D₂ receptor genes were added as template of the reaction. At the end of 2nd PCR, reaction products were digested with DpnI enzyme in order to eliminate template plasmids added to PCR reaction at the beginning, which are not PCR products. Template plasmids were isolated from *E. coli* cells; so that these plasmids were methylated within the bacterial cells during DNA synthesis. DpnI recognizes methylated GATC sequences; thus methylated template plasmids are digested; while new PCR products remain intact. After DpnI digestion for 3 hours, 2nd PCR products were transformed to *E. coli* cells and cells were grown in Ampicillin containing plates. The next day, consisted colonies were picked and grown in liquid medium to be able to isolate plasmids from the cells. Finally, the obtained isolated plasmids were screened with double digestion to check the insert size.

The wild type D₂ and A_{2A} receptors are between *NotI* and *HindIII* restriction sites within the pcDNA 3.1(-), so that the logic of this controlling procedure is observing size changes by digesting with these two enzymes. After digestion for overnight, digested plasmids were run on 1 % agarose gel as seen in Figure 3.2.

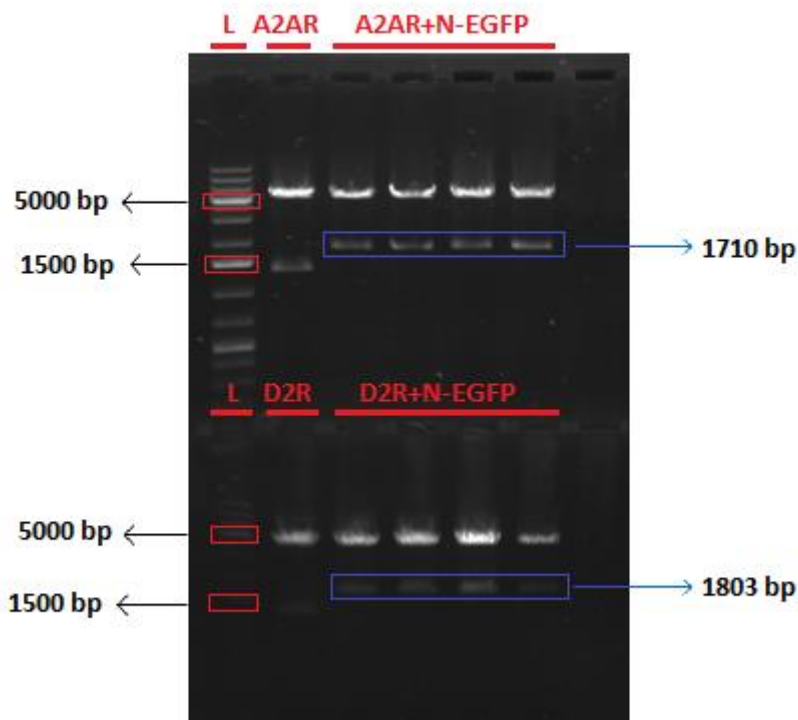


Figure 3.2 Agarose gel electrophoresis image of *NotI*&*HindIII* double-digestion screening of candidate A_{2A} and D₂ receptors tagged with N-EGFP in pcDNA 3.1 (-) vectors. Fermentas[®] GeneRuler™ 1 kb plus DNA Ladder was used.

As expected on the gel, wild type A_{2A} and D₂ receptors are seen as 1239 bp and 1332 bp, respectively. The addition of N-EGFP to these receptor genes must result in 471 bp increase in total size. In the direction of this expectation, all of the constructs in the image gave the expected sizes. The upper bands represent remaining pcDNA sequence after digestion, and as expected they are around 5400 bp.

After checking sizes of N-EGFP tagged receptors on agarose gels, the plasmids carrying these fusion proteins were sequenced for the final confirmation. According to sequencing results, N-EGFP tags were successfully inserted after C-termini of Adenosine A_{2A} (Accession Number: NM_000675) and Dopamine D₂ (Accession Number: NM_000795) receptor genes within pcDNA 3.1(-) plasmids. The confirmed coding sequences of receptor+N-EGFP fusions are given in Appendix F.

3.1.2 Labeling Adenosine A_{2A} and Dopamine D₂ Receptor Genes with C-EGFP Tags Using PCR Integration Method

For the construction of C-EGFP tagged receptors, same methodology was applied as described in 3.1.1. In the first PCR reaction, C-EGFP coding sequence was amplified with 30 bp overhangs to insert after C-terminus of receptors (see Appendix E for primers). pcDNA 3.1(-) vector containing EGFP gene was used as a template in the reaction in order to amplify only the C-EGFP portion. At the end, 1st PCR products were then run on 1% agarose gel as seen in Figure 3.3.

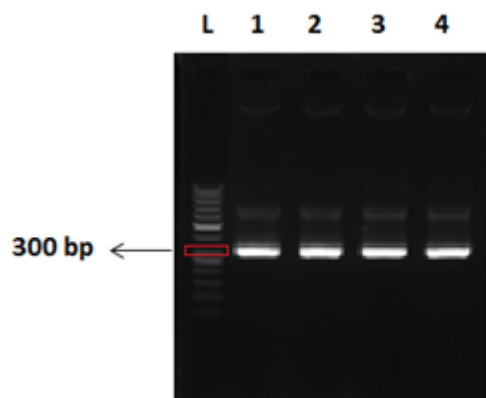


Figure 3.3 Agarose gel electrophoresis image of PCR amplified C-EGFP fragments with Adenosine A_{2A}R flanking ends (lane 1&2) and Dopamine D₂R flanking ends (lane 3&4). Fermentas[®] GeneRuler™ 50 bp DNA Ladder was used.

As expected, amplified C-EGFP tags gave the bands around 300 bp (C-EGFP tag is 249 bp; overhangs are 30 bp long). Afterwards, these products were eluted from the gel and used as a primer set in 2nd PCR. Adenosine A_{2A} or Dopamine D₂ receptor genes in pcDNA 3.1(-) were used as template plasmids for this integration reaction. At the end of 2nd PCR, products were digested with *DpnI* restriction enzyme to transform only the final PCR products into *E. coli* cells. The obtained colonies were then screened by digesting the isolated plasmids with *NotI* and *HindIII* enzymes.

After digestion for overnight, digested plasmids were run on 1% agarose gel as seen in Figure 3.4.

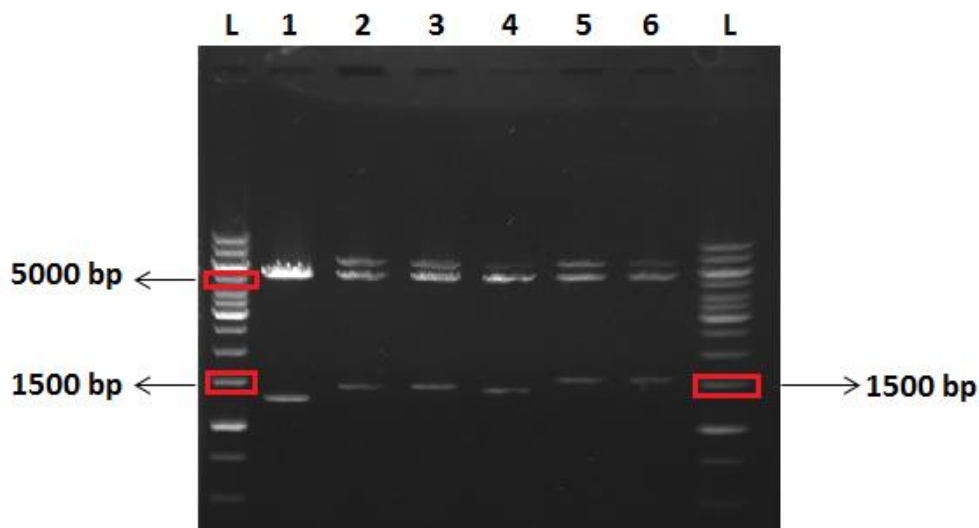


Figure 3.4 Agarose gel electrophoresis image of *NotI*&*HindIII* double-digestion screening of candidate A_{2A} and D_2 receptors tagged with C-EGFP in pcDNA 3.1 (-) vectors. Fermentas[®] GeneRuler™ 1 kb DNA Ladder was used. The wells were loaded with $A_{2A}R$ (1), $A_{2A}R+C-EGFP$ (2&3), D_2R (4), and $D_2R+C-EGFP$ (5&6).

As expected, wild type A_{2A} and D_2 receptors are seen as 1239 bp and 1332 bp, respectively. $A_{2A}R+C-EGFP$ and $D_2R+C-EGFP$ fusions displayed ~300 bp increase in size when compared with wild type corresponding. The upper bands represent remaining pcDNA sequence after digestion.

Additionally, the plasmids containing C-EGFP tagged receptors were sequenced for final validation. Obtained sequences confirmed that the receptors were successfully labeled with C-EGFP fragments after their C-termini. The coding sequences of receptor+C-EGFP fusions are given in Appendix F.

3.1.3 Reassembly of EGFP fragments in live cells

To show homo/hetero-dimerizations of A_{2A} and D₂ receptors, split EGFP partners (both N-EGFP and C-EGFP) were co-transfected into N2a cells. As described in methodology, 750 ng of split-EGFP tagged receptor containing plasmids were co-transfected to cells using Lipofectamine_{TM} LTX with Plus_{TM} reagents. 40-48 hours after transfection, cells were observed under laser scanning confocal microscope with single track configuration (Track 2), as shown in Figure 2.3.

By this way, homodimerization of Adenosine A_{2A} receptors has been detected in live N2a cells, as shown in Figure 3.5. As expected, A_{2A} receptors are seen as dimers significantly on the plasma membrane where they function.

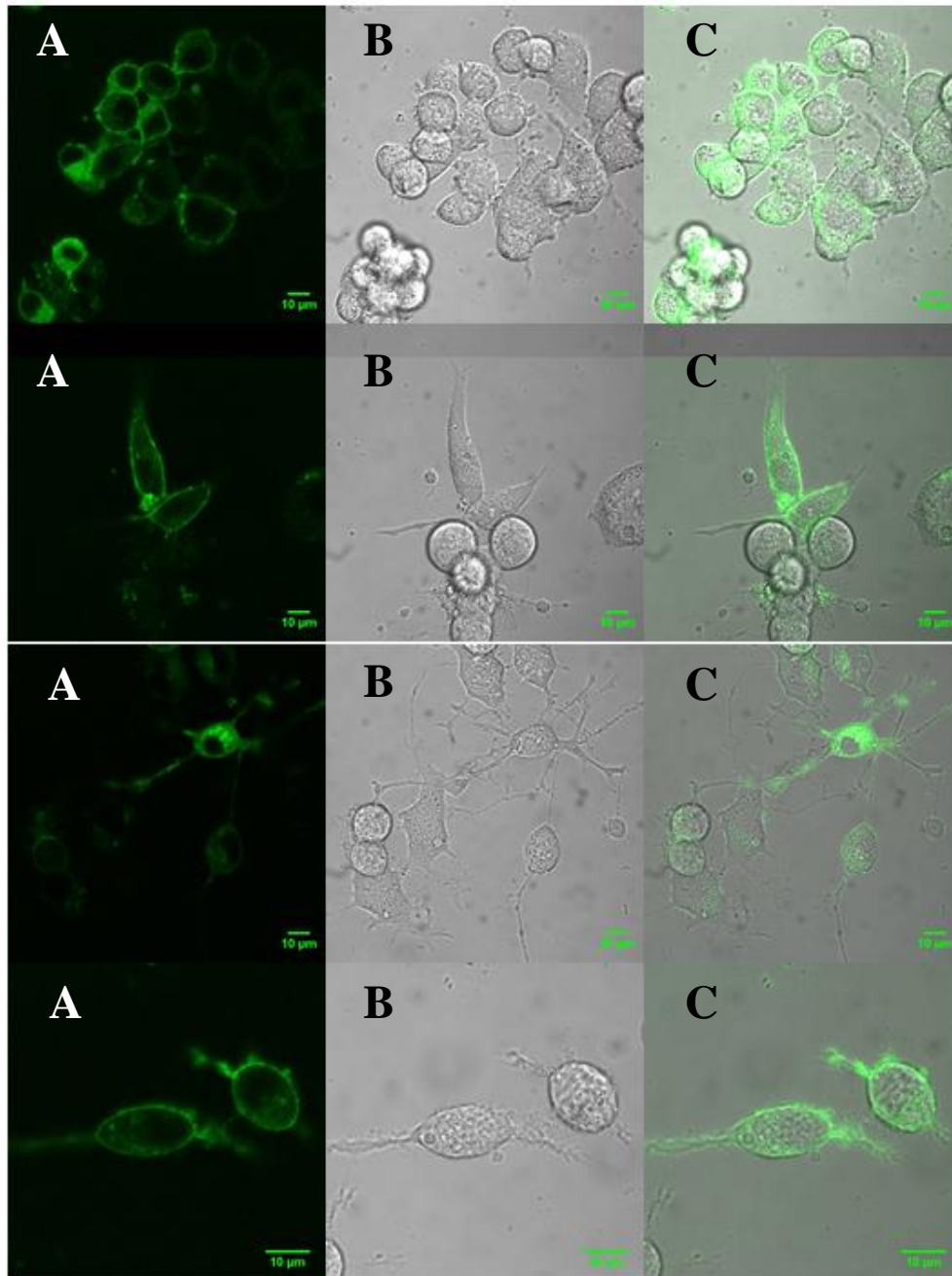


Figure 3.5 N2a cells co-transfected with $A_{2A}R+N$ -EGFP and $A_{2A}R+C$ -EGFP fusion proteins. (A) Images were taken from EGFP channel. (B) Images were taken from bright field channel. (C) Images were obtained by merging channel (A) and (B).

Similarly, homodimerization of Dopamine D₂ receptors and; heterodimerization of A_{2A} and D₂ receptors have been studied under the same conditions. However, no proper EGFP signal was obtained on the plasma membrane from the cells co-transfected with D₂R+N-EGFP and D₂R+C-EGFP fusion proteins or D₂R+N-EGFP and A_{2A}R+C-EGFP fusion proteins or A_{2A}R+N-EGFP and D₂R+C-EGFP fusion proteins. Although some fragmentary intracellular signals with very low intensity have been detected in the studies of homo/hetero-dimerizations of Dopamine D₂ receptors (see Figure 3.6 and 3.7), it is hard to conclude that dimerizations of D₂ receptors with each other and A_{2A} receptors has been detected successfully.

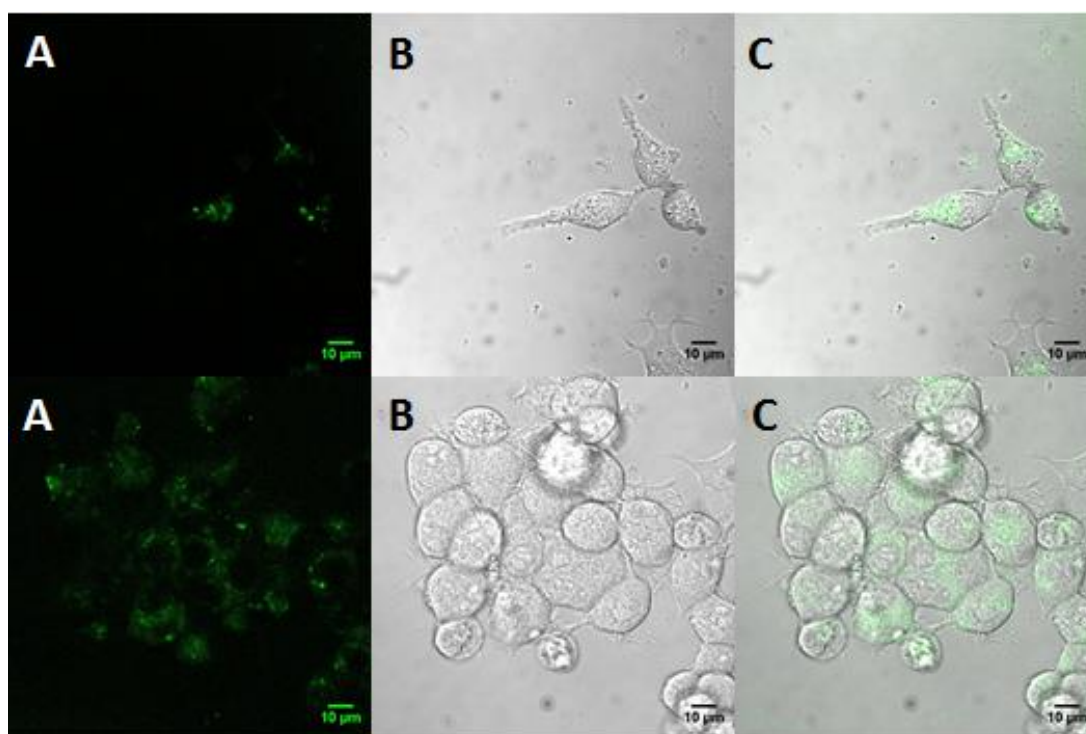


Figure 3.6 N2a cells co-transfected with D₂R+N-EGFP and D₂R+C-EGFP fusion proteins. (A) Images were taken from EGFP channel. (B) Images were taken from bright field channel. (C) Images were obtained by merging channel (A) and (B).

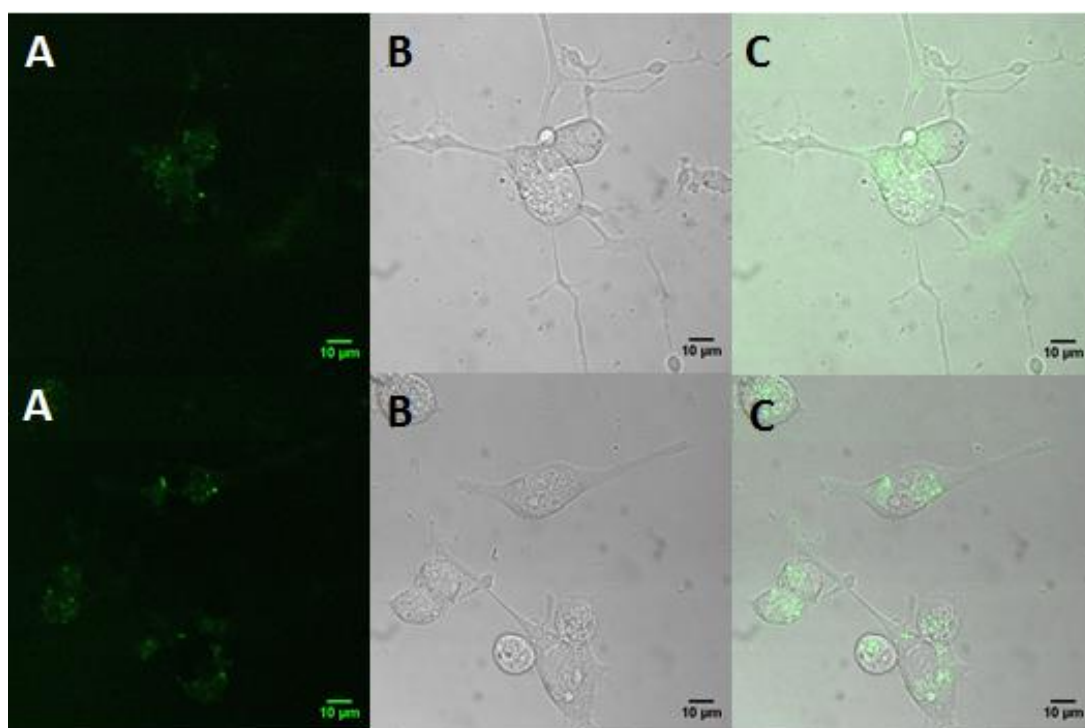


Figure 3.7 N2a cells co-transfected with D₂R+N-EGFP and A_{2A}R+C-EGFP (first row) or A_{2A}R+N-EGFP and D₂R+C-EGFP (second row) fusion proteins. (A) Images were taken from EGFP channel. (B) Images were taken from bright field channel. (C) Images were obtained by merging channel (A) and (B).

Unlike in the homodimerization of Adenosine A_{2A} receptors, Dopamine D₂ receptors are seen to dimerize in intracellular parts of the cells and the obtained signals are much weaker compared to signals resulting from A_{2A}R homodimerization. For the reconstitution of EGFP signal, insertion positions of split-EGFP fragments should be favorable. In other words, upon interactions of D₂ receptors with each other and/or A_{2A} receptors, the split EGFP tags might not complement due to improper orientation according to each other. Thus, labeling D₂ receptors with split-EGFP tags from their different positions; such as N-terminal or a proper site within C-tail, could solve the weak-signal problems by providing flexibility to increase the possibility of association of fluorescent fragments. Alternatively, insertion of split-EGFP tags after

C-termini of D₂ receptors might affect proper folding or structure of these receptors, resulting in the prevention of these proteins from interacting on the membrane. In other respects, interactions with G-proteins on the membrane might lead to critical conformational changes for D₂ receptors, driving split fragments apart from each other. That's why D₂ receptor homodimerization might not be visible as EGFP signal specifically on the membrane. Additionally, labeling of D₂ receptor genes with fluorescent tags might attenuate trafficking of these receptors to the membrane; thus we couldn't detect D₂ receptor interactions on the plasma membrane.

It is also noteworthy to express that spontaneous reassembly of N-EGFP and C-EGFP tags is highly unlikely since the affinity between these fragments is too low when co-expressed together (Magliery *et al.*, 2005). Even so to validate that A_{2A}R homo-dimerization was detected not due to the spontaneous reassembly of these split tags, pcDNA vectors containing only N-EGFP and only C-EGFP fragments were co-transfected to live N2a cells as a negative control. As expected, no assembled EGFP signal was detected from these cells.

3.2 Detection of homo/hetero-dimerizations between Adenosine A_{2A} and Dopamine D₂ Receptors by use of FRET

In addition to BiFC assay, physical homo/hetero-dimerizations between A_{2A} and D₂ receptors were studied with FRET technique to consolidate results obtained from BiFC study. In this study, EGFP and mCherry fluorescent proteins were chosen to be used in FRET experiments due to their suitable excitation and emission spectrums when compared to each other.

3.2.1 Validation of Adenosine A_{2A} and Dopamine D₂ Receptors tagged with full length mCherry and EGFP

cDNA clones of Adenosine A_{2A} receptor and Dopamine D₂ receptor were obtained in pDNR-Dual and pDONR221 vectors, respectively. For direct expression in N2a cells, receptor genes were transferred into a mammalian expression vector pcDNA 3.1 (-); by cutting from *NotI* and *HindIII* sites and cloned to the same RE sites of pcDNA 3.1 (-) (see Appendix D). After inserting the receptor genes into expression vector, the fluorescent protein genes, EGFP and mCherry, were fused to C-termini of these receptors by use of PCR integration method. All of the details about these tagging studies are demonstrated in a thesis “Optimization of FRET Method to Detect Dimerization of Dopamine D₂ and Adenosine A_{2A} Receptors in Live cells” by Gökhan Ünlü.

Since these fusion proteins were placed between *NotI* and *HindIII* sites within the pcDNA 3.1(-), plasmids containing Adenosine A_{2A} receptor and Dopamine D₂ receptor fused to fluorescent proteins were digested with *NotI* and *HindIII* restriction enzymes in order to check for their sizes. Afterwards, the digested plasmids were run on 1 % agarose gel as seen in Figure 3.8.

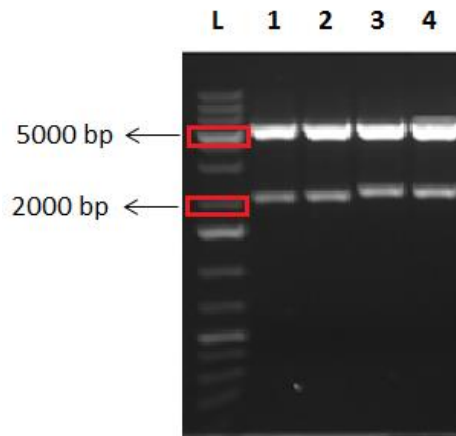


Figure 3.8 Agarose gel electrophoresis image of digested pcDNA 3.1(-) vectors containing Adenosine A_{2A} receptor and Dopamine D₂ receptor fused to EGFP/mCherry. Fermentas[®] GeneRuler™ 1 kb plus DNA Ladder was used. The wells were loaded with A_{2A}R-mCherry (1), A_{2A}R-EGFP (2), D₂R-EGFP (3), D₂R-mCherry (4).

As expected after digestion, Adenosine A_{2A} receptor and Dopamine D₂ receptor genes fused to EGFP or mCherry proteins gave the bands around 2000 bp (A_{2A} receptor gene without the stop codon is 1236 bp, D₂ receptor gene without the stop codon is 1329 bp, EGFP gene is 720 bp and mCherry gene is 711 bp) . The remainder pcDNA 3.1(-) vector sequence is seen on the top of the gel image, as 5.4 kb.

To additionally confirm the constructs for the insertion of EGFP and mCherry genes after target receptor genes, the prepared plasmids were sent for sequencing. According to sequencing results, EGFP (Accession Number: AAB02574) and mCherry (Accession Number: ACO48282) genes were successfully inserted after C-termini of Adenosine A_{2A} (Accession Number: NM_000675) and Dopamine D₂

receptor genes (Accession Number: NM_000795) within pcDNA 3.1(-) plasmids. The coding sequences of receptor+EGFP/mCherry fusions are given in Appendix F.

After tagging these target receptors, the functionalities of EGFP or mCherry tagged Adenosine A_{2A} and Dopamine D₂ receptors were tested in a study “The Functional Assessment of Fluorescently Tagged Adenosine A_{2A} and Dopamine D₂ Receptors and Qualitative Analysis of Dimerization of Adenosine A_{2A} and Dopamine D₂ Receptors by Using FRET”, conducted by Selin Akkuzu. In this study C-terminally tagged receptors were analyzed in terms of their abilities to change cAMP concentration within the cells by use of a cAMP-GloTM assay, commercially available by Promega Corporation. At the end of this study, it has been shown that C-terminally tagged A_{2A} and D₂ receptors are as functional as wild type receptors.

After confirming the sequences of functional pre-prepared constructs, complementary pairs of these plasmids were transfected to N2a cells to study homo/hetero-dimerization between these receptors by use of FRET assay.

3.2.2 Homodimerization of Adenosine A_{2A} receptors

To study interactions between Adenosine A_{2A} receptors, 500 ng of pcDNA 3.1(-) _ A_{2A}R+EGFP and 500 ng of pcDNA 3.1(-) _ A_{2A}R+mCherry plasmids were co-transfected to N2a cells using Lipofectamine LTX and Plus reagents. 40-48 hours after transfection, the cells were imaged under laser scanning confocal microscope. For FRET analysis with PixFRET, an imageJ plugin, three sets of experiments were prepared including the cells containing only A_{2A}R+EGFP, only A_{2A}R+mCherry and containing both. These three sets were observed with different configurations as illustrated in Figure 2.2 and 2.3. The images taken from cells containing only EGFP tagged receptors and only mCherry tagged receptors were used to determine bleed-

throughs by using PixFRET. This program calculates bleed-throughs coming from cells transfected with single fluorescent proteins, thus calculates FRET efficiency by eliminating these determined noise bleed-throughs.

To calculate donor bleed-through coming from EGFP proteins, N2a cells transfected only with EGFP tagged A_{2A} receptors were examined with Track 1 and Track 2 configurations (see Figure 3.9); whereas, acceptor bleed-through coming from mCherry proteins was calculated from the cells transfected only with mCherry tagged A_{2A} receptors under Track 1 and Track 3 (see Figure 3.10).

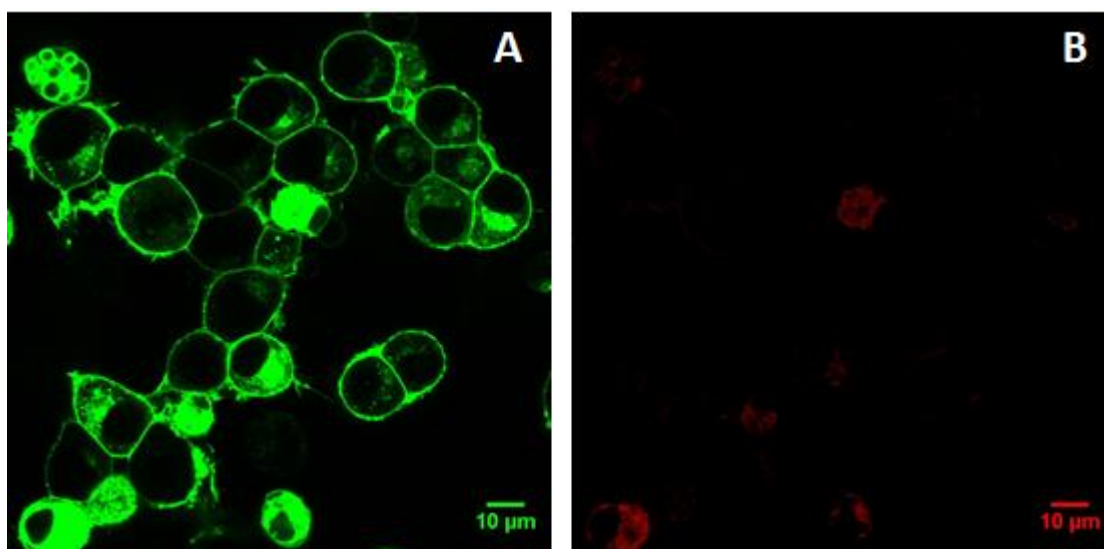


Figure 3.9 N2a cells transfected only with $A_{2A}R$ + EGFP. Images were taken from Track 2-EGFP channel (A) and Track 1-FRET channel (B).

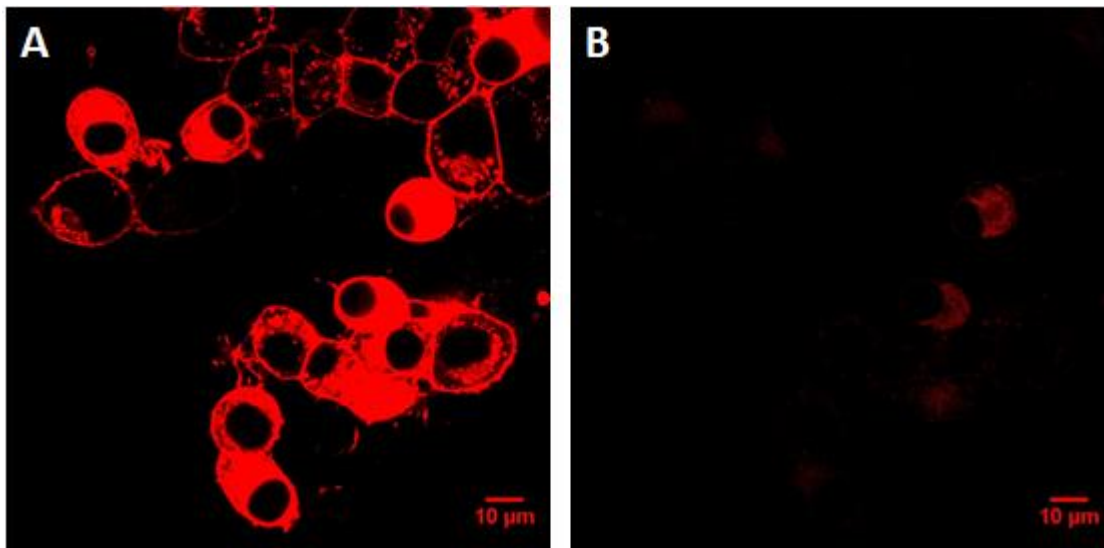


Figure 3.10 N2a cells transfected only with A_{2A}R + mCherry. Images were taken from Track 3-mCherry channel (A) and Track 1-FRET channel (B).

After these images were used with Pix-FRET to normalize bleed-throughs, images taken from double-transfected cells with all three of the tracks were used to calculate FRET efficiencies. The program computes FRET by analyzing the images pixel by pixel in these three channel settings and after calculation of FRET efficiencies, images can be artificially colored to represent localization and efficiency of FRET in live cells (see Figure 3.11 and 3.12). The images representing FRET efficiency (labeled as E) were colored based on five different colors, each indicating a specific range of FRET efficiency. As defined on the calibration bars of these images, blue pixels, green pixels, yellow pixels, red pixels and gray pixels represent the intervals of 1-10, 10-20, 20-30, 30-40 and 40-50 % FRET efficiencies, respectively.

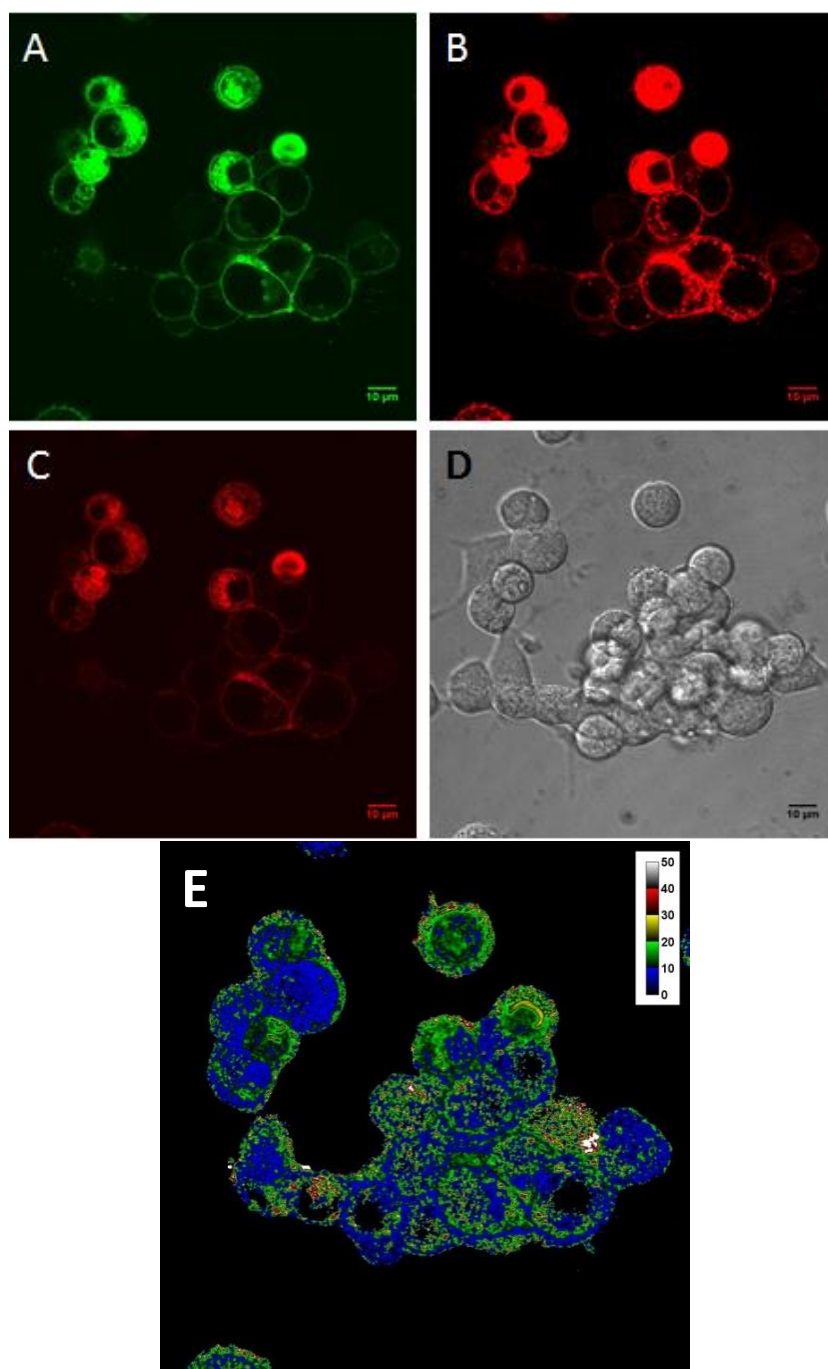


Figure 3.11 Representative images (#1) of N2a cells transfected with A_{2A}R+EGFP and A_{2A}R+mCherry. Images were taken from Track 2-EGFP channel (A), Track 3-mCherry channel (B), Track 1-FRET channel (C) and Channel D-bright field (D). Image (E) shows pixels where FRET occurs.

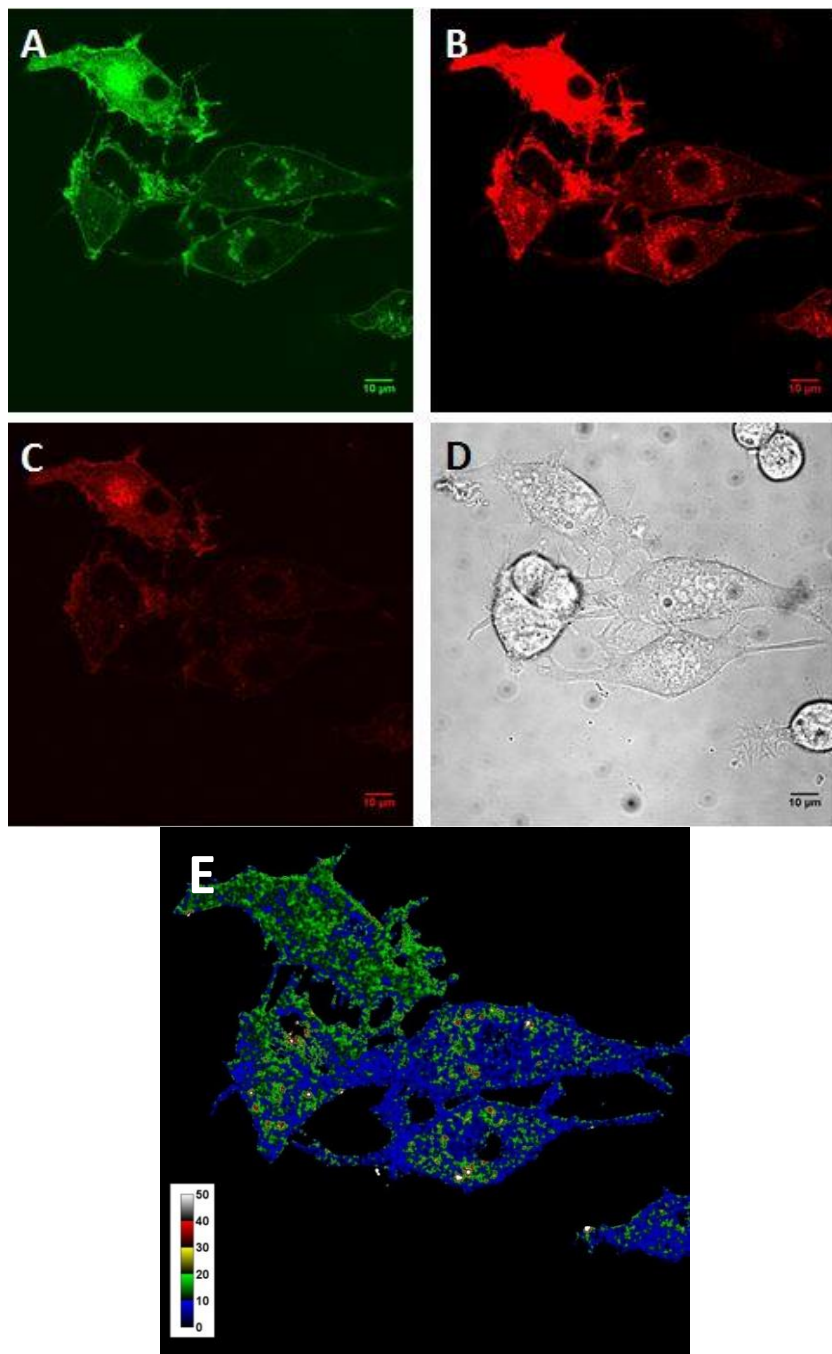


Figure 3.12 Representative images (#2) of N2a cells transfected with $A_{2A}R$ +EGFP and $A_{2A}R$ +mCherry. Images were taken from Track 2-EGFP channel (A), Track 3-mCherry channel (B), Track 1-FRET channel (C) and Channel D-bright field (D). Image (E) shows pixels where FRET occurs.

After coloring FRET efficiency images for qualitative analysis, a region of interest was drawn around the cells to obtain a histogram giving the pixel counts and computed FRET efficiencies quantitatively. A representative histogram is given in Figure 3.13.

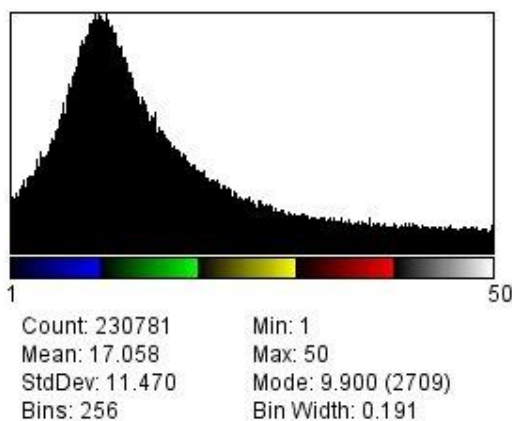


Figure 3.13 Representative histogram image where blue colored zone is in the range between 1-10, green colored zone is in the range between 10-20, yellow colored zone is in the range between 20-30, red colored zone is in the range between 30-40 and gray colored zone is in the range between 40-50.

Histograms of all images were recorded and data is shown in Appendix G.

Additionally, effects of A_{2A}R-agonist, CGS-21680, on the homodimerization of Adenosine A_{2A} receptors were examined. 1 hour before the imaging, cells were treated with 200 nM CGS-21680 and images were captured in similar ways, to analyze FRET efficiencies. Bleed-through images were similarly used to eliminate background signal and FRET efficiencies in live N2a cells were represented both qualitatively (see Figure 3.14) and quantitatively. Histograms of all images taken from treated cells were also recorded and shown in Appendix G.

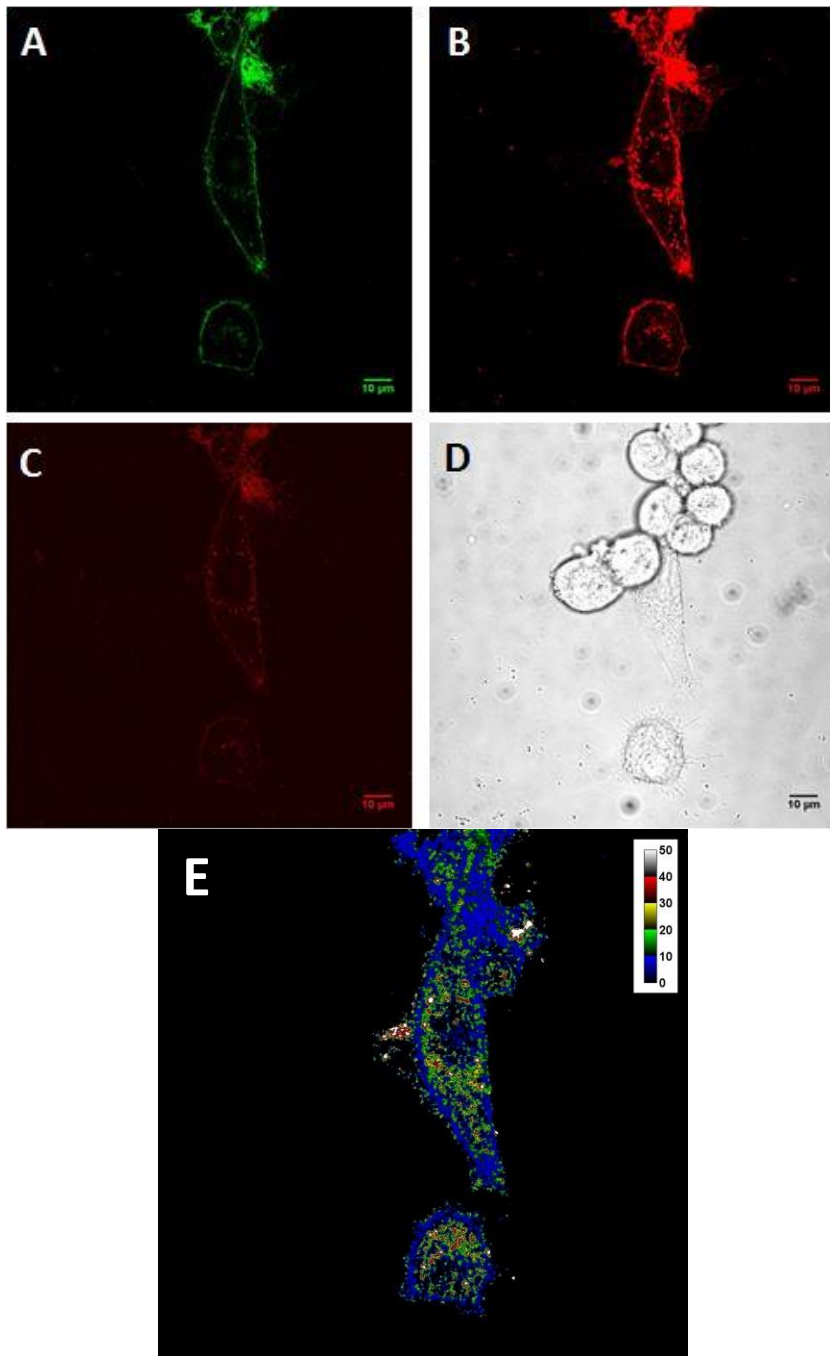


Figure 3.14 Representative images of N2a cells transfected with $A_{2A}R$ +EGFP and $A_{2A}R$ +mCherry; and treated with CGS-21680. Images were taken from Track 2-EGFP channel (A), Track 3-mCherry channel (B), Track 1-FRET channel (C) and Channel D-bright field (D). Image (E) shows pixels where FRET occurs.

After 20 images for each treated and untreated cells were analyzed by PixFRET to determine FRET efficiencies, mean of total efficiencies were calculated and it is found that untreated cells gave 14.542 % FRET efficiency for A_{2A}R dimerizations, while treated cells gave 14.179 % efficiency for FRET. Detections of FRET were then used to quantify the distance between donor and acceptor molecules by use of the formula, $E = R_0^6 / (R_0^6 + r^6)$, where E stands for FRET efficiency, r for distance between fluorophores and R₀ for Förster distance. R₀ is a standard value for a specific FRET pair which is 5.1 nm for EGFP-mCherry. By inserting R₀ and FRET efficiency values to their places in the formula, real distance between fluorophores could be calculated. According to this formula, average distance between EGFP and mCherry which are fused to interacting A_{2A} receptors is 6.85 nm in untreated cells, whereas 6.89 nm in treated cells.

Moreover, in order to conclude about the effects of using 200 nM agonist CGS-21680 on homodimerization of adenosine receptors, student's t-test was applied to compare FRET efficiencies of treated and untreated cells. It has been detected that use of CGS-21680 did not significantly change the distances between donor and acceptor molecules (Figure 3.15).

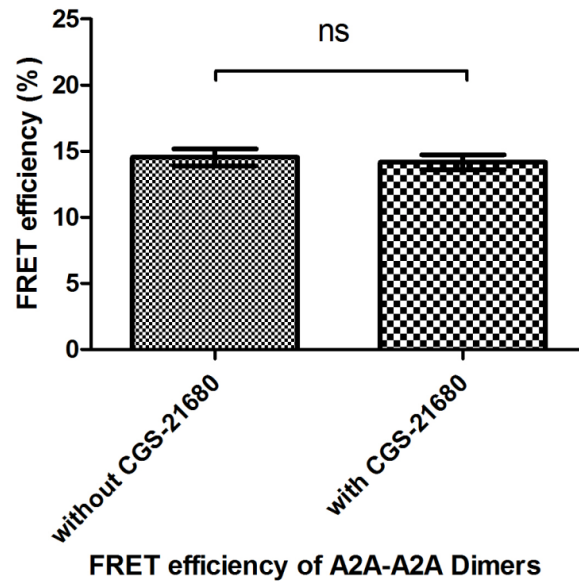


Figure 3.15 Graph of student's t-test results expressing effects of use of agonist CGS-21680 on homodimerization of Adenosine A_{2A} receptors. Mean of FRET efficiency for untreated cells is 14.542 %, while it is 14.179 % for treated cells. Their t-test results were not different from each other with p value < 0.05.

In addition to total means, specific ranges of FRET efficiencies were also compared between treated and untreated cells. For every efficiency ranges (1-10%, 10-20%, 20-30%, 30-40% and 40-50%), histograms were taken separately; so that pixel counts of every range was recorded. By comparing with the total pixel count giving FRET, the percentage of every range in the cells was detected. Average distributions of efficiency ranges based on pixel count in treated and untreated cells are displayed in Figure 3.16.

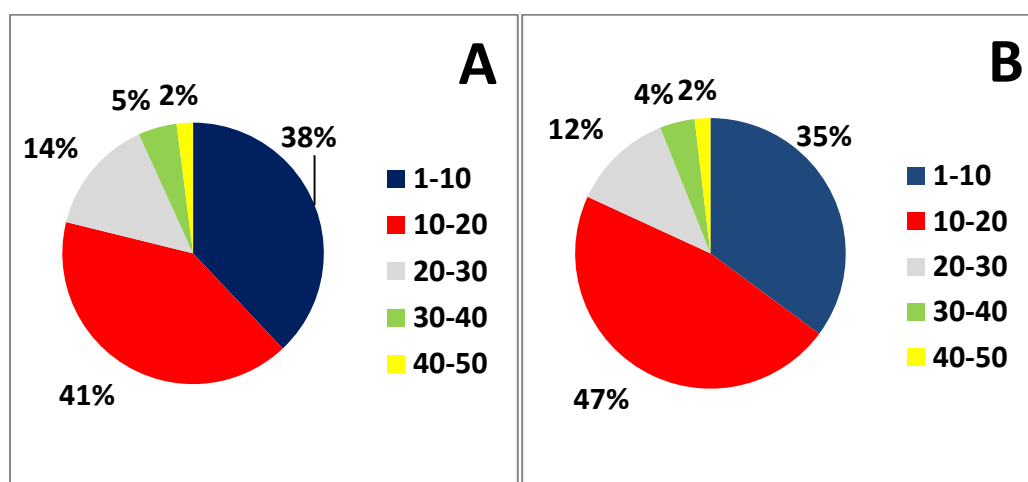


Figure 3.16 Mean distributions of efficiency ranges in N2a cells transfected with $A_{2A}R+EGFP$ and $A_{2A}R+mCherry$ genes. A) untreated ; B) treated with CGS-21680.

Consequently, homodimerization of $A_{2A}R$ s has been shown by using both BiFC and FRET assays in this study. BiFC assay results suggested that $A_{2A}R$ homodimers are densely formed on the plasma membrane; however, according to FRET results, this dimerization occurs also in the intracellular regions. Indeed, most of the cells gave higher FRET efficiencies in their intracellular regions compared to membrane. The intracellular FRET signals may come from ER and Golgi apparatus where the membrane proteins are concentrated during their synthesis and trafficking. In other words, Adenosine A_{2A} receptors may form homodimers early in ER and/or Golgi, and then these homodimers may be carried to the plasma membrane within intracellular vesicles. To comment on the story of dimerization, this hypothesis should be tested by using organelle markers in future studies. Moreover, relatively lower FRET signals coming from the membrane might be caused by interactions with other proteins, especially G proteins. On the membrane, functional $A_{2A}R$ -homodimer interacts with G_s proteins and this interaction may lead to critical conformational changes on receptor dimers, making fluorescent proteins fused to the receptors become distant from each other.

Previous studies suggested that activation of A_{2A}R by an agonist do not influence the degree of receptor homo/hetero-dimerization (Canals *et al.*, 2004; Kamiya *et al.*, 2003). In this study, we also couldn't detect a significant effect of A_{2A}R agonist, CGS-21680, on the homodimerization of receptors by means of average FRET efficiency values and distribution of different ranges of FRET signal in the cells.

3.2.3 Homodimerization of Dopamine D₂ Receptors

To study homodimerization of Dopamine D₂ receptors, 500 ng of pcDNA 3.1(-) _ D₂R + EGFP and pcDNA 3.1(-) _ D₂R + mCherry plasmids were co-transfected to N2a cells using Lipofectamine LTX and Plus reagents. 40-48 hours after transfection, the cells were imaged under laser scanning confocal microscope. For FRET analysis with PixFRET, bleed-through experiments and FRET sets were prepared in a similar way described in part 3.2.2.

To calculate donor bleed-through coming from EGFP, N2a cells transfected only with EGFP tagged D₂ receptors were observed with Track 1 and Track 2 configurations (see Figure 3.17); while cells transfected only with mCherry tagged D₂ receptors were observed with Track 1 and Track 3 to estimate acceptor bleed-through coming from mCherry (see Figure 3.18).

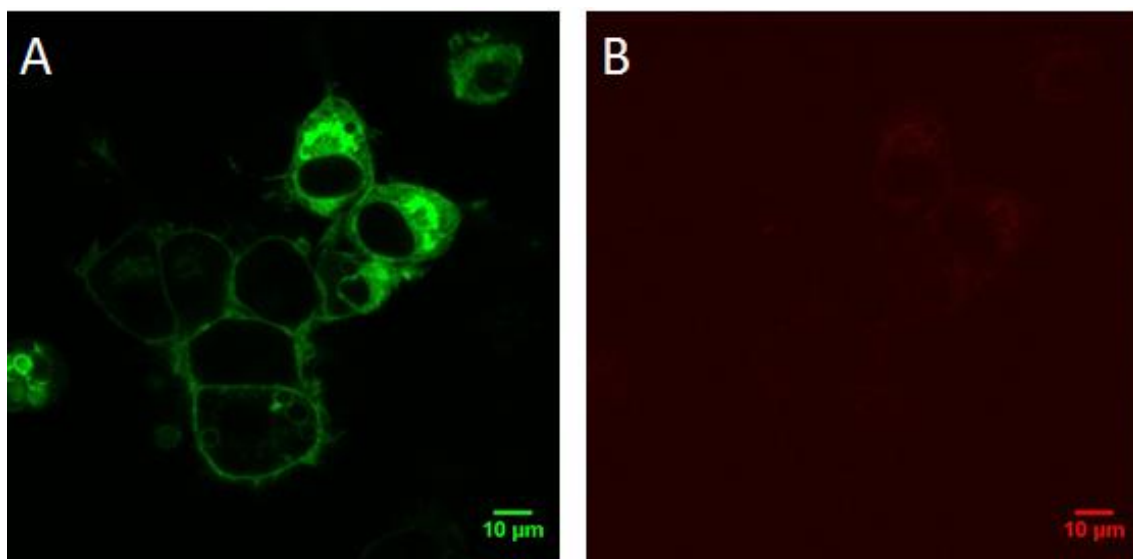


Figure 3.17 N2a cells transfected only with D₂R + EGFP. Images were taken from Track 2-EGFP channel (A) and Track 1-FRET channel (B).

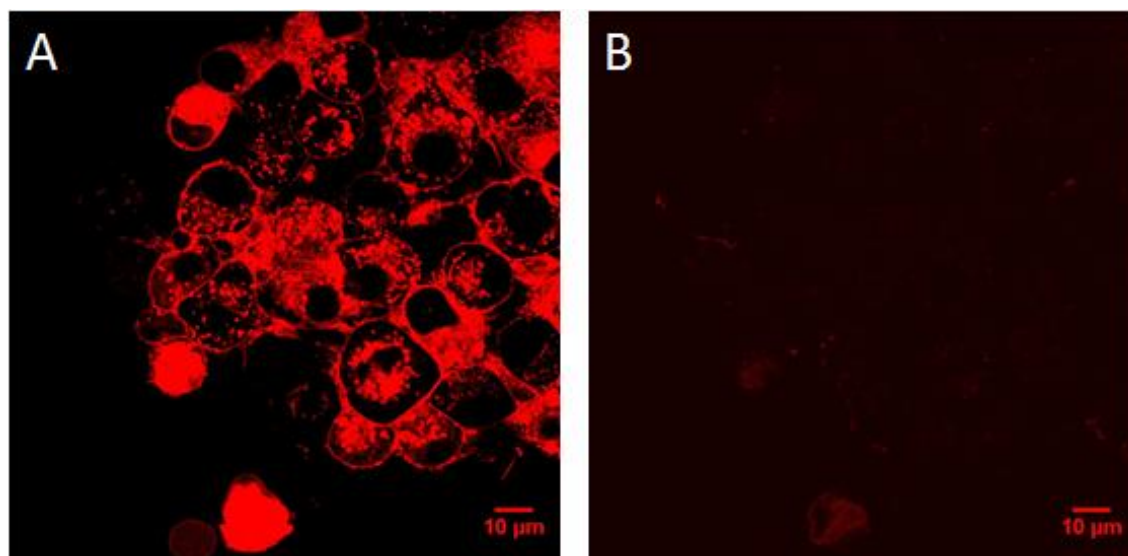


Figure 3.18 N2a cells transfected only with D₂R + mCherry. Images were taken from Track 3-mCherry channel (A) and Track 1-FRET channel (B).

These bleed-through images were used with PixFRET to eliminate background noise in FRET calculations. Afterwards, images taken from double-transfected cells with all three tracks were analyzed by using PixFRET and FRET efficiencies were detected. Sample microscopic images obtained to study this homodimerization and their artificially colored FRET efficiency images are given in Figure 3.19 and 3.20. As indicated in the calibration bars of images (E), blue pixels, green pixels, yellow pixels, red pixels and gray pixels represent the intervals of 1-6, 6-12, 12-18, 18-24 and 24-30 % FRET efficiencies, respectively.

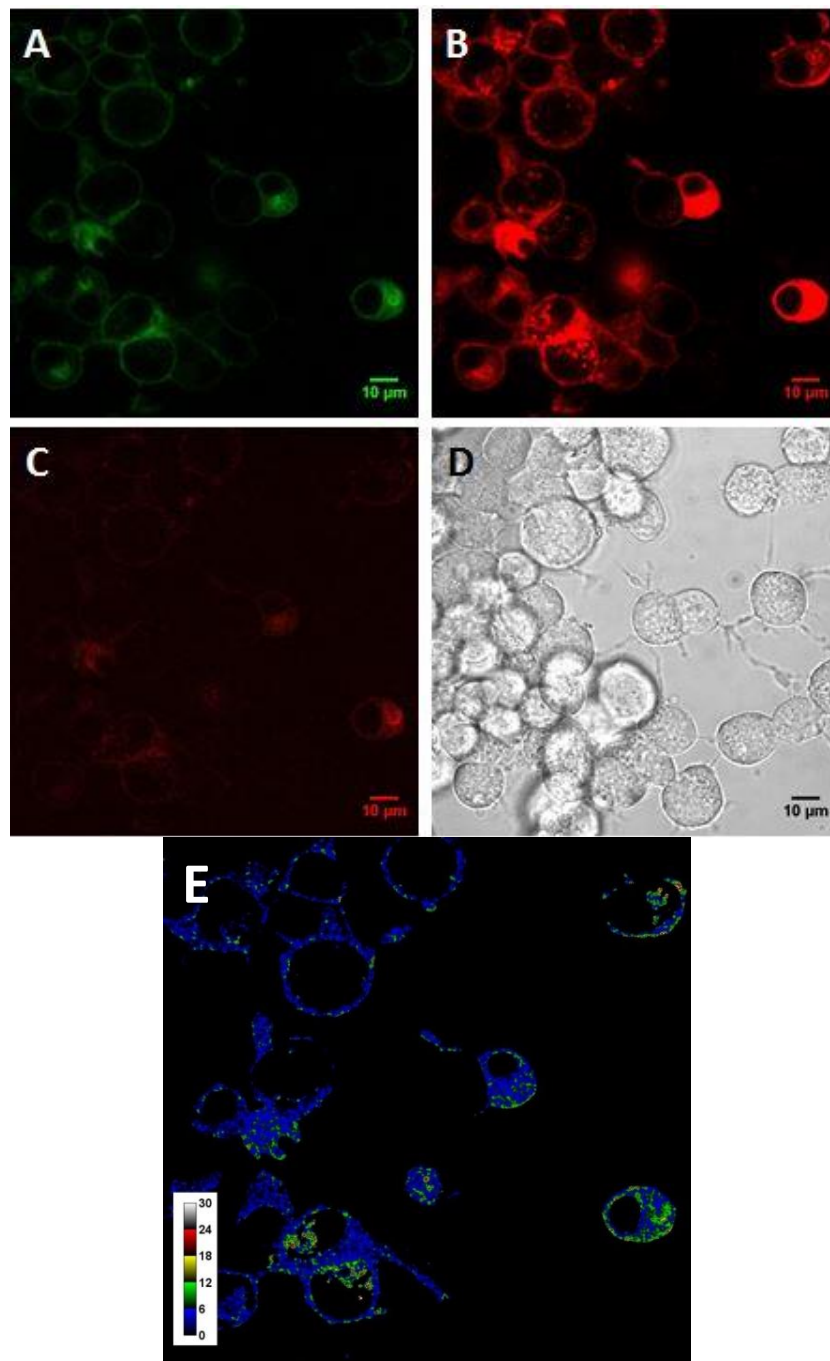


Figure 3.19 Representative images (#1) of N2a cells transfected with D₂R+EGFP and D₂R+mCherry. Images were taken from Track 2-EGFP channel (A), Track 3-mCherry channel (B), Track 1-FRET channel (C) and Channel D-bright field (D). Image (E) shows pixels where FRET occurs.

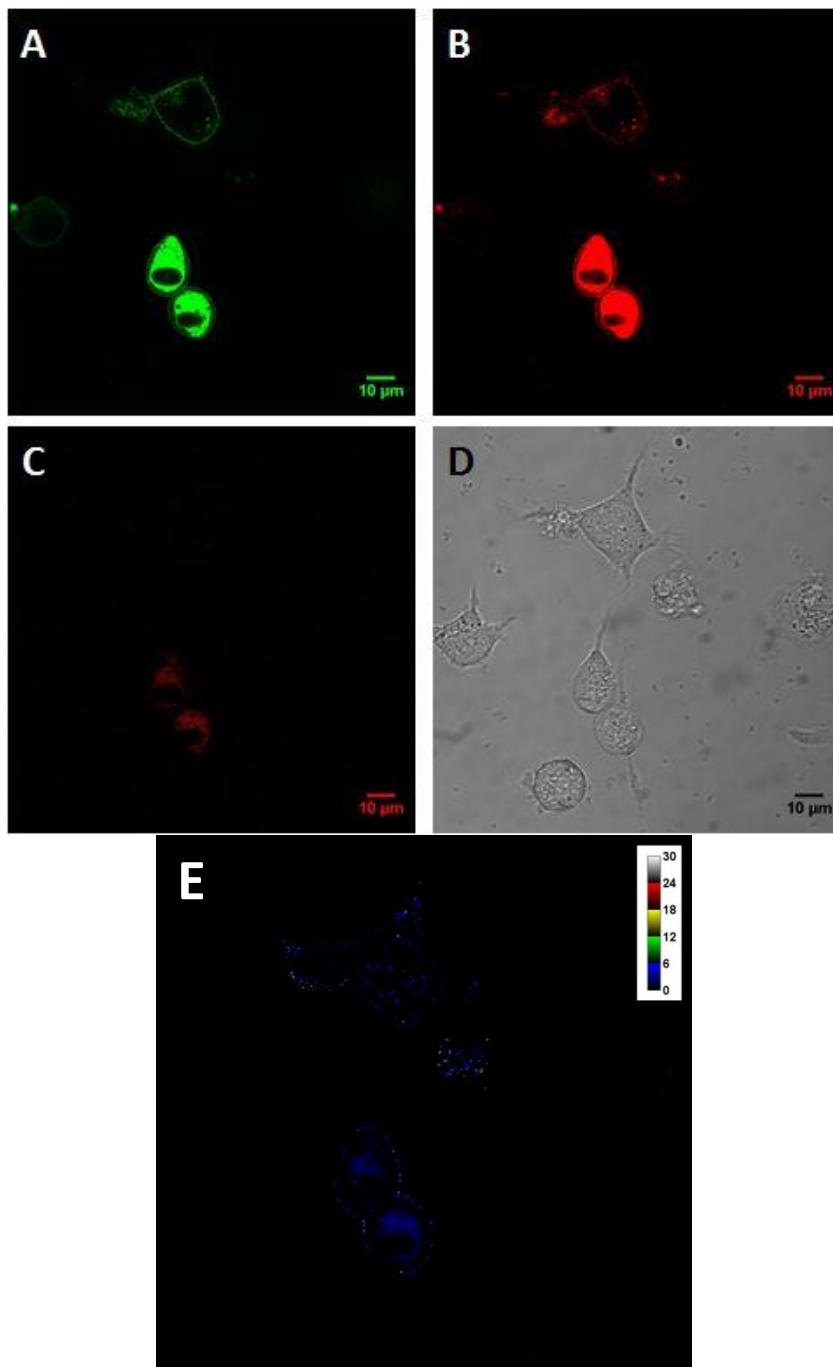


Figure 3.20 Representative images (#2) of N2a cells transfected with D₂R+EGFP and D₂R+mCherry. Images were taken from Track 2-EGFP channel (A), Track 3-mCherry channel (B), Track 1-FRET channel (C) and Channel D-bright field (D). Image (E) shows pixels where FRET occurs.

After mapping FRET efficiency images to see localization of FRET within cells, a region of interest was drawn around the cells to obtain histograms giving the pixel counts and quantitative values of FRET efficiencies. Recorded data from histograms is given in Appendix G.

Moreover, effects of D₂R-agonist, quinpirole, on the dimerization of Dopamine D₂ receptors were studied. 1 hour before the imaging, cells were treated with 10 μ M quinpirole. Single-plasmid transfected experiments were analyzed similarly to calculate bleed-throughs. At the end, PixFRET gave the representative images to demonstrate FRET efficiency distributions within the cells (see Figure 3.21). Histograms of all images taken from treated cells were also recorded and data is shown in Appendix G.

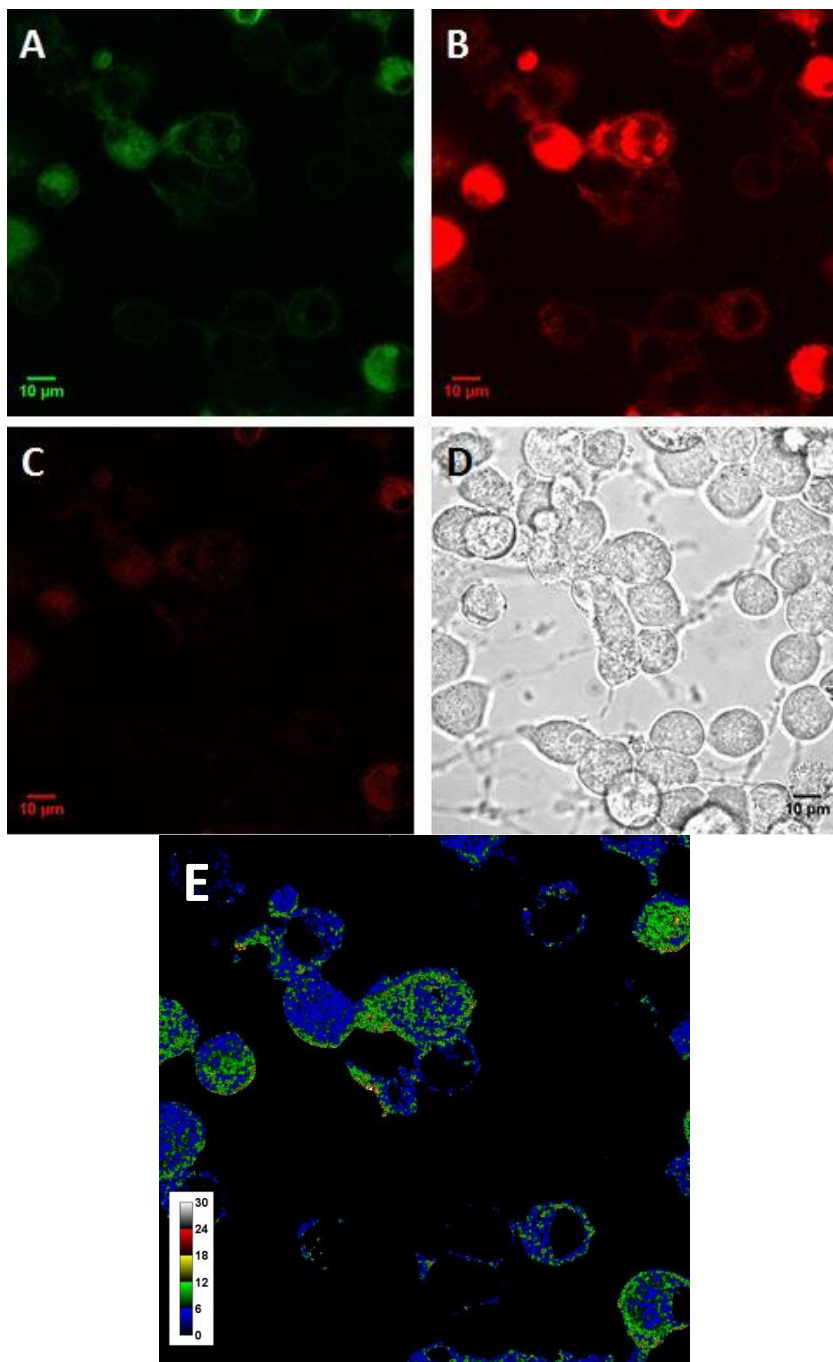


Figure 3.21 Representative images of N2a cells transfected with D₂R+EGFP and D₂R+mCherry; and treated with quinpirole. Images were taken from Track 2-EGFP channel (A), Track 3-mCherry channel (B), Track 1-FRET channel (C) and Channel D-bright field (D). Image (E) shows pixels where FRET occurs.

After 20 images for each treated and untreated cells were analyzed by PixFRET to determine FRET efficiencies, mean of total efficiencies were calculated and it is found that untreated cells gave 5.432 % FRET efficiency for D₂R dimerizations, while treated cells gave 6.036 % efficiency for FRET. Then, real distance between fluorophores was calculated from the formula, $E = R_0^6 / (R_0^6 + r^6)$, by using quantified FRET efficiency values. It is found that average distance between EGFP and mCherry which are fused to interacting D₂ receptors is 8.21 nm in untreated cells, whereas 8.06 nm in treated cells.

Furthermore, student's t-test was applied to compare FRET efficiencies of treated and untreated cells under the investigation of D₂R dimerization. It has been detected that use of 10 μM quinpirole did not significantly affect the distances between donor and acceptor molecules (Figure 3.22).

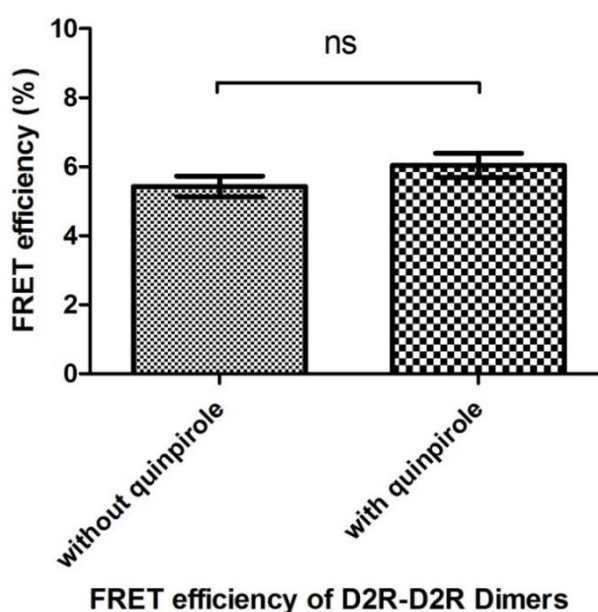


Figure 3.22 Graph of student's t-test results expressing effects of use of agonist quinpirole on homodimerization of Dopamine D₂ receptors. Mean of FRET efficiency for untreated cells is 5.43 %, while it is 6.04 % for treated cells. Their t-test results were not different from each other with p value < 0.05.

Specific ranges of FRET efficiencies were also compared between treated and untreated cells. For every efficiency ranges (1-6 %, 6-12 %, 12-18 %, 18-24 % and 24-30 %), histograms were taken separately and the percentage of every range in the cells was detected. Average distributions of efficiency ranges based on pixel count in treated and untreated cells are displayed in Figure 3.23.

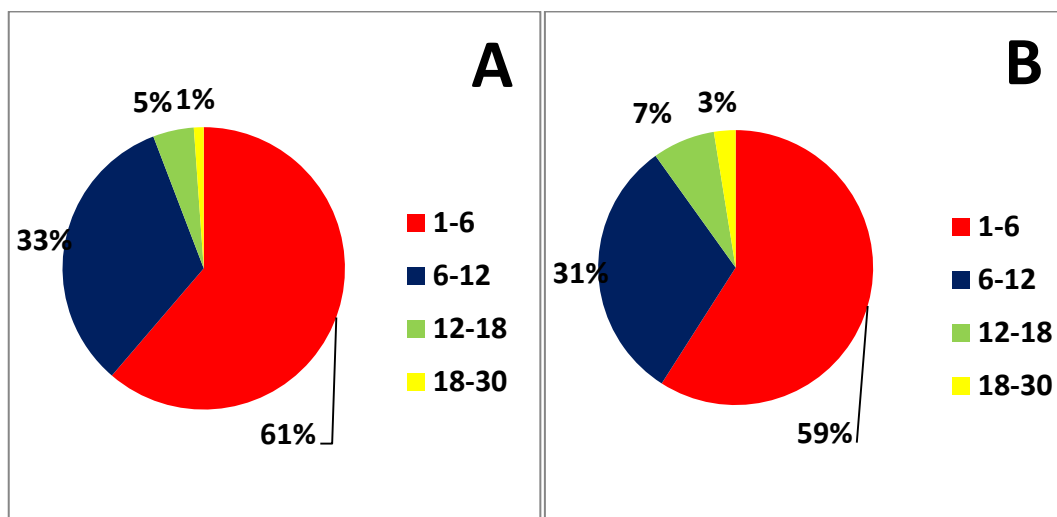


Figure 3.23 Mean distributions of efficiency ranges in N2a cells co-transfected with D₂R+EGFP and D₂R +mCherry genes. A) untreated ; B) treated with quinpirole.

Consequently, much weaker signals were detected from the homodimerization of D₂ receptors, compared to A_{2A}R homodimers. First of all, BiFC assay results have shown that Dopamine D₂ receptors are seen to dimerize in intracellular parts of the cells and reassembly signals were very weak. Secondly, FRET data suggested that homodimerization between D₂Rs occurs on the plasma membrane but stronger signals were collected from intracellular regions. The intracellular FRET signals might be due to the D₂R-D₂R dimer formations early in ER and or Golgi, similar to the hypothesis of A_{2A}R dimer formation. As described in 3.2.2, interaction with other membrane proteins; such as G_i protein, may affect the distance between fluorophores fused to interacting receptors; thus weaker FRET signal might be observed on the

cell surface. Moreover, a study has shown that D₂Rs are mostly found intracellularly, since they are usually retained in the ER (Prou *et al.*, 2001). There are some hypotheses about the intracellular retention of these receptors. First of all, imperfect folding of the receptor fused to a different protein may cause some defects in posttranslational modifications, such as glycosylation. Such defects may promote a fast retrieval of the receptors from the intermediate compartment of Golgi complex (Gahmberg & Tolvanen, 1996). Secondly, there may be a constitutive endocytosis of these receptors resulting in the accumulation of receptors inside the cells (Vickery & von Zastrow, 1999). Alternatively, a molecular partner that may be required for the maintenance of the receptor at the plasma membrane may be lacking in cell cultures used in the experiments (Prou *et al.*, 2001).

Nonetheless, the FRET efficiency was quite low both on the membrane and in the intracellular compartments to conclude about the homodimerization of D₂Rs. Orientation of acceptor and donor molecules might not be proper upon dimerization of receptors; thus we might not observe sufficient FRET signal. Thus, labeling D₂R from its different position; such as N-terminal or a proper site within C-tail, could provide higher FRET signals to detect homodimerization. On the other side, insertion of fluorescent protein might affect proper folding of the receptor; thus D₂R-homodimerization might be destroyed due to such structural alterations.

Although some studies have suggested that Dopamine D₂ dimerization in the plasma membrane is significantly increased by the stimulation with specific agonists (Dziedzicka-Wasylewska *et al.*, 2006), other studies have shown that formation of D₂R oligomers is not affected by treatment with agonist (Canals *et al.*, 2003). In this study, we also couldn't detect a significant effect of D₂R agonist, quinpirole, on the homodimerization of receptors by means of average FRET efficiency values and distribution of different ranges of FRET signal in the cells.

3.2.4 Heterodimerization of Adenosine A_{2A} and Dopamine D₂ Receptors

To investigate heterodimerization of Adenosine A_{2A} and Dopamine D₂ receptors, 500 ng of pcDNA 3.1(-) _ A_{2A}R + EGFP and 500 ng of pcDNA 3.1(-) _ D₂R + mCherry plasmids were co-transfected to N2a cells using Lipofectamine LTX and Plus reagents. 40-48 hours after transfection, the cells were imaged under laser scanning confocal microscope. Three sets of experiments were designed for FRET analysis with PixFRET, as described in part 3.2.2.

To calculate donor and acceptor bleed-throughs, N2a cells transfected only with EGFP tagged A_{2A} receptors were observed with Track 1 and Track 2 configurations (see Figure 3.9); and cells transfected only with mCherry tagged D₂ receptors were observed with Track 1 and Track 3 configurations (see Figure 3.18), respectively. Later on, images taken from double-transfected cells with all three tracks (see Figure 3.24 and 3.25) were analyzed with PixFRET and obtained FRET efficiency images were artificially colored to represent localization of dimerization. As indicated in the calibration bars of images (E), blue pixels, green pixels, yellow pixels, red pixels and gray pixels represent the intervals of 1-10, 10-20, 20-30, 30-40 and 40-50 % FRET efficiencies, respectively.

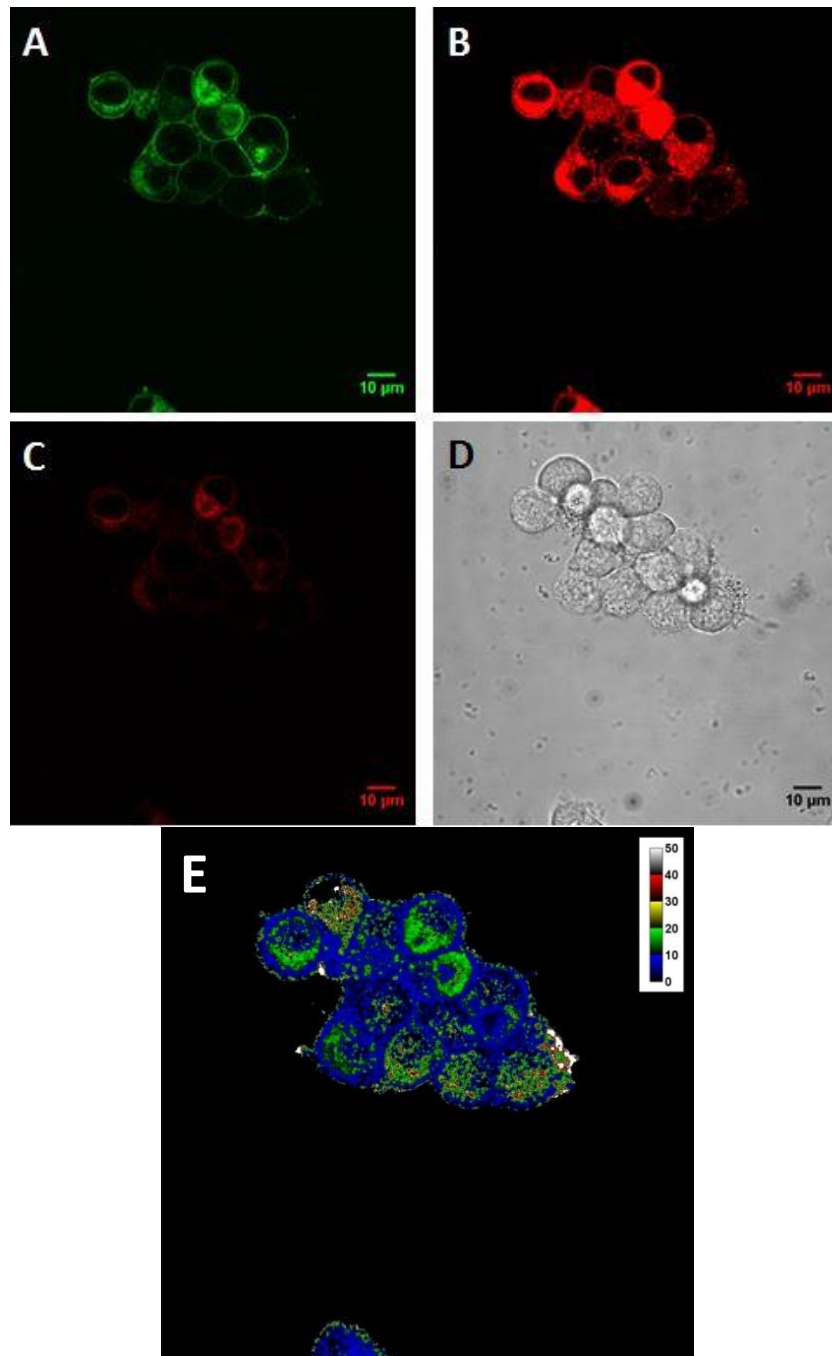


Figure 3.24 Representative images (#1) of N2a cells co-transfected with $A_{2A}R+EGFP$ and $D_2R+mCherry$. Images were taken from Track 2-EGFP channel (A), Track 3-mCherry channel (B), Track 1-FRET channel (C) and Channel D-bright field (D). Image (E) shows pixels where FRET occurs.

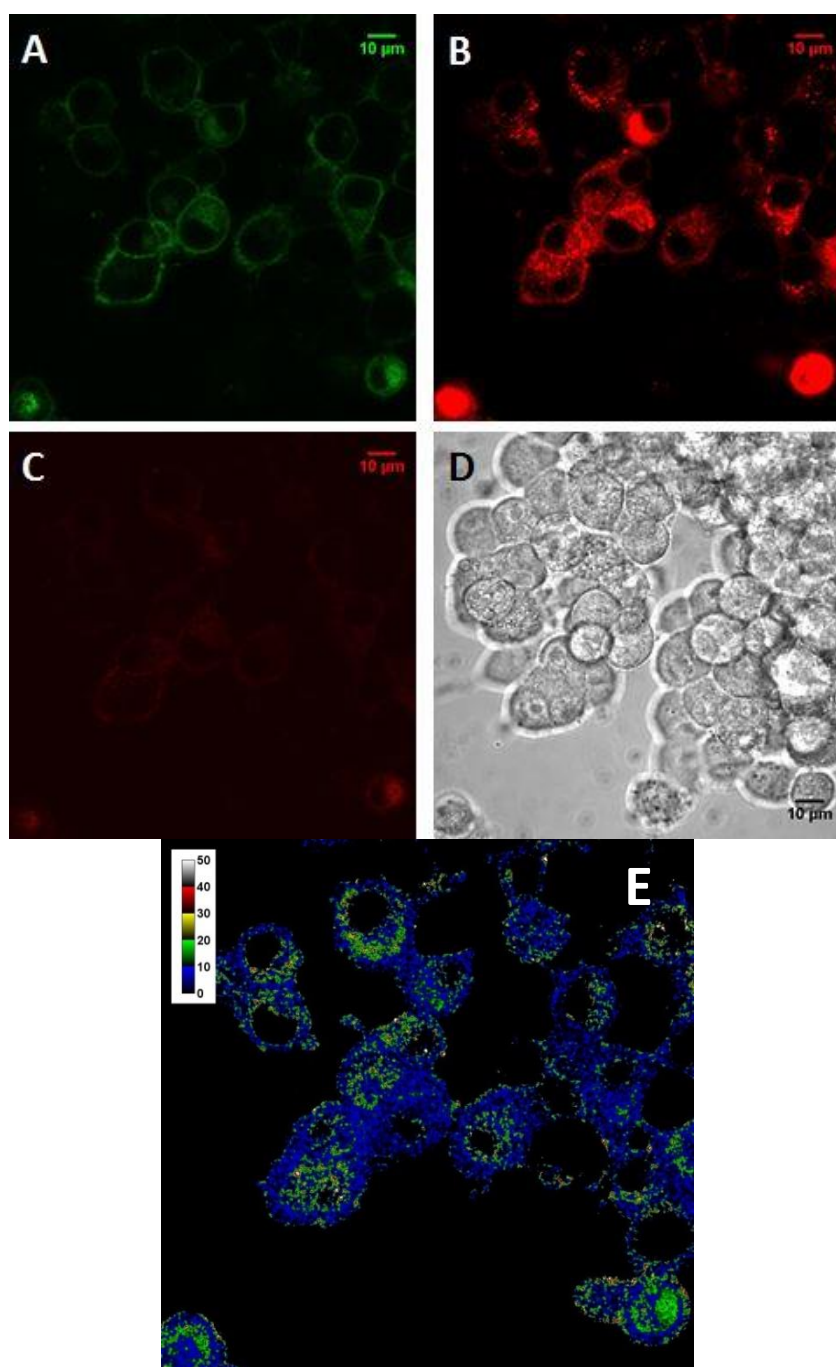


Figure 3.25 Representative images (#2) of N2a cells co-transfected with $A_{2A}R+EGFP$ and $D_2R+mCherry$. Images were taken from Track 2-EGFP channel (A), Track 3-mCherry channel (B), Track 1-FRET channel (C) and Channel D-bright field (D). Image (E) shows pixels where FRET occurs.

After heterodimerizations were detected from FRET images, a region of interest was drawn around the cells to obtain histograms quantifying pixel counts and FRET efficiencies. Recorded data is demonstrated in Appendix G.

Combined actions of A_{2A}R-agonist (CGS-21680) and D₂R-agonist (quinpirole) were also investigated in this study. 1 hour before the imaging, cells were co-treated with 200 nM CGS-21680 and 10 μM quinpirole. After estimating bleed-throughs by use of PixFRET, FRET analysis was performed in a similar manner (see Figure 3.26). Recorded data taken from histograms is given in Appendix G.

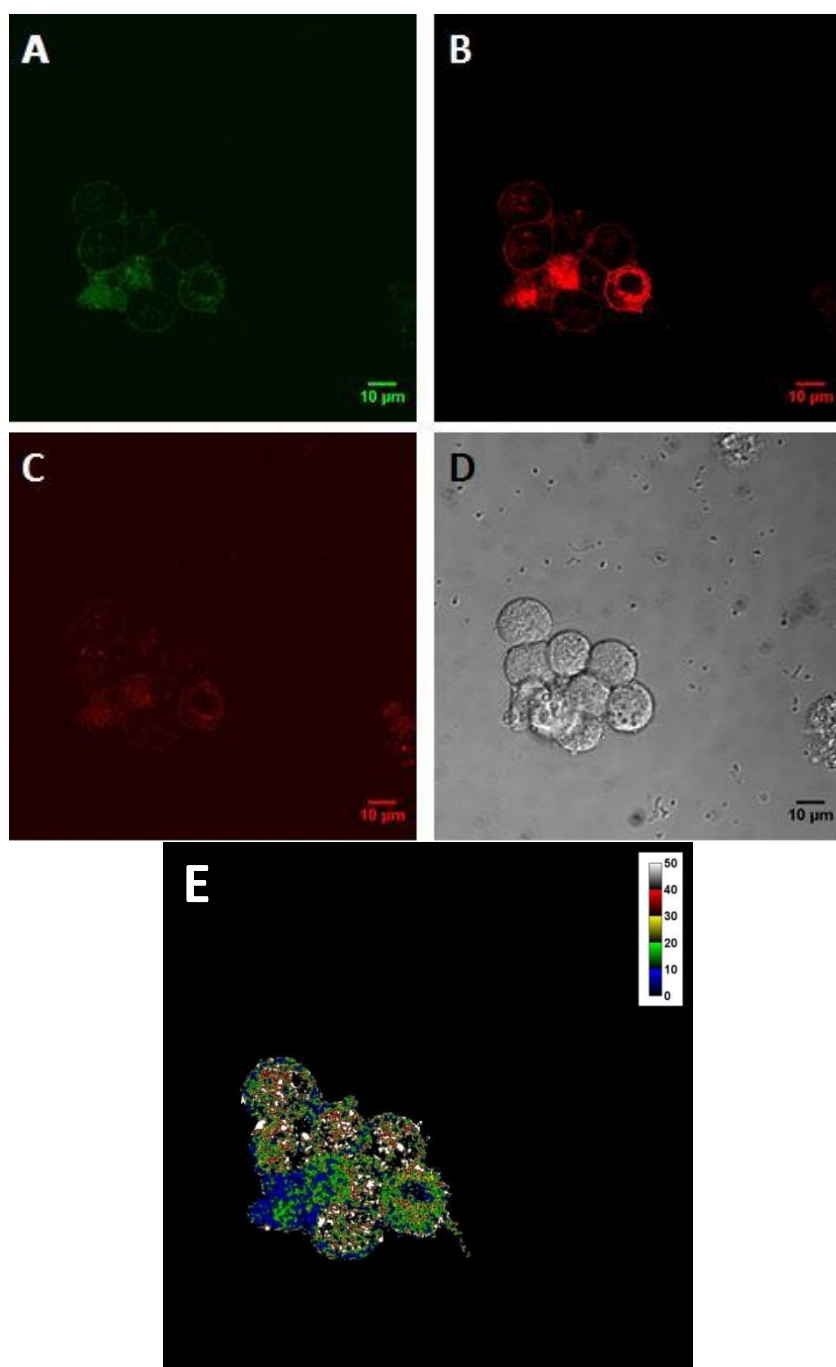


Figure 3.26 Representative images of N2a cells co-transfected with A_{2A}R+EGFP and D₂R+mCherry; and co-treated with CGS-21680 and quinpirole. Images were taken from Track 2-EGFP channel (A), Track 3-mCherry channel (B), Track 1-FRET channel (C) and Channel D-bright field (D). Image (E) shows pixels where FRET occurs.

After 20 images for each treated and untreated cells were analyzed by PixFRET, mean of total efficiencies were calculated and it is found that untreated cells gave 14.91 % FRET efficiency for heterodimerizations, while treated cells gave 16.06 % efficiency for FRET. Next, it is found from the formula, $E = R_0^6 / (R_0^6 + r^6)$, that the average distance between EGFP and mCherry which are fused to interacting receptors is 6.82 nm in untreated cells, whereas 6.72 nm in treated cells.

Moreover, student's t-test was carried out to compare FRET efficiencies of treated and untreated cells under the investigation of A_{2A}R-D₂R interactions. It has been detected that combined use of CGS-21680 and quinpirole did not affect the distances between donor and acceptor molecules significantly (Figure 3.27).

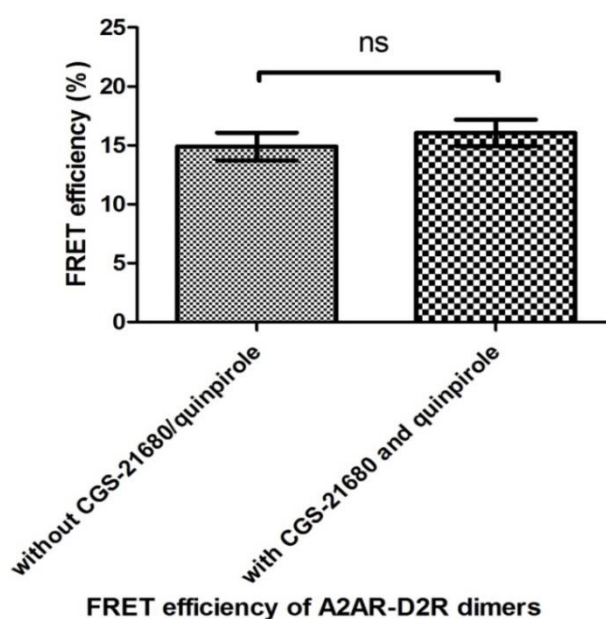


Figure 3.27 Graph of student's t-test results demonstrating combined effects of CGS-21680 and quinpirole on heterodimerization of A_{2A} and D₂ receptors. Mean of FRET efficiency for untreated cells is 14.91 %, while it is 16.06 % for treated cells. Their t-test results were not different from each other with p value < 0.05.

After comparing total means, specific ranges of FRET efficiencies were also analyzed to compare treated and untreated cells. The percentage of every range (1-10 %, 10-20 %, 20-30 %, 30-40 % and 40-50 %) was computed from the histograms obtained for every separate range (See Figure 3.28).

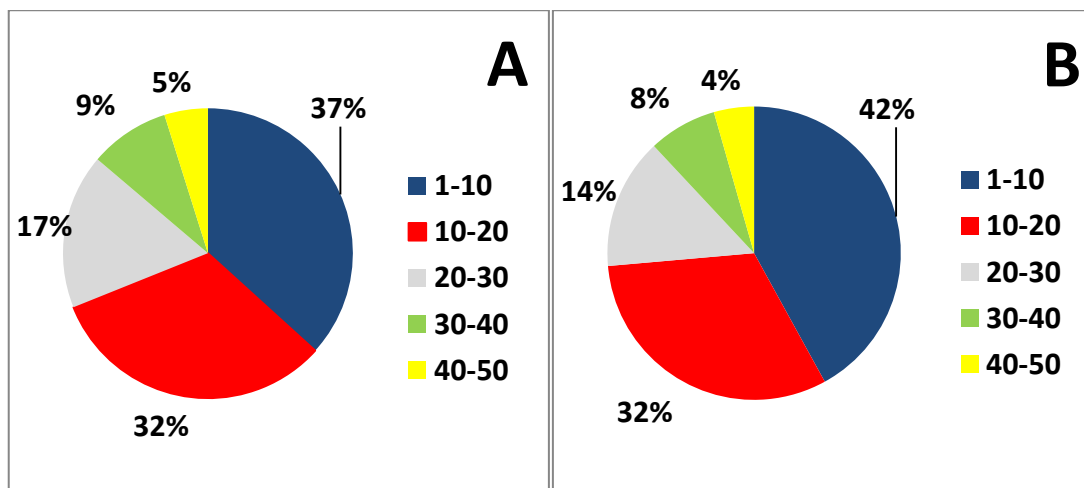


Figure 3.28 Mean distributions of efficiency ranges in N2a cells co-transfected with $A_{2A}R$ +EGFP and D_2R +mCherry genes. A) untreated ; B) co-treated with CGS-21680 and quinpirole.

Although heterodimerization of $A_{2A}R$ and D_2R couldn't be observed using BiFC assay, this dimerization gave signals in FRET experiments. BiFC assay results gave very weak reassembly signals from intracellular compartments for the heterodimerization of $A_{2A}R$ and D_2R . On the other hand, FRET images demonstrated the localization of this dimerization throughout the cell, with stronger efficiencies in intracellular regions. Similar to homodimerizations, heterodimerization between these two receptors may begin early in ER and/or Golgi, and then heterodimers may be carried to the plasma membrane in intracellular vesicles. It would be helpful to work with organelle markers for the detection of formation and trafficking of homo-heterodimers. As mentioned before, relatively lower FRET signals coming from the cell surface might be due to the interaction of dimers with other proteins, especially

G proteins, changing distance between EGFP and mCherry fluorophores. Despite fluorescent proteins were in a close distance on the plasma membrane to give FRET, they might not properly oriented to complement each other upon dimerization. That may be the reason of lack of EGFP signal on the membrane during BiFC experiments. Therefore, labeling receptors, especially D₂Rs, from its different position could solve this problem.

Likewise in the homodimerization studies, activation of both A_{2A}R and D₂R by their agonists also did not significantly change average FRET efficiency and distribution of different FRET signal ranges in this heterodimerization study.

3.3 Detection of physical interactions between Adenosine A_{2A} and NMDA Receptors by use of FRET

cDNA clones of NR1 subunit was obtained in pReceiver vector and for direct expression in N2a cells, NR1-subunit gene was transferred into the mammalian expression vector pcDNA 3.1 (-). NR1 gene was inserted between *NheI* and *NotI* cut sites within the pcDNA 3.1(-) (see Appendix D). After inserting this NMDA subunit into expression vector, the fluorescent protein genes, EGFP and mCherry, were inserted after 870th amino acid of NR1 by use of PCR integration method. All of the details about these tagging studies are demonstrated in a thesis “Comparison of Fluorescent Protein Labelled and Wild Type NMDA Receptor Distribution” by Şeyda Pirinçi.

Since labeled NR1 genes were placed between *NheI* and *NotI* sites within the pcDNA 3.1(-), plasmids containing NR1 subunit fused to fluorescent proteins were digested with corresponding restriction enzymes in order to check for their sizes.

Afterwards, the digested plasmids were run on 1% agarose gel as seen in Figure 3.29.

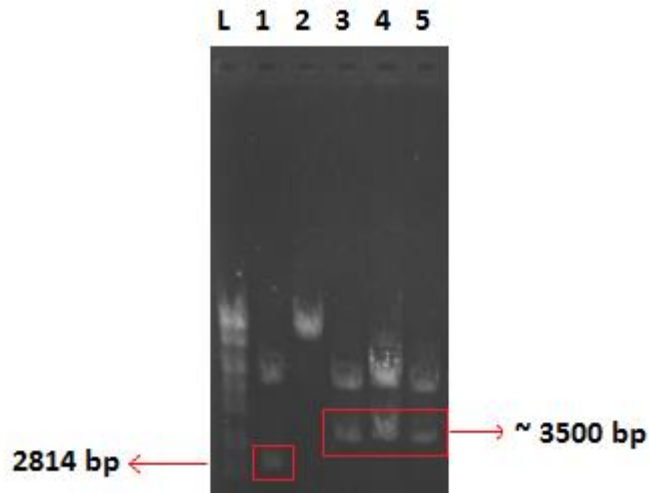


Figure 3.29 Agarose gel electrophoresis image of digested pcDNA 3.1(-) vectors containing NR1 subunit fused to EGFP/mCherry. Fermentas[®] GeneRuler[™] 1 kb plus DNA Ladder was used. The wells were loaded with untagged NR1 (1), NR1-EGFP (2&3), NR1-mCherry (4&5).

As expected after digestion, NR1 subunit genes fused to EGFP or mCherry proteins gave the bands around 700 bp more than their untagged versions, except NR1-EGFP in the well number 2. (NR1 gene is 2814 bp, EGFP gene is 720 bp and mCherry gene is 711bp).

After confirming these pre-prepared constructs in terms of their sizes, N2a cells were co-transfected with 500 ng of pcDNA 3.1(-)_{A_{2A}R}+EGFP, 750 ng of pcDNA 3.1(-)_{NR1}+mCherry and 750 ng of pcDNA 3.1(-)_{NR2B} plasmids in order to study possible physical interactions between Adenosine A_{2A} receptors and NMDA ion channels. Since NR1 subunit cannot leave the ER alone, untagged NR2B subunit was also added to transfection mixture to stimulate NMDA trafficking to the membrane.

40-48 hours after transfection, the cells were imaged under laser scanning confocal microscope.

For bleed-through estimations, images taken from the cells containing only A_{2A}R+EGFP or only A_{2A}R+mCherry were used by PixFRET (see Figure 3.9 and 3.10). Later on, images taken from triple-transfected cells with all three of the tracks (see Figure 3.30 and 3.31) were used to detect FRET efficiencies. Obtained images representing FRET efficiencies were artificially colored (images E) based on five different colors, each indicating a specific range of FRET efficiency. As defined on the calibration bars of these images, blue pixels, green pixels, yellow pixels, red pixels and gray pixels represent the intervals of 1-6, 6-12, 12-18, 18-24 and 24-30 % FRET efficiencies, respectively.

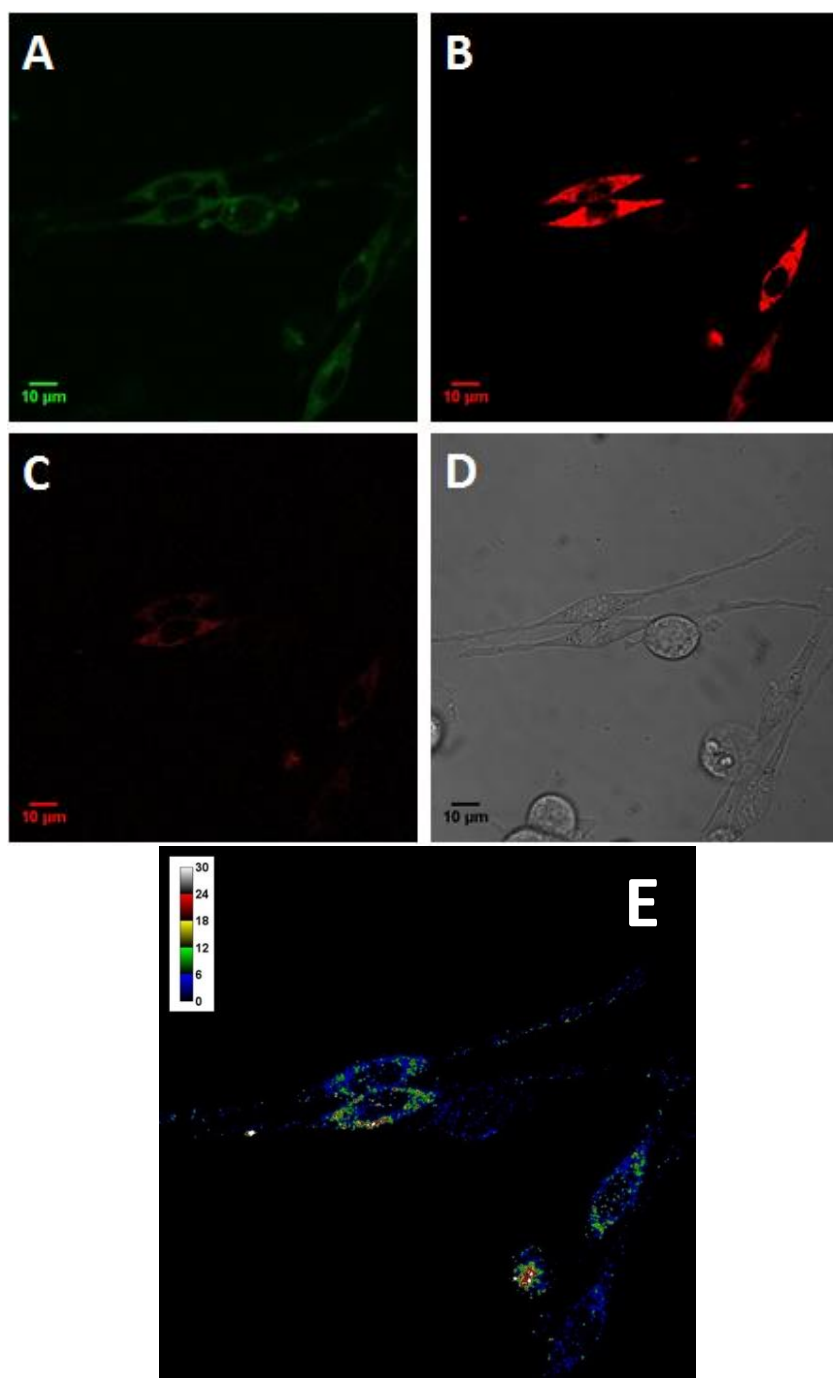


Figure 3.30 Representative images (#1) of N2a cells transfected with $A_{2A}R+EGFP$, NR1+mCherry and NR2B. Images were taken from Track 2-EGFP channel (A), Track 3-mCherry channel (B), Track 1-FRET channel (C) and Channel D-bright field (D). Image (E) shows pixels where FRET occurs.

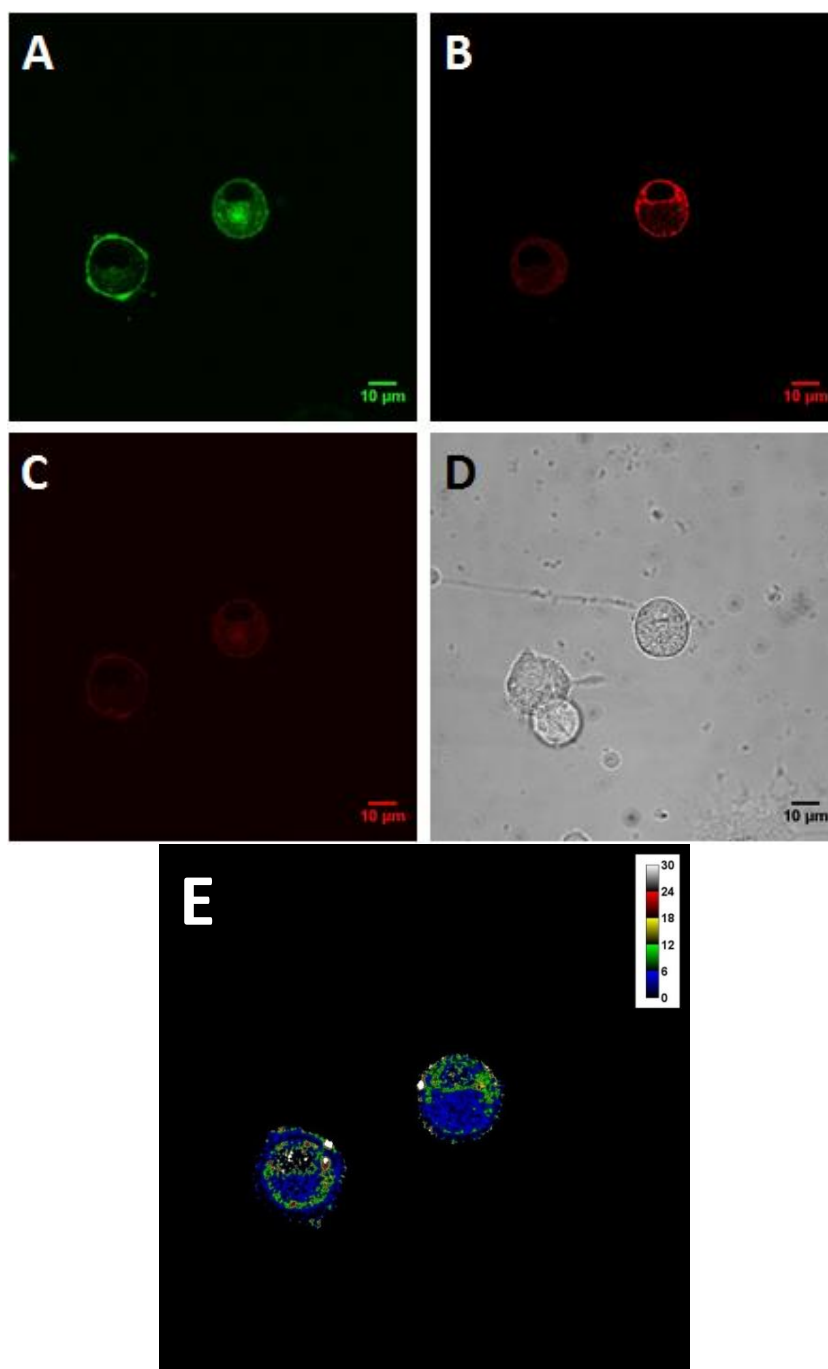


Figure 3.31 Representative images (#2) of N2a cells transfected with A_{2A}R+EGFP, NR1+mCherry and NR2B. Images were taken from Track 2-EGFP channel (A), Track 3-mCherry channel (B), Track 1-FRET channel (C) and Channel D-bright field (D). Image (E) shows pixels where FRET occurs.

After coloring FRET efficiency images to see localization of FRET within cells, a region of interest was drawn around the cells to obtain histograms giving the pixel counts and quantitative values of FRET efficiencies. Recorded data from histograms is given in Appendix G.

After 20 images of N2a cells were analyzed by PixFRET, mean of total FRET efficiency was calculated as 8.295 % for A_{2A}R-NR1 heterodimerization. Next, average distance between EGFP and mCherry which are fused to interacting receptors was calculated from the formula, $E = R_0^6 / (R_0^6 + r^6)$, as 7.61 nm.

For every FRET efficiency ranges (1-6 %, 6-12 %, 12-18 %, 18-24 % and 24-30 %), histograms were taken separately and average distribution of different ranges within cells was shown in Figure 3.32.

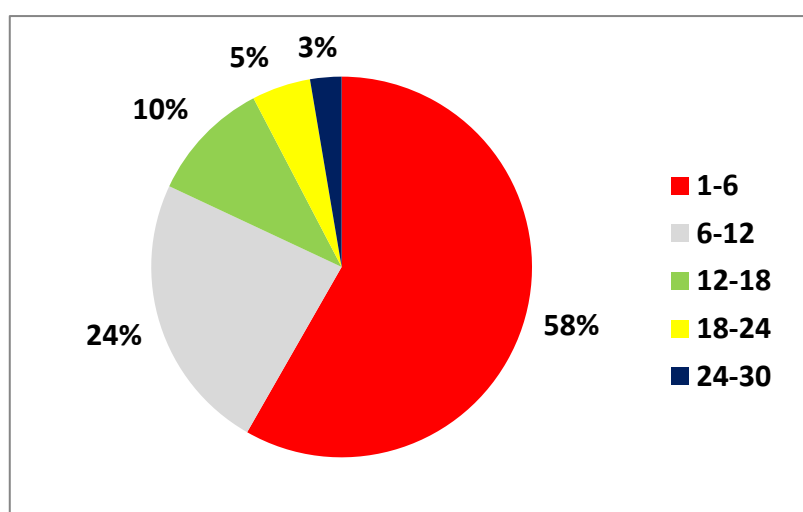


Figure 3.32 Mean distributions of efficiency ranges in N2a cells transfected with A_{2A}R+EGFP, NR1+mCherry and NR2B genes.

In this study, interaction of A_{2A}R with NMDAR has been shown with 8.30 % FRET efficiency on average, which is less than that of A_{2A}R homodimerization or heterodimerization with D₂Rs. NMDA channels are large tetrameric membrane proteins, thus their interaction with other membrane proteins may be more complex, keeping fused fluorescent tags apart from each other. Additionally, intracellular compartments gave a little bit higher FRET signal compared to cell surface. That may be another example to early dimerizations of A_{2A}Rs in the ER and/or Golgi complex. Moreover, studying heterodimerization of A_{2A}R and NMDAR has an important drawback, too. In order to induce membrane-trafficking of functional NMDA channels, plasmids containing untagged NR2B subunit genes were also transfected to N2a cells, in addition to labelled NR1 subunits. In other words, it was difficult to control the insertion and expression of three different plasmids, containing A_{2A}R+EGFP, NR1-mCherry and NR2B, within the same cell.

CHAPTER 4

CONCLUSION

The aim of the study was to express fluorescently labelled Adenosine A_{2A}, Dopamine D₂ and NMDA receptors in live N2a mouse neuroblastoma cell line and detect homo- and/or hetero-dimerizations between these receptors by using Bimolecular Fluorescence Complementation (BiFC) and Fluorescent Resonance Energy Transfer (FRET) assays.

As a result, A_{2A}R and D₂R were successfully labeled with split-EGFP fragments from their C-termini and the receptors fused to complementary split-EGFP partners (both N- and C-EGFP) were co-transfected into N2a cells to detect dimerizations. By this way, homodimerization of Adenosine A_{2A} receptors has been detected mostly on the plasma membrane of live cells; whereas only some fragmentary intracellular signals with very low intensity have been observed in homo- and heterodimerization studies of Dopamine D₂ receptors.

To consolidate results obtained from BiFC studies, possible dimerizations were also studied with FRET method. At the end of study, dimerizations of A_{2A}R with each other and D₂R have been observed and quantified in live N2a cells. However, quantified FRET efficiency was quite low throughout the cells transfected with labelled D₂Rs to study their homodimer formations. In general, all dimerization studies gave higher FRET efficiencies in the intracellular compartments; thus formation and trafficking of these dimers should be tested by using organelle markers in future studies.

Using FRET method, A_{2A}R and D₂R agonists were tested to observe if they have any stimulatory or adverse effects on dimerization; however no significant effect was detected on observed dimerizations concluded from mean FRET efficiencies, while the distribution of FRET efficiencies had different distribution indicating the closeness of the receptors might be effected by the drug applications. Further studies are needed to identify the nature of this change. Additionally, possible neuropsychiatric drugs or dopamine and adenosine antagonists can be tested to study their probable effects on dimerizations in future studies.

Furthermore, interaction of A_{2A}R with NMDAR has been shown using FRET method for the first time in this study. At the present state of the study it is possible to combine BiFC and FRET techniques to study triple interaction comprising A_{2A}R, D₂R and NMDARs in a single complex. With the optimization of combining these two methods, possible homo- or heterooligomeric protein complexes composed of these receptors can be monitored to understand mechanisms of these interactions.

In further studies, three crucial experiments should be conducted to validate our fluorescence-based protein-protein interaction studies. Firstly, fluorescently labelled receptors should be tested for their functionalities on the plasma membrane. We hypothesized that A_{2A}R, D₂R and NMDARs function as dimers on the membrane; thus we should show that fluorescently labelled receptors are as functional as wild type ones. In a previous study, it has been shown that C-terminally tagged A_{2A} and D₂ receptors are as functional as wild type ones. Additionally, labelled NMDA receptors should be checked for their functionalities in a further study. Secondly, an experimental set should be prepared as negative control to confirm our FRET analysis. For this purpose, another GPCR, namely the human GABAB1b receptor, may be tagged fluorescently to be used as negative control. Since it is known that this receptor do not dimerize with A_{2A}R (Gandia *et al.*, 2008b), we will not able to detect FRET signal from co-expression of these two receptors. Finally, a recent study using computational structural analysis has emphasized the roles of helix 1 in A_{2A}R

dimerization and detected the role of highly conserved amino acids in helices 1, 2, 6 and 7 in maintaining the structure network (Fanelli & Felling, 2011). Therefore, these conserved sites will be mutated to observe if dimerizations occur from these regions.

REFERENCES

- Agnati, L. F., Ferré, S., Lluís, C., Franco, R., & Fuxe, K. (2003). Molecular mechanisms and therapeutic implications of intramembrane receptor/receptor interactions among heptahelical receptors with examples from the striatopallidal GABA neurons. *Pharmacological Reviews*, *55*, 509–550. doi:10.1124/pr.55.3.2.509
- Albertazzi, L., Arosio, D., Marchetti, L., Ricci, F., & Beltram, F. (2009). Quantitative FRET analysis with the E0GFP-mCherry fluorescent protein pair. *Photochemistry and Photobiology*, *85*, 287–297. doi:10.1111/j.1751-1097.2008.00435.x
- Alberts, B., Johnson, A., Lewis, J., Raff, M., Roberts, K., & Walter, P. (2002). *Molecular Biology of the Cell, Fourth Edition. Molecular Biology* (p. 1616).
- Auchampach, J. a, & Bolli, R. (1999). Adenosine receptor subtypes in the heart: therapeutic opportunities and challenges. *The American Journal of Physiology*, *276*(3 Pt 2), H1113–6. Retrieved from <http://www.ncbi.nlm.nih.gov/pubmed/10070100> [last accessed on 15 July 2014]
- Awobuluyi, M., Yang, J., Ye, Y., Chatterton, J. E., Godzik, A., Lipton, S. A., & Zhang, D. (2007). Subunit-specific roles of glycine-binding domains in activation of NR1/NR3 N-methyl-D-aspartate receptors. *Molecular Pharmacology*, *71*, 112–122. doi:10.1124/mol.106.030700
- Baines, C. P., Cohen, M. V., & Downey, J. M. (1999). Signal transduction in ischemic preconditioning: the role of kinases and mitochondrial K(ATP) channels. *Journal of Cardiovascular Electrophysiology*, *10*, 741–754.
- Beaulieu, J.-M., & Gainetdinov, R. R. (2011). The physiology, signaling, and pharmacology of dopamine receptors. *Pharmacological Reviews*, *63*, 182–217. doi:10.1124/pr.110.002642
- Benarroch, E. E. (2008). Adenosine and its receptors: Multiple modulatory functions and potential therapeutic targets for neurologic disease. *Neurology*, *70*, 231–236. doi:10.1212/01.wnl.0000297939.18236.ec
- Benquet, P., Gee, C. E., & Gerber, U. (2002). Two distinct signaling pathways upregulate NMDA receptor responses via two distinct metabotropic glutamate

- receptor subtypes. *The Journal of Neuroscience: The Official Journal of the Society for Neuroscience*, 22, 9679–9686.
- Berridge, M. J. (2012). Cell Signalling Biology: Module 3 - Ion Channels. *Biochemical Journal*. doi:10.1042/csb0001003
- Bezanilla, F. (2005). Voltage-gated ion channels. *NanoBioscience, IEEE Transactions on*, 4, 34–48. doi:10.1109/TNB.2004.842463
- Bouvier, M. (2001). Oligomerization of G-protein-coupled transmitter receptors. *Nature Reviews. Neuroscience*, 2, 274–286. doi:10.1038/35067575
- Bowery, N. G., & Enna, S. J. (2000). gamma-aminobutyric acid(B) receptors: first of the functional metabotropic heterodimers. *The Journal of Pharmacology and Experimental Therapeutics*, 292, 2–7.
- Broussard, J. a, Rappaz, B., Webb, D. J., & Brown, C. M. (2013). Fluorescence resonance energy transfer microscopy as demonstrated by measuring the activation of the serine/threonine kinase Akt. *Nature Protocols*, 8, 265–81. doi:10.1038/nprot.2012.147
- Brown, R. M., & Short, J. L. (2008). Adenosine A(2A) receptors and their role in drug addiction. *The Journal of Pharmacy and Pharmacology*, 60, 1409–1430. doi:10.1211/jpp/60.11.0001
- Bulenger, S., Marullo, S., & Bouvier, M. (2005). Emerging role of homo- and heterodimerization in G-protein-coupled receptor biosynthesis and maturation. *Trends in Pharmacological Sciences*. doi:10.1016/j.tips.2005.01.004
- Cabello, N., Gandía, J., Bertarelli, D. C. G., Watanabe, M., Lluís, C., Franco, R., ... Ciruela, F. (2009). Metabotropic glutamate type 5, dopamine D2 and adenosine A 2a receptors form higher-order oligomers in living cells. *Journal of Neurochemistry*, 109, 1497–1507. doi:10.1111/j.1471-4159.2009.06078.x
- Canals, M., Burgueño, J., Marcellino, D., Cabello, N., Canela, E. I., Mallol, J., ... Franco, R. (2004). Homodimerization of adenosine A2A receptors: Qualitative and quantitative assessment by fluorescence and bioluminescence energy transfer. *Journal of Neurochemistry*, 88, 726–734. doi:10.1046/j.1471-4159.2003.02200.x
- Canals, M., Marcellino, D., Fanelli, F., Ciruela, F., de Benedetti, P., Goldberg, S. R., ... Franco, R. (2003). Adenosine A2A-dopamine D2 receptor-receptor heteromerization: qualitative and quantitative assessment by fluorescence and

- bioluminescence energy transfer. *The Journal of Biological Chemistry*, 278, 46741–46749. doi:10.1074/jbc.M306451200
- Carroll, R. C., & Zukin, R. S. (2002). NMDA-receptor trafficking and targeting: Implications for synaptic transmission and plasticity. *Trends in Neurosciences*. doi:10.1016/S0166-2236(02)02272-5
- Cepeda, C., Buchwald, N. A., & Levine, M. S. (1993). Neuromodulatory actions of dopamine in the neostriatum are dependent upon the excitatory amino acid receptor subtypes activated. *Proceedings of the National Academy of Sciences of the United States of America*, 90, 9576–9580. doi:10.1073/pnas.90.20.9576
- Cepeda, C., & Levine, M. S. (1998). Dopamine and N-methyl-D-aspartate receptor interactions in the Neostriatum. *Developmental Neuroscience*. doi:10.1159/000017294
- Chikahisa, S., & Séi, H. (2011). The Role of ATP in Sleep Regulation. *Frontiers in Neurology*. doi:10.3389/fneur.2011.00087
- Choi, E. Y., Jeong, D., Park, K. W., & Baik, J. H. (1999). G protein-mediated mitogen-activated protein kinase activation by two dopamine D2 receptors. *Biochemical and Biophysical Research Communications*, 256, 33–40.
- Clegg, R. M. (1995). Fluorescence resonance energy transfer. *Current Opinion in Biotechnology*. doi:10.1016/0958-1669(95)80016-6
- Conte Camerino, D., Tricarico, D., & Desaphy, J. F. (2007). Ion Channel Pharmacology. *Neurotherapeutics*, 4, 184–198. doi:10.1016/j.nurt.2007.01.013
- Cornea, A., Janovick, J. A., Maya-Núñez, G., & Conn, P. M. (2001). Gonadotropin-releasing hormone receptor microaggregation. Rate monitored by fluorescence resonance energy transfer. *The Journal of Biological Chemistry*, 276, 2153–2158. doi:10.1074/jbc.M007850200
- Crespo, P., Xu, N., Simonds, W. F., & Gutkind, J. S. (1994). Ras-dependent activation of MAP kinase pathway mediated by G-protein beta gamma subunits. *Nature*, 369, 418–420. doi:10.1038/369418a0
- Cristalli, G., Lambertucci, C., Taffi, S., Vittori, S., & Volpini, R. (2003). Medicinal chemistry of adenosine A2A receptor agonists. *Current Topics in Medicinal Chemistry*, 3, 387–401.
- Crocker, A. D. (1994). Dopamine- mechanisms of action. *Experimental and Clinical Pharmacology*, 17(1), 17–21.

- Cronstein, B. N. (1994). Adenosine, an endogenous anti-inflammatory agent. *Journal of Applied Physiology (Bethesda, Md. : 1985)*, 76, 5–13.
- Cull-Candy, S., Brickley, S., & Farrant, M. (2001). NMDA receptor subunits: diversity, development and disease. *Current Opinion in Neurobiology*. doi:10.1016/S0959-4388(00)00215-4
- Cunha, R. A., Ferré, S., Vaugeois, J.-M., & Chen, J.-F. (2008). Potential therapeutic interest of adenosine A2A receptors in psychiatric disorders. *Current Pharmaceutical Design*, 14, 1512–1524. doi:10.1016/j.curobgyn.2005.11.001
- Dal Toso, R., Sommer, B., Ewert, M., Herb, A., Pritchett, D. B., Bach, A., ... Seeburg, P. H. (1989). The dopamine D2 receptor: two molecular forms generated by alternative splicing. *The EMBO Journal*, 8, 4025–4034.
- Day, R. N., & Davidson, M. W. (2009). The fluorescent protein palette: tools for cellular imaging. *Chemical Society Reviews*, 38, 2887–2921. doi:10.1039/b901966a
- Day, R. N., Periasamy, A., & Schaufele, F. (2001). Fluorescence resonance energy transfer microscopy of localized protein interactions in the living cell nucleus. *Methods (San Diego, Calif.)*, 25, 4–18. doi:10.1006/meth.2001.1211
- Demidov, V. V., Dokholyan, N. V., Witte-Hoffmann, C., Chalasani, P., Yiu, H.-W., Ding, F., ... Broude, N. E. (2006). Fast complementation of split fluorescent protein triggered by DNA hybridization. *Proceedings of the National Academy of Sciences of the United States of America*, 103, 2052–2056. doi:10.1073/pnas.0511078103
- Deupi, X., & Kobilka, B. (2007). Activation of G Protein-Coupled Receptors. *Advances in Protein Chemistry*. doi:10.1016/S0065-3233(07)74004-4
- Diniz, C., Borges, F., Santana, L., Uriarte, E., Oliveira, J. M. A., Gonçalves, J., & Fresco, P. (2008). Ligands and therapeutic perspectives of adenosine A(2A) receptors. *Current Pharmaceutical Design*, 14, 1698–1722. doi:10.2174/138161208784746842
- Dunwiddie, T. V., & Masino, S. A. (2001). The role and regulation of adenosine in the central nervous system. *Annual Review of Neuroscience*, 24, 31–55. doi:10.1146/annurev.neuro.24.1.31
- Durand, G. M., Bennett, M. V., & Zukin, R. S. (1993). Splice variants of the N-methyl-D-aspartate receptor NR1 identify domains involved in regulation by polyamines and protein kinase C. *Proceedings of the National Academy of*

Sciences of the United States of America, 90, 6731–6735.
doi:10.1073/pnas.90.20.9739a

- Dziedzicka-Wasylewska, M., Faron-Górecka, A., Andrecka, J., Polit, A., Kuśmider, M., & Wasylewski, Z. (2006). Fluorescence studies reveal heterodimerization of dopamine D1 and D2 receptors in the plasma membrane. *Biochemistry*, 45, 8751–8759. doi:10.1021/bi060702m
- Edmonds, B., Gibb, A. J., & Colquhoun, D. (1995). Mechanisms of Activation of Glutamate Receptors and the Time Course of Excitatory Synaptic Currents. *Annual Review of Physiology*, 57, 495–519.
- Eltzschig, H. K. (2013). Extracellular Adenosine Signaling in Molecular Medicine. *Journal of Molecular Medicine (Berlin, Germany)*, 91(2), 141–146. doi:10.1007/s00109-013-0999-z.Extracellular
- Eltzschig, H. K., Weissmüller, T., Mager, A., & Eckle, T. (2006). Nucleotide metabolism and cell-cell interactions. *Methods in Molecular Biology (Clifton, N.J.)*, 341, 73–87. doi:10.1385/1-59745-113-4:73
- Emilien, G., Maloteaux, J. M., Geurts, M., Hoogenberg, K., & Cragg, S. (1999). Dopamine receptors--physiological understanding to therapeutic intervention potential. *Pharmacology & Therapeutics*, 84, 133–156. doi:10.1016/S0163-7258(99)00029-7
- Faigle, M., Seessle, J., Zug, S., El Kasmi, K. C., & Eltzschig, H. K. (2008). ATP release from vascular endothelia occurs across Cx43 hemichannels and is attenuated during hypoxia. *PLoS ONE*, 3. doi:10.1371/journal.pone.0002801
- Fanelli, F., & Felling, A. (2011). Dimerization and ligand binding affect the structure network of A_{2A} adenosine receptor. *Biochimica et Biophysica Acta - Biomembranes*, 1808, 1256–1266. doi:10.1016/j.bbamem.2010.08.006
- Farina, A. N., Blain, K. Y., Maruo, T., Kwiatkowski, W., Choe, S., & Nakagawa, T. (2011). Separation of domain contacts is required for heterotetrameric assembly of functional NMDA receptors. *The Journal of Neuroscience: The Official Journal of the Society for Neuroscience*, 31, 3565–3579. doi:10.1523/JNEUROSCI.6041-10.2011
- Feige, J. N., Sage, D., Wahli, W., Desvergne, B., & Gelman, L. (2005). PixFRET, an ImageJ plug-in for FRET calculation that can accommodate variations in spectral bleed-throughs. *Microscopy Research and Technique*, 68, 51–58. doi:10.1002/jemt.20215

- Ferré, S., Ciruela, F., Canals, M., Marcellino, D., Burgueno, J., Casadó, V., ... Woods, A. (2004). Adenosine A2A-dopamine D2 receptor-receptor heteromers. Targets for neuro-psychiatric disorders. In *Parkinsonism and Related Disorders* (Vol. 10, pp. 265–271). doi:10.1016/j.parkreldis.2004.02.014
- Ferré, S., Diamond, I., Goldberg, S. R., Yao, L., Hourani, S. M. O., Huang, Z. L., ... Kitchen, I. (2007). Adenosine A2A receptors in ventral striatum, hypothalamus and nociceptive circuitry. Implications for drug addiction, sleep and pain. *Progress in Neurobiology*. doi:10.1016/j.pneurobio.2007.04.002
- Ferre, S., von Euler, G., Johansson, B., Fredholm, B. B., & Fuxe, K. (1991). Stimulation of high-affinity adenosine A2 receptors decreases the affinity of dopamine D2 receptors in rat striatal membranes. *Proceedings of the National Academy of Sciences of the United States of America*, 88, 7238–7241. doi:10.1073/pnas.88.16.7238
- Fiorentini, C., & Missale, C. (2004). Oligomeric assembly of dopamine D1 and glutamate NMDA receptors: molecular mechanisms and functional implications. *Biochemical Society Transactions*, 32, 1025–1028. doi:10.1042/BST0321025
- Forsythe, P., & Ennis, M. (1999). Adenosine, mast cells and asthma. *Inflammation Research*. doi:10.1007/s000110050464
- Franco, R., Casadó, V., Mallol, J., Ferrada, C., Ferré, S., Fuxe, K., ... Canela, E. I. (2006). The two-state dimer receptor model: a general model for receptor dimers. *Molecular Pharmacology*, 69, 1905–1912. doi:10.1124/mol.105.020685
- Fredholm, B. B. (1997). Adenosine and neuroprotection. *International Review of Neurobiology*, 40, 259–280.
- Fredholm, B. B., Chen, J.-F., Masino, S. A., & Vaugeois, J.-M. (2005). Actions of adenosine at its receptors in the CNS: insights from knockouts and drugs. *Annual Review of Pharmacology and Toxicology*, 45, 385–412. doi:10.1146/annurev.pharmtox.45.120403.095731
- Furukawa, H., Singh, S. K., Mancusso, R., & Gouaux, E. (2005). Subunit arrangement and function in NMDA receptors. *Nature*, 438, 185–192. doi:10.1038/nature04089
- Fuxe, K., O. Borroto-Escuela, D., Marcellino, D., Romero-Fernandez, W., Frankowska, M., Guidolin, D., ... Tanganelli, S. (2012). GPCR Heteromers and their Allosteric Receptor-Receptor Interactions. *Current Medicinal Chemistry*. doi:10.2174/092986712803414259

- Gahmberg, C. G., & Tolvanen, M. (1996). Why mammalian cell surface proteins are glycoproteins. *Trends in Biochemical Sciences*, *21*, 308–311.
- Gandia, J., Galino, J., Amaral, O. B., Soriano, A., Lluís, C., Franco, R., & Ciruela, F. (2008a). Detection of higher-order G protein-coupled receptor oligomers by a combined BRET-BiFC technique. *FEBS Letters*, *582*, 2979–2984. doi:10.1016/j.febslet.2008.07.045
- Gandia, J., Galino, J., Amaral, O. B., Soriano, A., Lluís, C., Franco, R., & Ciruela, F. (2008b). Detection of higher-order G protein-coupled receptor oligomers by a combined BRET-BiFC technique. *FEBS Letters*, *582*, 2979–2984. doi:10.1016/j.febslet.2008.07.045
- Giros, B., Sokoloff, P., Martres, M. P., Riou, J. F., Emorine, L. J., & Schwartz, J. C. (1989). Alternative splicing directs the expression of two D2 dopamine receptor isoforms. *Nature*, *342*, 923–926. doi:10.1038/342923a0
- Gordon, G. W., Berry, G., Liang, X. H., Levine, B., & Herman, B. (1998). Quantitative fluorescence resonance energy transfer measurements using fluorescence microscopy. *Biophysical Journal*, *74*, 2702–2713. doi:10.1016/S0006-3495(98)77976-7
- Greengard, P. (2001). The neurobiology of slow synaptic transmission. *Science (New York, N.Y.)*, *294*, 1024–1030. doi:10.1126/science.294.5544.1024
- Guo, W., Urizar, E., Kralikova, M., Mobarec, J. C., Shi, L., Filizola, M., & Javitch, J. A. (2008). Dopamine D2 receptors form higher order oligomers at physiological expression levels. *The EMBO Journal*, *27*, 2293–2304. doi:10.1038/emboj.2008.153
- Haas, H. L., & Selbach, O. (2000). Functions of neuronal adenosine receptors. *Naunyn-Schmiedeberg's Archives of Pharmacology*. doi:10.1007/s002100000314
- Harmar, A. J., Hills, R. A., Rosser, E. M., Jones, M., Buneman, O. P., Dunbar, D. R., ... Spedding, M. (2009). IUPHAR-DB: The IUPHAR database of G protein-coupled receptors and ion channels. *Nucleic Acids Research*, *37*. doi:10.1093/nar/gkn728
- Hart, M. L., Grenz, A., Gorzolla, I. C., Schittenhelm, J., Dalton, J. H., & Eltzschig, H. K. (2011). Hypoxia-inducible factor-1 α -dependent protection from intestinal ischemia/reperfusion injury involves ecto-5'-nucleotidase (CD73) and the A2B adenosine receptor. *Journal of Immunology (Baltimore, Md. : 1950)*, *186*, 4367–4374. doi:10.4049/jimmunol.0903617

- Hebert, D. N., & Molinari, M. (2007). In and out of the ER: protein folding, quality control, degradation, and related human diseases. *Physiological Reviews*, *87*, 1377–1408. doi:10.1152/physrev.00050.2006
- Hebert, T. E., Moffett, S., Morello, J. P., Loisel, T. P., Bichet, D. G., Barret, C., & Bouvier, M. (1996). A peptide derived from a beta2-adrenergic receptor transmembrane domain inhibits both receptor dimerization and activation. *The Journal of Biological Chemistry*, *271*, 16384–16392. doi:10.1074/jbc.271.27.16384
- Herrick-Davis, K., Grinde, E., & Mazurkiewicz, J. E. (2004). Biochemical and biophysical characterization of serotonin 5-HT_{2C} receptor homodimers on the plasma membrane of living cells. *Biochemistry*, *43*, 13963–13971. doi:10.1021/bi048398p
- Hillion, J., Canals, M., Torvinen, M., Casado, V., Scott, R., Terasmaa, A., ... Fuxe, K. (2002). Coaggregation, cointernalization, and codesensitization of adenosine A_{2A} receptors and dopamine D₂ receptors. *The Journal of Biological Chemistry*, *277*, 18091–18097. doi:10.1074/jbc.M107731200
- Hipsler, C., Bushlin, I., Gupta, A., Gomes, I., & Devi, L. A. (2010). Role of antibodies in developing drugs that target G-protein-coupled receptor dimers. *Mount Sinai Journal of Medicine*. doi:10.1002/msj.20199
- Horak, M., Chang, K., & Wenthold, R. J. (2008). Masking of the endoplasmic reticulum retention signals during assembly of the NMDA receptor. *The Journal of Neuroscience : The Official Journal of the Society for Neuroscience*, *28*, 3500–3509. doi:10.1523/JNEUROSCI.5239-07.2008
- Hu, C. D., Chinenov, Y., & Kerppola, T. K. (2002). Visualization of interactions among bZIP and Rel family proteins in living cells using bimolecular fluorescence complementation. *Molecular Cell*, *9*, 789–798. doi:10.1016/S1097-2765(02)00496-3
- Issafras, H., Angers, S., Bulenger, S., Blanpain, C., Parmentier, M., Labbé-Jullié, C., ... Marullo, S. (2002). Constitutive agonist-independent CCR5 oligomerization and antibody-mediated clustering occurring at physiological levels of receptors. *The Journal of Biological Chemistry*, *277*, 34666–34673. doi:10.1074/jbc.M202386200
- Jenner, P. (2003). A_{2A} antagonists as novel non-dopaminergic therapy for motor dysfunction in PD. *Neurology*, *61*, S32–S38. doi:10.1212/01.WNL.0000095209.59347.79

- Jordan, B. A., & Devi, L. A. (1999). G-protein-coupled receptor heterodimerization modulates receptor function. *Nature*, *399*, 697–700. doi:10.1038/21441
- Kamiya, T., Saitoh, O., Yoshioka, K., & Nakata, H. (2003). Oligomerization of adenosine A, *306*, 544–549. doi:10.1016/S0006-291X(03)00991-4
- Kanterman, R. Y., Mahan, L. C., Briley, E. M., Monsma, F. J., Sibley, D. R., Axelrod, J., & Felder, C. C. (1991). Transfected D2 dopamine receptors mediate the potentiation of arachidonic acid release in Chinese hamster ovary cells. *Molecular Pharmacology*, *39*, 364–369.
- Kerppola, T. K. (2006). Design and implementation of bimolecular fluorescence complementation (BiFC) assays for the visualization of protein interactions in living cells. *Nature Protocols*, *1*, 1278–1286. doi:10.1038/nprot.2006.201
- Kerppola, T. K. (2008). Bimolecular Fluorescence Complementation: Visualization of Molecular Interactions in Living Cells. *Methods in Cell Biology*. doi:10.1016/S0091-679X(08)85019-4
- Kerppola, T. K. (2009). Visualization of molecular interactions using bimolecular fluorescence complementation analysis: characteristics of protein fragment complementation. *Chemical Society Reviews*, *38*, 2876–2886. doi:10.1039/b909638h
- Kniazeff, J., Bessis, A.-S., Maurel, D., Ansanay, H., Prézeau, L., & Pin, J.-P. (2004). Closed state of both binding domains of homodimeric mGlu receptors is required for full activity. *Nature Structural & Molecular Biology*, *11*, 706–713. doi:10.1038/nsmb794
- Kobilka, B. K. (2007). G protein coupled receptor structure and activation. *Biochimica et Biophysica Acta*, *1768*, 794–807. doi:10.1016/j.bbamem.2006.10.021
- Köhr, G. (2006). NMDA receptor function: Subunit composition versus spatial distribution. *Cell and Tissue Research*. doi:10.1007/s00441-006-0273-6
- Lambright, D. G., Sondek, J., Böhm, A., Skiba, N. P., Hamm, H. E., & Sigler, P. B. (1996). The 2.0 Angstrom Crystal-Structure Of a Heterotrimeric G-Protein. *Nature*, *379*, 311–319.
- Latek, D., Modzelewska, A., Trzaskowski, B., Palczewski, K., & Filipek, S. (2012). G protein-coupled receptors--recent advances. *Acta Biochimica Polonica*, *59*, 515–29. Retrieved from <http://www.ncbi.nlm.nih.gov/pubmed/23251911> [last accessed on 13 July 2014]

- Laube, B., Hirai, H., Sturgess, M., Betz, H., & Kuhse, J. (1997). Molecular determinants of agonist discrimination by NMDA receptor subunits: Analysis of the glutamate binding site on the NR2B subunit. *Neuron*, *18*, 493–503. doi:10.1016/S0896-6273(00)81249-0
- Law, A. J., Weickert, C. S., Webster, M. J., Herman, M. M., Kleinman, J. E., & Harrison, P. J. (2003). Expression of NMDA receptor NR1, NR2A and NR2B subunit mRNAs during development of the human hippocampal formation. *European Journal of Neuroscience*, *18*, 1197–1205. doi:10.1046/j.1460-9568.2003.02850.x
- Lee, F. J. S., Xue, S., Pei, L., Vukusic, B., Chéry, N., Wang, Y., ... Liu, F. (2002). Dual regulation of NMDA receptor functions by direct protein-protein interactions with the dopamine D1 receptor. *Cell*, *111*, 219–230. doi:10.1016/S0092-8674(02)00962-5
- Lin, H.-H. (2013). G-protein-coupled receptors and their (Bio) chemical significance win 2012 Nobel Prize in Chemistry. *Biomedical Journal*, *36*, 118–24. doi:10.4103/2319-4170.113233
- Liu, L., Wong, T. P., Pozza, M. F., Lingenhohl, K., Wang, Y., Sheng, M., ... Wang, Y. T. (2004). Role of NMDA receptor subtypes in governing the direction of hippocampal synaptic plasticity. *Science (New York, N.Y.)*, *304*, 1021–1024. doi:10.1126/science.1101128
- Liu, X. Y., Chu, X. P., Mao, L. M., Wang, M., Lan, H. X., Li, M. H., ... Wang, J. Q. (2006). Modulation of D2R-NR2B Interactions in Response to Cocaine. *Neuron*, *52*, 897–909. doi:10.1016/j.neuron.2006.10.011
- Lledo, P. M., Homburger, V., Bockaert, J., & Vincent, J. D. (1992). Differential G protein-mediated coupling of D2 dopamine receptors to K⁺ and Ca²⁺ currents in rat anterior pituitary cells. *Neuron*, *8*, 455–463. doi:10.1016/0896-6273(92)90273-G
- Löffler, M., Morote-Garcia, J. C., Eltzhig, S. A., Coe, I. R., & Eltzhig, H. K. (2007). Physiological roles of vascular nucleoside transporters. *Arteriosclerosis, Thrombosis, and Vascular Biology*. doi:10.1161/ATVBAHA.106.126714
- Luo, Y., Kokkonen, G. C., Wang, X., Neve, K. A., & Roth, G. S. (1998). D2 dopamine receptors stimulate mitogenesis through pertussis toxin-sensitive G proteins and Ras-involved ERK and SAP/JNK pathways in rat C6-D2L glioma cells. *Journal of Neurochemistry*, *71*, 980–990.

- Lynch, D. R., & Guttman, R. P. (2002). Excitotoxicity: perspectives based on N-methyl-D-aspartate receptor subtypes. *The Journal of Pharmacology and Experimental Therapeutics*, *300*, 717–723. doi:10.1124/jpet.300.3.717
- MacDonald, M. L., Lamerdin, J., Owens, S., Keon, B. H., Bilter, G. K., Shang, Z., ... Westwick, J. K. (2006). Identifying off-target effects and hidden phenotypes of drugs in human cells. *Nature Chemical Biology*, *2*, 329–337. doi:10.1038/nchembio790
- Maggio, R., Vogel, Z., & Wess, J. (1993). Coexpression studies with mutant muscarinic/adrenergic receptors provide evidence for intermolecular “cross-talk” between G-protein-linked receptors. *Proceedings of the National Academy of Sciences of the United States of America*, *90*, 3103–3107. doi:10.1073/pnas.90.7.3103
- Magliery, T. J., Wilson, C. G. M., Pan, W., Mishler, D., Ghosh, I., Hamilton, A. D., & Regan, L. (2005). Detecting protein-protein interactions with a green fluorescent protein fragment reassembly trap: Scope and mechanism. *Journal of the American Chemical Society*, *127*, 146–157. doi:10.1021/ja046699g
- Mayer, M. L., & Armstrong, N. (2004). Structure and function of glutamate receptor ion channels. *Annual Review of Physiology*, *66*, 161–181. doi:10.1146/annurev.physiol.66.050802.084104
- McIlhinney, R. A., Philipps, E., Le Bourdelles, B., Grimwood, S., Wafford, K., Sandhu, S., & Whiting, P. (2003). Assembly of N-methyl-D-aspartate (NMDA) receptors. *Biochem Soc Trans*, *31*, 865–868. Retrieved from http://www.ncbi.nlm.nih.gov/entrez/query.fcgi?cmd=Retrieve&db=PubMed&dopt=Citation&list_uids=12887323 [last accessed on 5 August 2014]
- Milligan, G., & Bouvier, M. (2005). Methods to monitor the quaternary structure of G protein-coupled receptors. *FEBS Journal*. doi:10.1111/j.1742-4658.2005.04731.x
- Missale, C., Nash, S. R., Robinson, S. W., Jaber, M., & Caron, M. G. (1998). Dopamine receptors: from structure to function. *Physiological Reviews*, *78*, 189–225. doi:10.1186/1471-2296-12-32
- Monyer, H., Sprengel, R., Schoepfer, R., Herb, A., Higuchi, M., Lomeli, H., ... Seeburg, P. H. (1992). Heteromeric NMDA receptors: molecular and functional distinction of subtypes. *Science (New York, N.Y.)*, *256*, 1217–1221. doi:10.1126/science.256.5060.1217

- Mora, F., Segovia, G., & del Arco, A. (2008). Glutamate-dopamine-GABA interactions in the aging basal ganglia. *Brain Research Reviews*. doi:10.1016/j.brainresrev.2007.10.006
- Morari, M., Marti, M., Sbrenna, S., Fuxe, K., Bianchi, C., & Beani, L. (1998). Reciprocal dopamine-glutamate modulation of release in the basal ganglia. *Neurochemistry International*. doi:10.1016/S0197-0186(98)00052-7
- Morelli, M., Di Paolo, T., Wardas, J., Calon, F., Xiao, D., & Schwarzschild, M. A. (2007). Role of adenosine A2A receptors in parkinsonian motor impairment and l-DOPA-induced motor complications. *Progress in Neurobiology*. doi:10.1016/j.pneurobio.2007.07.001
- Navarro, G., Carriba, P., Gandía, J., Ciruela, F., Casadó, V., Cortés, A., ... Franco, R. (2008). Detection of heteromers formed by cannabinoid CB1, dopamine D2, and adenosine A2A G-protein-coupled receptors by combining bimolecular fluorescence complementation and bioluminescence energy transfer. *TheScientificWorldJournal*, 8, 1088–1097. doi:10.1100/tsw.2008.136
- Neve, K. A., Seamans, J. K., & Trantham-Davidson, H. (2004). Dopamine receptor signaling. *Journal of Receptor and Signal Transduction Research*, 24, 165–205. doi:10.1081/LRST-200029981
- Nishi, A., Snyder, G. L., Fienberg, A. A., Fisone, G., Aperia, A., Nairn, A. C., & Greengard, P. (1999). Requirement for DARPP-32 in mediating effect of dopamine D2 receptor activation. *European Journal of Neuroscience*, 11, 2589–2592. doi:10.1046/j.1460-9568.1999.00724.x
- Ohana, G., Bar-Yehuda, S., Barer, F., & Fishman, P. (2001). Differential effect of adenosine on tumor and normal cell growth: Focus on the A3 adenosine receptor. *Journal of Cellular Physiology*, 186, 19–23. doi:10.1002/1097-4652(200101)186:1<19::AID-JCP1011>3.0.CO;2-3
- Ohta, A., & Sitkovsky, M. (2001). Role of G-protein-coupled adenosine receptors in downregulation of inflammation and protection from tissue damage. *Nature*, 414(6866), 916–920. doi:10.1038/414916a
- Okada, Y., Miyamoto, T., & Toda, K. (2003). Dopamine modulates a voltage-gated calcium channel in rat olfactory receptor neurons. *Brain Research*, 968, 248–255. doi:10.1016/S0006-8993(03)02267-4
- Olah, M. E., & Stiles, G. L. (1995). Adenosine receptor subtypes: characterization and therapeutic regulation. *Annual Review of Pharmacology and Toxicology*, 35, 581–606. doi:10.1146/annurev.pa.35.040195.003053

- Ongini, E., Monopoli, A., Cacciari, B., & Baraldi, P. G. (2001). Selective adenosine A2A receptor antagonists. *Farmaco*, *56*(1-2), 87–90. doi:10.1016/S0014-827X(01)01024-2
- Ozawa, T., Takeuchi, M., Kaihara, A., Sato, M., & Umezawa, Y. (2001). Protein splicing-based reconstitution of split green fluorescent protein for monitoring protein-protein interactions in bacteria: Improved sensitivity and reduced screening time. *Analytical Chemistry*, *73*, 5866–5874. doi:10.1021/ac010717k
- Palczewski, K. (2010). Oligomeric forms of G protein-coupled receptors (GPCRs). *Trends in Biochemical Sciences*, *35*, 595–600. doi:10.1016/j.tibs.2010.05.002
- Paoletti, P., & Neyton, J. (2007). NMDA receptor subunits: function and pharmacology. *Current Opinion in Pharmacology*. doi:10.1016/j.coph.2006.08.011
- Pérez-Otaño, I., & Ehlers, M. D. (2004). Learning from NMDA receptor trafficking: Clues to the development and maturation of glutamatergic synapses. *NeuroSignals*. doi:10.1159/000077524
- Periasamy, A. (2001). Fluorescence resonance energy transfer microscopy: a mini review. *Journal of Biomedical Optics*, *6*, 287–291. doi:10.1117/1.1383063
- Pinna, A., Wardas, J., Simola, N., & Morelli, M. (2005). New therapies for the treatment of Parkinson's disease: adenosine A2A receptor antagonists. *Life Sciences*, *77*, 3259–3267. doi:10.1016/j.lfs.2005.04.029
- Pivonello, R., Ferone, D., Lombardi, G., Colao, A., Lamberts, S. W. J., & Hofland, L. J. (2007). Novel insights in dopamine receptor physiology. *European Journal of Endocrinology / European Federation of Endocrine Societies*, *156 Suppl*, S13–S21. doi:10.1530/eje.1.02353
- Polosa, R. (2002). Adenosine-receptor subtypes: their relevance to adenosine-mediated responses in asthma and chronic obstructive pulmonary disease. *The European Respiratory Journal: Official Journal of the European Society for Clinical Respiratory Physiology*, *20*, 488–496. doi:10.1183/09031936.02.01132002
- Poole, K., Moroni, M., & Lewin, G. R. (2014). Sensory mechanotransduction at membrane-matrix interfaces. *Pflügers Archiv - European Journal of Physiology*. doi:10.1007/s00424-014-1563-6
- Prou, D., Gu, W. J., Le Crom, S., Vincent, J. D., Salamero, J., & Vernier, P. (2001). Intracellular retention of the two isoforms of the D(2) dopamine receptor

- promotes endoplasmic reticulum disruption. *Journal of Cell Science*, *114*, 3517–3527.
- Prybylowski, K., & Wenthold, R. J. (2004). N-Methyl-D-aspartate receptors: subunit assembly and trafficking to the synapse. *The Journal of Biological Chemistry*, *279*(11), 9673–6. doi:10.1074/jbc.R300029200
- Purves, D., Augustine, G. J., Fitzpatrick, D., & Katz, L. (2001). Chapter 4: Channels and Transporters. In *Neuroscience (2nd edition)*. Sinauer Associates.
- Reutershan, J., Vollmer, I., Stark, S., Wagner, R., Ngamsri, K.-C., & Eltzschig, H. K. (2009). Adenosine and inflammation: CD39 and CD73 are critical mediators in LPS-induced PMN trafficking into the lungs. *The FASEB Journal: Official Publication of the Federation of American Societies for Experimental Biology*, *23*, 473–482. doi:10.1096/fj.08-119701
- Ribeiro, J. A. (2005). What can adenosine neuromodulation do for neuroprotection? *Current Drug Targets. CNS and Neurological Disorders*, *4*, 325–329. doi:10.2174/1568007054546090
- Richards, F. M. (1958). ON THE ENZYMIC ACTIVITY OF SUBTILISIN-MODIFIED RIBONUCLEASE. *Proceedings of the National Academy of Sciences of the United States of America*, *44*, 162–166. doi:10.1073/pnas.44.2.162
- Roman, R. M., & Fitz, J. G. (1999). Emerging Roles of Purinergic Signaling in Gastrointestinal. *Gastroenterology*, *116*(4), 964–979.
- Salter, M. W., & Kalia, L. V. (2004). Src kinases: a hub for NMDA receptor regulation. *Nature Reviews. Neuroscience*, *5*, 317–328. doi:10.1038/nrn1368
- Sang, K. P., Minh, D. N., Fischer, A., Luke, M. P. S., Affar, E. B., Dieffenbach, P. B., ... Tsai, L. H. (2005). Par-4 links dopamine signaling and depression. *Cell*, *122*, 275–287. doi:10.1016/j.cell.2005.05.031
- Sanz-Clemente, A., Nicoll, R. A., & Roche, K. W. (2012). Diversity in NMDA Receptor Composition: Many Regulators, Many Consequences. *The Neuroscientist*. doi:10.1177/1073858411435129
- Schorge, S., & Colquhoun, D. (2003). Studies of NMDA receptor function and stoichiometry with truncated and tandem subunits. *The Journal of Neuroscience: The Official Journal of the Society for Neuroscience*, *23*, 1151–1158. doi:23/4/1151 [pii]

- Schöneberg, T., Schulz, A., Biebermann, H., Hermsdorf, T., Römpler, H., & Sangkuhl, K. (2004). Mutant G-protein-coupled receptors as a cause of human diseases. *Pharmacology and Therapeutics*. doi:10.1016/j.pharmthera.2004.08.008
- Schulte, G. (2002). *Adenosine Receptor Signaling and the activation of mitogen activated protein kinases*. Retrieved from <http://publications.ki.se/xmlui/bitstream/handle/10616/37706/thesis.pdf?sequence=1> [last accessed on 16 July 2014]
- Schultz, W. (2007). Multiple dopamine functions at different time courses. *Annual Review of Neuroscience*, 30, 259–288. doi:10.1146/annurev.neuro.28.061604.135722
- Schwarzschild, M. A., Agnati, L., Fuxe, K., Chen, J.-F., & Morelli, M. (2006). Targeting adenosine A2A receptors in Parkinson's disease. *Trends in Neurosciences*, 29, 647–654. doi:10.1016/j.tins.2006.09.004
- Scott, D. B., Blanpied, T. A., Swanson, G. T., Zhang, C., & Ehlers, M. D. (2001). An NMDA receptor ER retention signal regulated by phosphorylation and alternative splicing. *The Journal of Neuroscience: The Official Journal of the Society for Neuroscience*, 21, 3063–3072. doi:10.1523/JNEUROSCI.2199-01.2001 [pii]
- Seabrook, G. R., Knowles, M., Brown, N., Myers, J., Sinclair, H., Patel, S., ... McAllister, G. (1994). Pharmacology of high-threshold calcium currents in GH4C1 pituitary cells and their regulation by activation of human D2 and D4 dopamine receptors. *British Journal of Pharmacology*, 112, 728–734.
- Seidel, M. G., Klinger, M., Freissmuth, M., & Höller, C. (1999). Activation of mitogen-activated protein kinase by the A(2A)-adenosine receptor via a rap1-dependent and via a p21(ras)-dependent pathway. *The Journal of Biological Chemistry*, 274, 25833–25841. doi:10.1074/jbc.274.36.25833
- Shi, Y., Liu, X., Gebremedhin, D., Falck, J. R., Harder, D. R., & Koehler, R. C. (2008). Interaction of mechanisms involving epoxyeicosatrienoic acids, adenosine receptors, and metabotropic glutamate receptors in neurovascular coupling in rat whisker barrel cortex. *Journal of Cerebral Blood Flow and Metabolism: Official Journal of the International Society of Cerebral Blood Flow and Metabolism*, 28, 111–125. doi:10.1038/sj.jcbfm.9600511
- Shimomura, O., Johnson, H. F., & Saiga, Y. (1962). Extraction, Purification and Properties of Aequorin, a Bioluminescent Protein from the Luminous Hydromedusan, Aequorea. *Journal of Cellular and Comparative Physiology*, 59(3), 223–229.

- Shin, H. K., Park, S. N., & Hong, K. W. (2000). Implication of adenosine A2(A) receptors in hypotension-induced vasodilation and cerebral blood flow autoregulation in rat pial arteries. *Life Sciences*, *67*, 1435–1445. doi:10.1016/S0024-3205(00)00737-2
- Sidhu, A., & Niznik, H. B. (2000). Coupling of dopamine receptor subtypes to multiple and diverse G proteins. *International Journal of Developmental Neuroscience*. doi:10.1016/S0736-5748(00)00033-2
- Snyder, G. L., Fienberg, A. A., Haganir, R. L., & Greengard, P. (1998). A dopamine/D1 receptor/protein kinase A/dopamine- and cAMP-regulated phosphoprotein (Mr 32 kDa)/protein phosphatase-1 pathway regulates dephosphorylation of the NMDA receptor. *The Journal of Neuroscience: The Official Journal of the Society for Neuroscience*, *18*, 10297–10303.
- Standley, S., Roche, K. W., McCallum, J., Sans, N., & Wenthold, R. J. (2000). PDZ domain suppression of an ER retention signal in NMDA receptor NR1 splice variants. *Neuron*, *28*, 887–898. doi:10.1016/S0896-6273(00)00161-6
- Stephenson, F. A. (2001). Subunit characterization of NMDA receptors. *Current Drug Targets*, *2*, 233–239. doi:10.2174/1389450013348461
- Svenningsson, P., Le Moine, C., Fisone, G., & Fredholm, B. B. (1999). Distribution, biochemistry and function of striatal adenosine A(2A) receptors. *Progress in Neurobiology*. doi:10.1016/S0301-0082(99)00011-8
- Szöllosi, J., Damjanovich, S., Nagy, P., Vereb, G., & Mátyus, L. (2006). Principles of resonance energy transfer. *Current Protocols in Cytometry / Editorial Board, J. Paul Robinson, Managing Editor ... [et Al.], Chapter 1, Unit 1.12*. doi:10.1002/0471142956.cy0112s38
- Takeda, S., Kadowaki, S., Haga, T., Takaesu, H., & Mitaku, S. (2002). Identification of G protein-coupled receptor genes from the human genome sequence. *FEBS Letters*, *520*, 97–101. doi:10.1016/S0014-5793(02)02775-8
- Terrillon, S., & Bouvier, M. (2004). Roles of G-protein-coupled receptor dimerization. *EMBO Reports*, *5*, 30–34. doi:10.1038/sj.embor.7400052
- Terrillon, S., Durroux, T., Mouillac, B., Breit, A., Ayoub, M. A., Taulan, M., ... Bouvier, M. (2003). Oxytocin and vasopressin V1a and V2 receptors form constitutive homo- and heterodimers during biosynthesis. *Molecular Endocrinology (Baltimore, Md.)*, *17*, 677–691. doi:10.1210/me.2002-0222

- Traynelis, S. F., Hartley, M., & Heinemann, S. F. (1995). Control of proton sensitivity of the NMDA receptor by RNA splicing and polyamines. *Science (New York, N.Y.)*, 268, 873–876. doi:10.1126/science.7754371
- Tsien, R. Y. (1998). The green fluorescent protein. *Annual Review of Biochemistry*, 67, 509–544. doi:10.1146/annurev.biochem.67.1.509
- Tymianski, M., Charlton, M. P., Carlen, P. L., & Tator, C. H. (1993). Source specificity of early calcium neurotoxicity in cultured embryonic spinal neurons. *The Journal of Neuroscience: The Official Journal of the Society for Neuroscience*, 13, 2085–2104.
- Venkatakrishnan, A. J., Deupi, X., Lebon, G., Tate, C. G., Schertler, G. F., & Babu, M. M. (2013). Molecular signatures of G-protein-coupled receptors. *Nature*, 494, 185–194. doi:10.1038/nature11896
- Vickery, R. G., & von Zastrow, M. (1999). Distinct dynamin-dependent and -independent mechanisms target structurally homologous dopamine receptors to different endocytic membranes. *The Journal of Cell Biology*, 144, 31–43. doi:10.1083/jcb.144.1.31
- Vriens, J., Nilius, B., & Voets, T. (2014). Peripheral thermosensation in mammals. *Nature Reviews. Neuroscience*. doi:10.1038/nrn3784
- Wenthold, R. J., Al-Hallaq, R. A., Swanwick, C. C., & Petralia, R. S. (2008). Molecular Properties and Cell Biology of the NMDA Receptor. In *Structural And Functional Organization Of The Synapse* (pp. 317–367). Springer US. doi:10.1007/978-0-387-77232-5_12
- Wenthold, R. J., Prybylowski, K., Standley, S., Sans, N., & Petralia, R. S. (2003). Trafficking of NMDA receptors. *Annual Review of Pharmacology and Toxicology*, 43, 335–358. doi:10.1146/annurev.pharmtox.43.100901.135803
- Wietek, J., Wiegert, J. S., Adeishvili, N., Schneider, F., Watanabe, H., Tsunoda, S. P., ... Hegemann, P. (2014). Conversion of channelrhodopsin into a light-gated chloride channel. *Science (New York, N.Y.)*, 344, 409–12. doi:10.1126/science.1249375
- Woo, N. H., Teng, H. K., Siao, C.-J., Chiaruttini, C., Pang, P. T., Milner, T. A., ... Lu, B. (2005). Activation of p75NTR by proBDNF facilitates hippocampal long-term depression. *Nature Neuroscience*, 8, 1069–1077. doi:10.1038/nn1510
- Wu, J., Xie, N., Zhao, X., Nice, E. C., & Huang, C. (2012). Dissection of aberrant GPCR signaling in tumorigenesis--a systems biology approach. *Cancer*

Genomics & Proteomics, 9, 37–50. Retrieved from <http://www.ncbi.nlm.nih.gov/pubmed/22210047> [last accessed on 12 July 2014]

- Xia, H., Hornby, Z. D., & Malenka, R. C. (2001). An ER retention signal explains differences in surface expression of NMDA and AMPA receptor subunits. *Neuropharmacology*, 41, 714–723. doi:10.1016/S0028-3908(01)00103-4
- Xia, Z., & Liu, Y. (2001). Reliable and Global Measurement of Fluorescence Resonance Energy Transfer Using Fluorescence Microscopes. *Biophysical Journal*. doi:10.1016/S0006-3495(01)75886-9
- Zamyatnin, A. A., Solovyev, A. G., Bozhkov, P. V., Valkonen, J. P. T., Morozov, S. Y., & Savenkov, E. I. (2006). Assessment of the integral membrane protein topology in living cells. *Plant Journal*, 46, 145–154. doi:10.1111/j.1365-313X.2006.02674.x
- Zawarynski, P., Talerico, T., Seeman, P., Lee, S. P., O'Dowd, B. F., & George, S. R. (1998). Dopamine D2 receptor dimers in human and rat brain. *FEBS Letters*, 441, 383–386.
- Zito, K., & Scheuss, V. (2010). NMDA Receptor Function and Physiological Modulation. In *Encyclopedia of Neuroscience* (pp. 1157–1164). doi:10.1016/B978-008045046-9.01225-0
- Zukin, R. S., & Bennett, M. V. (1995). Alternatively spliced isoforms of the NMDAR1 receptor subunit. *Trends in Neurosciences*, 18, 306–313. doi:10.1016/0166-2236(95)93920-S

APPENDIX A

COMPOSITIONS OF CELL CULTURE SOLUTIONS

Table A. 1 Composition of D-MEM with high glucose

COMPONENT	CONCENTRATION (mg/L)
Amino Acids	
Glycine	30
L-Arginine hydrochloride	84
L-Cysteine 2HCl	63
L-Glutamine	580
L-Histidine hydrochloride-H ₂ O	42
L-Isoleucine	105
L-Leucine	105
L-Lysine hydrochloride	146
L-Methionine	30
L-Phenylalanine	66
L-Serine	42
L-Threonine	95
L-Tryptophan	16
L-Tyrosine	72
L-Valine	94
Vitamins	
Choline chloride	4
D-Calcium pantothenate	4

Folic acid	4
Niacinamide	4
Pyridoxine hydrochloride	4
Riboflavin	0.4
Thiamine hydrochloride	4
i-Inositol	7.2
Inorganic Salts	
Calcium chloride	264
Ferric nitrate	0.1
Magnesium sulfate	200
Potassium chloride	400
Sodium bicarbonate	3700
Sodium chloride	6400
Sodium phosphate monobasic	141
Other components	
D-Glucose (Dextrose)	4500
Phenol Red	15
Sodium pyruvate	110

Table A. 2 Composition of 1X Phosphate Buffered Saline (PBS) solution

NaCl	8 g/L
KCl	0.2 g/L
Na ₂ HPO ₄	1.44 g/L
KH ₂ PO ₄	0.24 g/L

The components are dissolved within dH₂O. After adjustment of pH to 7.4, solution is autoclaved for sterile usage.

APPENDIX B

COMPOSITION AND PREPARATION OF BACTERIAL CULTURE MEDIUM

Luria Bertani (LB) Medium

10 g/L Tryptone

5 g/L Yeast Extract

5 g/L NaCl

15 g/L agar is added for solid medium preparation.

The pH of the medium is adjusted to 7.0.

APPENDIX C

COMPOSITIONS OF BUFFERS AND SOLUTIONS

1X NEBuffer 4:

20 mM Tris-acetate

50 mM Potassium Acetate

10 mM Magnesium Acetate

1mM Dithiothreitol

pH: 7.9 at 25°C

1X NEB-CutSmart™ Buffer:

50 mM Potassium Acetate

20 mM Tris-acetate

10 mM Magnesium Acetate

100 µg/ml BSA

pH 7.9 at 25°C

1X T4 DNA Ligase Reaction Buffer:

50 mM Tris-HCl

10 mM MgCl₂

1 mM ATP

10 mM Dithiothreitol

pH: 7.5 at 25°C

10X TBE (Tris -Borate -EDTA) Buffer:

108 g/L Tris Base

55 g/L Boric Acid

40 mL/L 20 mM EDTA

1X TBE Buffer was used for agarose gel electrophoresis.

6X Loading Dye :

10 mM Tris-HCl (pH: 7.6)

0.03% Bromophenol Blue

0.03% Xylene Cyanol FF

60% Glycerol

60 mM EDTA

APPENDIX D

PLASMID MAPS

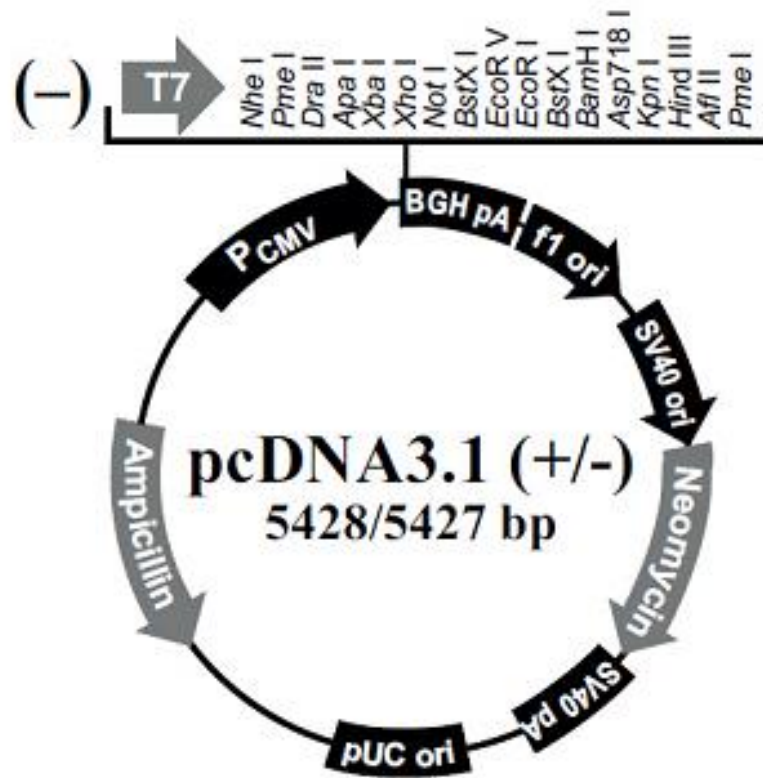


Figure D. 1 Map of pcDNA 3.1 (-) (taken from Invitrogen® Life Technologies)

APPENDIX E

PRIMERS

Primers to amplify N-EGFP tag with A_{2A}R flanking ends

Forward primer:

5' - **cccctggcccaggatggagcaggagtgtcc****ATGGTGAGCAAGGGCGAGGAG** - 3'

Yellow region: last 30 bp of A_{2A}R without stop codon

Green region: beginning of EGFP sequence

Reverse primer:

5' - **gaggctgatcagcggtttaaacttaagctt****TTA****CTTGTCGGCCATGATATAGACG** - 3'

Gray region: first 30 bp of the pcDNA 3.1(-), which directly follow A_{2A}R sequence

Green region: end of N-EGFP fragment (**TTA** was inserted as stop codon of N-EGFP tag)

Primers to amplify N-EGFP tag with D₂R flanking ends

Forward primer:

5' - **cgcaaggccttcctgaagatcctccactgc****ATGGTGAGCAAGGGCGAGGAG** - 3'

Red region: last 30 bp of D₂R without stop codon

Green region: beginning of EGFP sequence

Reverse primer: same as that of A_{2A}R

Primers to amplify C-EGFP tag with A_{2A}R flanking ends

Forward primer:

5' - **cccctggcccaggatggagcaggagtgtcc**CAGAAGAACGGCATCAAGG - 3'

Yellow region: last 30 bp of A_{2A}R without stop codon

Green region: beginning of C-EGFP fragment

Reverse primer:

5' - **ctgatcagcggtttaacttaagcttcc**TACTTGTACAGCTCGTCCATGCC - 3'

Gray region: first 30 bp of the pcDNA 3.1(-), which directly follow A_{2A}R sequence

Green region: end of EGFP sequence (with stop codon)

Primers to amplify C-EGFP tag with D₂R flanking ends

Forward primer:

5' - **cgcaaggccttctgaagatcctccactgc**CAGAAGAACGGCATCAAGG - 3'

Red region: last 30 bp of D₂R without stop codon

Green region: beginning of C-EGFP fragment

Reverse primer: same as that of A_{2A}R

APPENDIX F

CODING SEQUENCES OF FUSION PROTEINS

Coding sequence of N-EGFP tagged A_{2A} receptor: Black sequence corresponds to A_{2A} receptor; while green sequence represents N-EGFP sequence. A stop codon was inserted at the end of N-EGFP tag.

```
ATGCCCATCATGGGCTCCTCGGTGTACATCACGGTGGAGCTGGCCATTGCTGTGCTGGCCATCC
TGGGCAATGTGCTGGTGTGCTGGGCCGTGTGGCTCAACAGCAACCTGCAGAACGTCACCAACTA
CTTTGTGGTGTCACTGGCGGCGGCCGACATCGCAGTGGGTGTGCTCGCCATCCCCTTTGCCATC
ACCATCAGCACC GGTTCTGCGCTGCCTGCCACGGCTGCCTCTTCATTGCCTGCTTCGTCCTGG
TCCTCACGCAGAGCTCCATCTTCAGTCTCCTGGCCATCGCCATTGACCGCTACATTGCCATCCG
CATCCCGCTCCGGTACAATGGCTTGGTGACCGGCACGAGGGCTAAGGGCATCATTGCCATCTGC
TGGGTGCTGTGCTTTGCCATCGGCCTGACTCCCATGCTAGGTTGGAACAACCTGCGGTGAGCCAA
AGGAGGGCAAGAACCCTCCCAGGGCTGCGGGGAGGGCCAAGTGGCCTGTCTCTTTGAGGATGT
GGTCCCCATGAAC TACATGGTGTACTTCAACTTCTTTGCCTGTGTGCTGGTGGCCCTGCTGCTC
ATGCTGGGTGTCTATTTGCGGATCTTCCTGGCGGCGGACGACAGCTGAAGCAGATGGAGAGCC
AGCCTCTGCCGGGGGAGCGGGCACGGTCCACACTGCAGAAGGAGGTCCATGCTGCCAAGTCACT
GGCCATCATTGTGGGGCTCTTTGCCCTCTGCTGGCTGCCCTACACATCATCAACTGCTTCACT
TTCTTCTGCCCCGACTGCAGCCACGCCCCCTCTCTGGCTCATGTACCTGGCCATCGTCCTCTCCC
ACACCAATTTCGGTTGTGAATCCCTTCATCTACGCCTACCGTATCCGCGAGTTCGCCAGACCTT
CCGCAAGATCATTTCGCAGCCACGTCCTGAGGCAGCAAGAACCTTCAAGGCAGCTGGCACCAGT
GCCCCGGTCTTGGCAGCTCATGGCAGTGACGGAGAGCAGGTCAGCCTCCGTCTCAACGGCCACC
CGCCAGGAGTGTGGGCCAACGGCAGTGCTCCCCACCCTGAGCGGAGGCCCAATGGCTACGCCCT
GGGGCTGGT GAGTGGAGGGAGTGCCCAAGAGTCCCAGGGGAACACGGGCCTCCCAGACGTGGAG
CTCCTTAGCCATGAGCTCAAGGGAGTGTGCCAGAGCCCCCTGGCCTAGATGACCCCTGGCCC
AGGATGGAGCAGGAGTGTCCATGGT GAGCAAGGGCGAGGAGCTGTTACCGGGGTGGTGGCCAT
CCTGGTCGAGCTGGACGGCGACGTAAACGGCCACAAGTTCAGCGTGTCCGGCGAGGGCGAGGGC
GATGCCACCTACGGCAAGCTGACCCTGAAGTTCATCTGCACCACCGGCAAGCTGCCCGTGCCCT
GGCCCACCCTCGTGACCACCCTGACCTACGGCGTGCAGTGCTTCAGCCGCTACCCCGACCACAT
GAAGCAGCAGACTTCTTCAAGTCCGCCATGCCCGAAGGCTACGTCCAGGAGCGCACCATCTTC
TTCAAGGACGACGGCAACTACAAGACCCGCGCCGAGGTGAAGTTCGAGGGCGACACCCTGGTGA
ACCGCATCGAGCTGAAGGGCATCGACTTCAAGGAGGACGGCAACATCCTGGGGCACAAAGCTGGA
GTACAAC TACAACAGCCACAACGTCTATATCATGGCCGACAAGTAA
```

Coding sequence of N-EGFP tagged D₂ receptor: Black sequence corresponds to D₂ receptor; while green sequence represents N-EGFP sequence. A stop codon was inserted at the end of N-EGFP tag.

```
ATGGATCCACTGAATCTGTCCTGGTATGATGATGATCTGGAGAGGCAGAACTGGAGCC
GGCCCTTCAACGGGTGACAGCGGAAGGCGGACAGACCCCACTACAACACTACTATGCCAC
ACTGCTCACCCCTGCTCATCGTGTGCATCGTCTTCGGCAACGTGCTGGTGTGCATGGCT
GTGTCCCAGGAGAAAGGCGCTGCAGACCACCAACTACCTGATCGTCAGCCTCGCAG
TGGCCGACCTCCTCGTCGCCACACTGGTTCATGCCCTGGGTTGTCTACCTGGAGGTGGT
AGGTGAGTGGAAATTCAGCAGGATTCACTGTGACATCTTCGTCACCTGGACGTCATG
ATGTGCACGGCGAGCATCCTGAACTTGTGTGCCATCAGCATCGACAGGTACACAGCTG
TGGCCATGCCCATGCTGTACAATACGCGCTACAGCTCCAAGCGCCGGGTACCCGTCAT
GATCTCCATCGTCTGGGTCTGTCCTTACCATCTCCTGCCCACTCCTCTTCGGACTC
AATAACGCAGACCAGAACGAGTGCATCATTGCCAACCAGGCTTCGTTGGTCTACTCCT
CCATCGTCTCCTTCTACGTGCCCTTCAATTGTCACCCTGCTGGTCTACATCAAGATCTA
CATTGTCTCCGAGACGCCGCAAGCGAGTCAACACCAAACGCAGCAGCCGAGCTTTC
AGGGCCACCTGAGGGCTCCACTAAAGGGCAACTGTACTCACCCGAGGACATGAAAC
TCTGCACCGTTATCATGAAGTCTAATGGGAGTTTCCAGTGAACAGGCGGAGAGTGGA
GGCTGCCCGGCGAGCCAGGAGCTGGAGATGGAGATGCTCTCCAGCACCAGCCCAACC
GAGAGGACCCGGTACAGCCCCATCCCAACCAGCCACCACCAGCTGACTCTCCCCGACC
CGTCCCACCATGGTCTCCACAGCACTCCCGACAGCCCCGCCAAACCAGAGAAGAATGG
GCATGCCAAAGACCACCCCAAGATTGCCAAGATCTTTGAGATCCAGACCATGCCCAAT
GGCAAACCCGGACCTCCCTCAAGACCATGAGCCGTAGGAAGCTCTCCAGCAGAAGG
AGAAGAAAGCCACTCAGATGCTCGCCATTGTTCTCGGCGTGTTTCATCATCTGCTGGCT
GCCCTTCTTTCATCACACACATCCTGAACATACTGTGACTGCAACATCCCGCCTGTC
CTGTACAGCGCCTTACAGTGGCTGGGCTATGTCAACAGCGCCGTGAACCCCATCATCT
ACACCACCTTCAACATTGAGTTCGCCAAGGCCTTCTGAAGATCCTCCACTGCATGGT
GAGCAAGGGCGAGGAGCTGTTACCCGGGTTGGTGCCCATCCTGGTTCGAGCTGGACGGC
GACGTAACCGCCACAAGTTCAGCGTGTCCGGCGAGGGCGAGGGCGATGCCACCTACG
GCAAGCTGACCCTGAAGTTCATCTGCACCACCGGCAAGCTGCCCGTGCCCTGGCCAC
CCTCGTGACCACCCTGACCTACGGCGTGCAGTGTTCAGCCGCTACCCGACCACATG
AAGCAGCAGACTTCTTCAAGTCCGCCATGCCCGAAGGCTACGTCCAGGAGCGCACCA
TCTTCTTCAAGGACGACGGCAACTACAAGACCCGCGCCGAGGTGAAGTTCGAGGGCGA
CACCTGGTGAACCGCATCGAGCTGAAGGGCATCGACTTCAAGGAGGACGGCAACATC
CTGGGGACAAGCTGGAGTACAACAGCCACAACGTCTATATCATGGCCGACA
AGTAA
```

Coding sequence of C-EGFP tagged A_{2A} receptor: Black sequence corresponds to A_{2A} receptor; while green sequence represents C-EGFP sequence.

```
ATGCCCATCATGGGCTCCTCGGTGTACATCACGGTGGAGCTGGCCATTGCTGTGCTGGCCATCC
TGGGCAATGTGCTGGTGTGCTGGGCCGTGTGGCTCAACAGCAACCTGCAGAACGTCACCAACTA
CTTTGTGGTGTCACTGGCGGCGGCCGACATCGCAGTGGGTGTGCTCGCCATCCCCTTTGCCATC
ACCATCAGCACCGGGTTCTGCGCTGCCACGGCTGCCTCTTCATTGCCTGCTTCGTCCTGG
TCCTCACGCAGAGCTCCATCTTCAGTCTCCTGGCCATCGCCATTGACCGCTACATTGCCATCCG
CATCCCGCTCCGGTACAATGGCTTGGTGACCGGCACGAGGGCTAAGGGCATCATTGCCATCTGC
TGGGTGCTGTGCTTTGCCATCGGCCTGACTCCCATGCTAGGTTGGAACAACCTGCGGTCAGCCAA
AGGAGGGCAAGAACCACTCCCAGGGCTGCGGGGAGGGCCAAGTGGCCTGTCTCTTTGAGGATGT
GGTCCCCATGAACTACATGGTGTACTTCAACTTCTTTGCCTGTGTGCTGGTGCCCTGCTGCTC
ATGCTGGGTGTCTATTTGCGGATCTTCCTGGCGGCGGACGACAGCTGAAGCAGATGGAGAGCC
AGCCTCTGCCGGGGGAGCGGGCACGGTCCACACTGCAGAAGGAGGTCCATGCTGCCAAGTCACT
GGCCATCATTGTGGGGCTCTTTGCCCTCTGCTGGCTGCCCTACACATCATCAACTGCTTCACT
TTCTTCTGCCCCGACTGCAGCCACGCCCTCTCTGGCTCATGTACCTGGCCATCGTCCTCTCCC
ACACCAATTCGGTTGTGAATCCCTTCATCTACGCCTACCGTATCCGCGAGTTCGGCCAGACCTT
CCGCAAGATCATTTCGAGCCACGTCCTGAGGCAGCAAGAACCTTTCAAGGCAGCTGGCACCAGT
GCCCCGGTCTTGGCAGCTCATGGCAGTGACGGAGAGCAGGTCAGCCTCCGTCTCAACGGCCACC
CGCCAGGAGTGTGGGCCAACGGCAGTGCTCCCCACCCTGAGCGGAGGCCAATGGCTACGCCCT
GGGGCTGGTGTAGTGGAGGGAGTGCCCAAGAGTCCCAGGGGAACACGGGCCTCCCAGACGTGGAG
CTCCTTAGCCATGAGCTCAAGGGAGTGTGCCAGAGCCCCCTGGCCTAGATGACCCCTGGCCC
AGGATGGAGCAGGAGTGTCCAGAAAGAACGGCATCAAGGTGAACTTCAAGATCCGCCACAACAT
CGAGGACGGCAGCGTGCAGCTCGCCGACCACTACCAGCAGAACACCCCCATCGGGCAGGGCCCC
GTGCTGCTGCCCCGACAACCACTACCTGAGCACCCAGTCCAAGCTTAGCAAAGACCCCAACGAGA
AGCGCGATCACATGGTCTCTGCTGGAGTTTCGTGACCGCCGCGGGGATCACTCTCGGCATGGACGA
GCTGTACAAGTAA
```

Coding sequence of C-EGFP tagged D₂ receptor: Black sequence corresponds to D₂ receptor; while green sequence represents C-EGFP sequence.

```
ATGGATCCACTGAATCTGTCCTGGTATGATGATGATCTGGAGAGGCAGAACTGGAGCC
GGCCCTTCAACGGGTGACAGCGGAAGGCGGACAGACCCCACTACAACACTACTATGCCAC
ACTGCTCACCCCTGCTCATCGCTGTCATCGTCTTCGGCAACGTGCTGGTGTGCATGGCT
GTGTCCCGCGAGAAGGCGCTGCAGACCACCACTACCTGATCGTCAGCCTCGCAG
TGGCCGACCTCCTCGTCGCCACACTGGTCATGCCCTGGGTTGTCTACCTGGAGGTGGT
AGGTGAGTGGAAATTCAGCAGGATTCCTGTGACATCTTCGTCACTCTGGACGTCATG
ATGTGCACGGCGAGCATCCTGAACTTGTGTGCCATCAGCATCGACAGGTACACAGCTG
TGGCCATGCCCATGCTGTACAATACGCGCTACAGCTCCAAGCGCCGGGTACCCGTCAT
GATCTCCATCGTCTGGGTCTGTCCTTCACCATCTCCTGCCCACTCCTCTTCGGACTC
AATAACGCAGACCAGAACGAGTGCATCATTGCCAACC CGCCTTCGTGGTCTACTCCT
CCATCGTCTCCTTCTACGTGCCCTTCATTGTCACCCTGCTGGTCTACATCAAGATCTA
CATTGTCTCCTCCGCGAGACGCCGCAAGCGAGTCAACACCAAACGCAGCAGCCGAGCTTTC
AGGGCCACCTGAGGGCTCCACTAAAGGGCAACTGTACTCACCCGAGGACATGAAAC
TCTGCACCGTTATCATGAAGTCTAATGGGAGTTTCCAGTGAACAGGCGGAGAGTGGA
GGCTGCCCCGGCGAGCCAGGAGCTGGAGATGGAGATGCTCTCCAGCACCAGCCCACCC
GAGAGGACCCGGTACAGCCCCATCCCACCCAGCCACCACCAGCTGACTCTCCCCGACC
CGTCCCACCATGGTCTCCACAGCACTCCCGACAGCCCCGCCAAACCAGAGAAGAATGG
GCATGCCAAAGACCACCCCAAGATTGCCAAGATCTTTGAGATCCAGACCATGCCCAAT
GGCAAACCCGGACCTCCCTCAAGACCATGAGCCGTAGGAAGCTCTCCCAGCAGAAGG
AGAAGAAAGCCACTCAGATGCTCGCCATTGTTCTCGGCGTGTTCATCATCTGCTGGCT
GCCCTTCTTCATCACACACATCCTGAACATACACTGTGACTGCAACATCCCCGCTGTC
CTGTACAGCGCCTTCACGTGGCTGGGCTATGTCAACAGCGCCGTGAACCCCATCATCT
ACACCACCTTCAACATTGAGTTCGCAAGGCCTTCTGAAGATCCTCCACTGCGAGAA
GAACGGCATCAAGGTGAACTTCAAGATCCGCCACAACATCGAGGACGGCAGCGTGCAG
CTCGCCGACCACTACCAGCAGAACACCCCATCGGCGACGGCCCCGTGCTGCTGCCCG
ACAACCACTACCTGAGCACCCAGTCCAAGCTTAGCAAAGACCCCAACGAGAAGCGCGA
TCACATGGTCTGCTGGAGTTCGTGACCGCCCGGGGATCACTCTCGGCATGGACGAG
CTGTACAAGTAA
```

Coding sequence of mCherry tagged A_{2A} receptor: Black sequence corresponds to A_{2A} receptor; while red sequence represents mCherry sequence.

```
ATGCCCATCATGGGCTCCTCGGTGTACATCACGGTGGAGCTGGCCATTGCTGTGCTGGCCATCC
TGGGCAATGTGCTGGTGTGCTGGGCCGTGTGGCTCAACAGCAACCTGCAGAACGTCACCAACTA
CTTTGTGGTGTCACTGGCGGGCGGCCGACATCGCAGTGGGTGTGCTCGCCATCCCCTTTGCCATC
ACCATCAGCACCGGGTTCTGCGCTGCCTGCCACGGCTGCCTCTTCATTGCCTGCTTCGTCCTGG
TCCTCACGCAGAGCTCCATCTTCAGTCTCCTGGCCATGCCATTGACCGTACATTGCCATCCG
CATCCCGCTCCGGTACAATGGCTTGGTGACCGGCACGAGGGCTAAGGGCATCATTGCCATCTGC
TGGGTGCTGTGCTTTGCCATCGGCCTGACTCCCATGCTAGGTTGGAACAACGCGGTCAGCCAA
AGGAGGGCAAGAACCACTCCCAGGGCTGCGGGGAGGGCCAAGTGGCCTGTCTCTTTGAGGATGT
GGTCCCCATGAACTACATGGTGTACTTCAACTTCTTTGCCTGTGTGCTGGTGGCCCTGCTGCTC
ATGCTGGGTGTCTATTTGCGGATCTTCTGGCGGCGGACGACAGCTGAAGCAGATGGAGAGCC
AGCCTCTGCCGGGGGAGCGGGCACGGTCCACACTGCAGAAGGAGGTCCATGCTGCCAAGTCACT
GGCCATCATTGTGGGGCTCTTTGCCCTCTGCTGGCTGCCCTACACATCATCAACTGCTTCACT
TTCTTCTGCCCCGACTGCAGCCACGCCCTCTCTGGCTCATGTACCTGGCCATCGTCTCTCCC
ACACCAATTCGGTTGTGAATCCCTTCATCTACGCCATACCGTATCCGCGAGTTCGGCCAGACCTT
CCGCAAGATCATTTCGAGCCACGTCTGAGGCAGCAAGAACCTTTCAAGGCAGCTGGCACCAGT
GCCCCGGTCTTGGCAGCTCATGGCAGTGACGGAGAGCAGGTGAGCCTCCGCTCTCAACGGCCACC
CGCCAGGAGTGTGGGCCAACGGCAGTGCTCCCCACCCTGAGCGGAGGCCCAATGGCTACGCCCT
GGGGCTGGTGTGAGTGGAGGGAGTGCCCAAGAGTCCCAGGGGAACACGGGCCTCCCAGACGTGGAG
CTCCTTAGCCATGAGCTCAAGGGAGTGTGCCAGAGCCCCCTGGCCTAGATGACCCCTGGCCC
AGGATGGAGCAGGAGTGTCCATGGTGAGCAAGGGCGAGGAGGATAACATGGCCATCATCAAGGA
GTTTCATGCGCTTCAAGGTGCACATGGAGGGCTCCGTGAACGGCCACGAGTTCGAGATCGAGGGC
GAGGGCGAGGGCCGCCCTACGAGGGCACCCAGACCGCCAAGCTGAAGGTGACCAAGGGTGGCC
CCCTGCCCTTCGCTGGGACATCCTGTCCCCCTCAGTTCATGTACGGCTCCAAGGCCTACGTGAA
GCACCCCGCCGACATCCCCGACTACTTGAAGCTGTCTTCCCCGAGGGCTTCAAGTGGGAGCGC
GTGATGAACTTCGAGGACGGCGGCGTGGTACCCTGACCCAGGACTCCTCCCTGCAGGACGGCG
AGTTCATCTACAAGGTGAAGCTGCGCGCACCAACTTCCCCCTCCGACGGCCCCGTAATGCAGAA
GAAGACCATGGGCTGGGAGGCCTCCTCCGAGCGGATGTACCCCGAGGACGGCGCCCTGAAGGGC
GAGATCAAGCAGAGGCTGAAGCTGAAGGACGGCGGCCACTACGACGCTGAGGTCAAGACCACCT
ACAAGGCCAAGAAGCCCCTGCAGCTGCCCGGCGCTACAACGTCAACATCAAGTTGGACATCAC
CTCCACAACGAGGACTACACCATCGTGGAACAGTACGAACGCGCCGAGGGCCGCACTCCACC
GGCGGCATGGACGAGCTGTACAAGTAA
```

Coding sequence of EGFP tagged A_{2A} receptor: Black sequence corresponds to A_{2A} receptor; while green sequence represents EGFP sequence.

```
ATGCCCATCATGGGCTCCTCGGTGTACATCACGGTGGAGCTGGCCATTGCTGTGCTGGCCATCC
TGGGCAATGTGCTGGTGTGCTGGGCCGTGTGGCTCAACAGCAACCTGCAGAACGTCACCAACTA
CTTTGTGGTGTCACTGGCGGGCGGCCGACATCGCAGTGGGTGTGCTCGCCATCCCCTTTGCCAT
CACCATCAGCACCGGGTTCTGCGCTGCCACGGCTGCCTCTTCATTGCCTGCTTCGTCTCTG
GTCCTCACGCAGAGCTCCATCTTCAGTCTCCTGGCCATCGCCATTGACCGCTACATTGCCATCC
GCATCCCGCTCCGGTACAATGGCTTGGTGAACGGGACGAGGGCTAAGGGCATCATTGCCATCTG
CTGGGTGCTGTGCTTTGCCATCGGCCTGACTCCCATGCTAGGTTGGAACAACCTGCGGTGAGCCA
AAGGAGGGCAAGAACCCTCCAGGGCTGCGGGGAGGGCCAAGTGGCCTGTCTCTTTGAGGATG
TGGTCCCATGAACACATGGTGTACTTCAACTTCTTTGCCTGTGTGCTGGTGCCCTGTCTGCT
CATGCTGGGTGTCTATTTGCGGATCTTCTGCGGGCGCGACGACAGCTGAAGCAGATGGAGAGC
CAGCCTCTGCGGGGGAGCGGGCACGGTCCACACTGCAGAAGGAGGTCCATGCTGCCAAGTCAC
TGGCCATCATTGTGGGGCTCTTTGCCCTCTGCTGGCTGCCCTACACATCATCAACTGCTTCAC
TTTCTTCTGCCCCGACTGCAGCCACGCCCTCTCTGGCTCATGTACCTGGCCATCGTCTCTCTCC
CACACCAATTCGGTGTGAATCCCTTCATCTACGCTACCGTATCCGCGAGTTCCGCCAGACCT
TCCGCAAGATCATTGCGAGCCACGTCTGAGGCAGCAAGAACCCTTTCAAGGCAGCTGGCACCAG
TGCCCGGTCTTGGCAGCTCATGGCAGTGACGGAGAGCAGGTGAGCCTCCGTCTCAACGGCCAC
CCGCCAGGAGTGTGGGCCAACGGCAGTGCTCCCCACCCTGAGCGGAGGCCCAATGGCTACGCC
TGGGGCTGGTGTGAGTGGAGGGAGTGCCCAAGAGTCCCAGGGGAACACGGGCCTCCCAGACGTGGA
GCTCCTTAGCCATGAGCTCAAGGGAGTGTGCCAGAGCCCCCTGGCCTAGATGACCCCCCTGGCC
CAGGATGGAGCAGGAGTGTCCATGGTGTAGCAAGGGCGAGGAGCTGTTACCGGGGTGGTGCCCA
TCCTGGTGTGAGCTGGACGGCGACGTAACCGGCCACAAGTTTCAGCGTGTCCGGCGAGGGCGAGGG
CGATGCCACCTACGGCAAGCTGACCCTGAAGTTTCATCTGCACCACCGGCAAGCTGCCCGTGGCC
TGGCCCACCCTCGTGACCACCCTGACCTACGGCGTGCAGTGCTTCAGCCGCTACCCCGACCACA
TGAAGCAGCAGACTTCTTCAAGTCCGCCATGCCCCGAAGGCTACGTCCAGGAGCGCACCATCTT
CTTCAAGGACGACGGCAACTACAAGACCCGCGCCGAGGTGAAGTTTCGAGGGCGACACCCTGGTG
AACCGCATCGAGCTGAAGGGCATCGACTTCAAGGAGGACGGCAACATCCTGGGGCACAAGCTGG
AGTACAACACAGCCACAACGTCTATATCATGGCCGACAAGCAGAAGAACGGCATCAAGGT
GAACTTCAAGATCCGCCACAACATCGAGGACGGCAGCGTGCAGCTCGCCGACCACTACCAGCAG
AACACCCCATCGGGCAGCGCCCCGTGCTGCTGCCCCGACAACCACTACCTGAGCACCAGTCCA
AGCTTAGCAAAGACCCCAACGAGAAGCGGATCACATGGTCTGCTGGAGTTCGTGACCGCCGC
CGGGATCACTCTCGGCATGGACGAGCTGTACAAGTAA
```

Coding sequence of mCherry tagged D₂ receptor: Black sequence corresponds to D₂ receptor; while red sequence represents mCherry sequence.

```
ATGGATCCACTGAATCTGTCTCTGGTATGATGATGATCTGGAGAGGCAGAACTGGAGCC
GGCCCTTCAACGGGTCAGACGGGAAGGCGGACAGACCCCACTACAACACTACTATGCCAC
ACTGCTCACCTGCTCATCGCTGTCATCGTCTTCGGCAACGTGCTGGTGTGCATGGCT
GTGTCCC CGGAGAAGGCGCTGCAGACCACCACCAACTACCTGATCGTCAGCCTCGCAG
TGGCCGACCTCCTCGTCGCCACACTGGTCATGCCCTGGGTTGTCTACCTGGAGGTGGT
AGGTGAGTGGAAATTCAGCAGGATTCACCTGTGACATCTTCGTCACTCTGGACGTCATG
ATGTGCACGGCGAGCATCCTGAACTTGTGTGCCATCAGCATCGACAGGTACACAGCTG
TGGCCATGCCCATGCTGTACAATACGCGCTACAGCTCCAAGCGCCGGGTACCCGTCAT
GATCTCCATCGTCTGGGTCCTGTCTTACCATCTCCTGCCACTCCTCTTCGGACTC
AATAACGCAGACCAGAACGAGTGCATCATTGCCAACCCGGCCTTCGTGGTCTACTCCT
CCATCGTCTCCTTCTACGTGCCCTTCATTGTCAACCTGCTGGTCTACATCAAGATCTA
CATTGTCTCTCCGACAGACGCCGCAAGCGAGTCAACACCAAACGCAGCAGCCGAGCTTTC
AGGGCCACCTGAGGGCTCCACTAAAGGGCAACTGTACTCACCCCGAGGACATGAAAC
TCTGCACCGTTATCATGAAGTCTAATGGGAGTTTCCAGTGAACAGGCGGAGAGTGGAA
GGCTGCCCCGGCGAGCCCAGGAGCTGGAGATGGAGATGCTCTCCAGCACCAGCCCACCC
GAGAGGACCCGGTACAGCCCCATCCACCCAGCCACCACCAGCTGACTCTCCCCGACC
CGTCCCACCATGGTCTCCACAGCACTCCCACAGCCCCGCAAACCAGAGAAGAATGG
GCATGCCAAAGACCACCCCAAGATTGCCAAGATCTTTGAGATCCAGACCATGCCAAT
GGCAAACCCGGACCTCCCTCAAGACCATGAGCCGTAGGAAGCTCTCCAGCAGAAGG
AGAAGAAAGCCACTCAGATGCTCGCCATTGTTCTCGGCGTGTTCATCATCTGCTGGCT
GCCCTTCTTTCATCACACACATCCTGAACATACACTGTGACTGCAACATCCCCGCTGTC
CTGTACAGCGCCTTACGTGGCTGGGCTATGTCAACAGCGCCGTGAACCCCATCATCT
ACACCACCTTCAACATTGAGTTCCGCAAGGCCTTCCTGAAGATCCTCCACTGCATGGT
GAGCAAGGGCGAGGAGGATAACATGGCCATCATCAAGGAGTTCATGCGCTTCAAGGTG
CACATGGAGGGCTCCGTGAACGGCCACGAGTTCGAGATCGAGGGCGAGGGCGAGGGCC
GCCCCACGAGGGCACCCAGACCCCAAGCTGAAGGTGACCAAGGGTGGCCCCCTGCC
CTTCGCCCTGGGACATCCTGTCCCCTCAGTTCATGTACGGCTCCAAGGCCTACGTGAAG
CACCCCGCCGACATCCCCGACTACTTGAAGCTGTCTTCCCCGAGGGCTTCAAGTGGG
AGCGCGTGATGAACTTCGAGGACGGCGGCGTGGTGACCGTGACCCAGGACTCCTCCCT
GCAGGACGGCGAGTTCATCTACAAGGTGAAGCTGCGCGGCACCAACTTCCCCTCCGAC
GGCCCCGTAATGCAGAAGAAGACCATGGGCTGGGAGGCTCCTCCGAGCGGATGTACC
CCGAGGACGGCGCCCTGAAGGGCGAGATCAAGCAGAGGCTGAAGCTGAAGGACGGCGG
CCACTACGACGCTGAGGTCAAGACCACCTACAAGGCCAAGAAGCCGTGCAGCTGCC
GGCGCCTACAACGTCAACATCAAGTTGGACATCACCTCCACAACGAGGACTACACCA
TCGTGGAACAGTACGAACGCGCCGAGGGCCGCACTCCACCGCGGCATGGACGAGCT
GTACAAGTAA
```

Coding sequence of EGFP tagged D₂ receptor: Black sequence corresponds to D₂ receptor; while green sequence represents EGFP sequence.

```
ATGGATCCACTGAATCTGTCCTGGTATGATGATGATCTGGAGAGGCAGAACTGGAGCCGGCCCT
TCAACGGGTGTCAGACGGGAAGGCGGACAGACCCCACTACAACACTACTATGCCACACTGCTCACCCCT
GCTCATCGCTGTCATCGTCTTCGGCAACGTGCTGGTGTGCATGGCTGTGTCCCGCGAGAAGGCG
CTGCAGACCACCACCAACTACCTGATCGTCAGCCTCGCAGTGGCCGACCTCCTCGTCGCCACAC
TGGTCATGCCCTGGGTTGTCTACCTGGAGGTGGTAGGTGAGTGGAAATTCAGCAGGATTCCTG
TGACATCTTCGTCACTCTGGACGTCATGATGTGCACGGCGAGCATCCTGAACTTGTGTGCCATC
AGCATCGACAGGTACACAGCTGTGGCCATGCCCATGCTGTACAATACGCGCTACAGCTCCAAGC
GCCGGGTACCCGTGATGATCTCCATCGTCTGGGTCTGTCTTACCATCTCCTGCCACTCCT
CTTCGGACTCAATAACGCAGACCAGAACGAGTGCATCATTGCCAACCCGGCCTTCGTGGTCTAC
TCCTCCATCGTCTCCTTCTACGTGCCCTTCATTGTCACCCTGCTGGTCTACATCAAGATCTACA
TTGTCTCCGCGAGACGCCGCAAGCGAGTCAACACCAACGCAGCAGCCGAGCTTTCAGGGCCCA
CCTGAGGGCTCCACTAAAGGGCAACTGTACTCACCCCGAGGACATGAAACTCTGCACCGTTATC
ATGAAGTCTAATGGGAGTTTTCCAGTGAACAGGCGGAGAGTGGAGGCTGCCCGGCGAGCCAGG
AGCTGGAGATGGAGATGCTCTCCAGCACCAGCCCACCCGAGAGGACCCGGTACAGCCCCATCCC
ACCCAGCCACCACCAGCTGACTCTCCCCGACCCGTCCCACCATGGTCTCCACAGCACTCCCGAC
AGCCCCGCCAAACCAGAGAAGAATGGGCATGCCAAAGACCACCCCAAGATTGCCAAGATCTTTG
AGATCCAGACCATGCCAATGGCAAAACCCGGACCTCCCTCAAGACCATGAGCCGTAGGAAGCT
CTCCCAGCAGAAGGAGAAGAAAGCCACTCAGATGCTCGCCATTGTTCTCGGCGTGTTCATCATC
TGCTGGCTGCCCTTCTTCATCACACACATCCTGAACATACTACTGTGACTGCAACATCCCGCCTG
TCCTGTACAGCGCCTTCACGTGGCTGGGCTATGTCAACAGCGCCGTGAACCCCATCATCTACAC
CACCTTCAACATTGAGTTCGCGAAGGCCTTCTGAAGATCCTCCACTGCATGGTGAGCAAGGGC
GAGGAGCTGTTACCCGGGGTGGTGCCCATCCTGGTTCGAGCTGGACGGCGACGTAAACGGCCACA
AGTTCAGCGTGTCCGGCGAGGGCGAGGGCGATGCCACCTACGGCAAGCTGACCCTGAAGTTCAT
CTGCACCACCGGCAAGCTGCCCGTGCCTGGCCACCCCTCGTGACCACCCCTGACCTACGGCGTG
CAGTGCTTCAGCCGCTACCCCGACCACATGAAGCAGCAGACTTCTTCAAGTCCGCCATGCCCG
AAGGCTACGTCCAGGAGCGACCCATCTTCTTCAAGGACGACGGCAACTACAAGACCCGCGCGA
GGTGAAGTTCGAGGGCGACACCCTGGTGAACCGCATCGAGCTGAAGGGCATCGACTTCAAGGAG
GACGGCAACATCCTGGGGCACAAGCTGGAGTACAACATAACAGCCACAACGTCTATATCATGG
CCGACAAGCAGAAGAACGGCATCAAGGTGAACTTCAAGATCCGCCACAACATCGAGGACGGCAG
CGTGAGCTCGCCGACCACTACCAGCAGAACACCCCATCGGCGACGGCCCCGTGCTGCTGCCC
GACAACCACTACCTGAGCACCCAGTCCAAGCTTAGCAAAGACCCCAACGAGAAGCGCGATCACA
TGGTCTGCTGGAGTTCGTGACCGCCGCGGGATCACTCTCGGCATGGACGAGCTGTACAAGTA
A
```

APPENDIX G

FRET EFFICIENCY DATA

Table G. 1 FRET data of A_{2A}R- A_{2A}R homodimerization

Without agonist			
	Pixel count	Cell number on image	Mean of FRET efficiency
image 1	347081	7	19.387
image 2	189972	8	16.997
image 3	124452	2	14.645
image 4	153589	5	17.607
image 5	227612	7	17.284
image 6	319980	8	15.917
image 7	586703	26	15.246
image 8	204272	13	18.650
image 9	72846	4	16.831
image 10	51797	4	10.119
image 11	383103	11	13.184
image 12	294096	8	16.706
image 13	409144	16	11.591
image 14	275206	14	11.624
image 15	433162	23	12.433
image 16	305379	16	12.227
image 17	471845	16	12.258
image 18	401796	22	10.158
image 19	474246	28	12.602
image 20	245487	8	15.369
		Total cell number:	Total mean:
		246	14.542

Table G. 1 cont'd FRET data of A_{2A}R- A_{2A}R homodimerization

With agonist			
	Pixel count	Cell number on image	Mean of FRET efficiency
image 1	190971	9	17.574
image 2	361980	16	17.887
image 3	365255	19	15.198
image 4	267168	8	16.213
image 5	463681	20	15.017
image 6	443223	17	17.518
image 7	60032	6	17.111
image 8	87432	5	11.520
image 9	134835	7	11.904
image 10	387698	15	11.887
image 11	486020	13	11.671
image 12	336606	17	17.349
image 13	279709	11	11.665
image 14	402073	13	11.968
image 15	22782	1	16.145
image 16	627901	40	11.461
image 17	263841	14	11.290
image 18	394394	11	14.893
image 19	262436	8	13.456
image 20	402866	16	11.849
		Total cell number:	Total mean:
		266	14.179

Table G. 2 FRET data of D₂R- D₂R homodimerization

Without agonist			
	Pixel count	Cell number on image	Mean of FRET efficiency
image 1	38008	11	5.644
image 2	22878	10	7.423
image 3	27111	12	7.823
image 4	11281	4	2.987
image 5	165072	12	6.643
image 6	108210	12	5.439
image 7	73820	9	5.759
image 8	184793	12	5.990
image 9	48953	6	5.940
image 10	174233	15	5.239
image 11	133957	6	5.745
image 12	30060	2	5.633
image 13	150002	7	6.357
image 14	70	5	4.415
image 15	304	15	6.278
image 16	24	1	6.533
image 17	4768	2	3.281
image 18	4234	7	3.979
image 19	80752	18	3.618
image 20	3401	12	3.906
		total cell number:	total mean:
		178	5.432

Table G.2 cont'd FRET data of D₂R- D₂R homodimerization

With agonist			
	Pixel count	Cell number on image	Mean of FRET efficiency
image 1	39789	6	8.049
image 2	4157	2	4.562
image 3	5566	6	3.422
image 4	18762	10	3.888
image 5	12811	3	6.363
image 6	976	5	4.719
image 7	60406	8	7.269
image 8	18866	1	7.261
image 9	53917	5	6.528
image 10	56544	6	6.143
image 11	101285	11	5.171
image 12	66369	4	7.116
image 13	23151	4	8.720
image 14	32586	13	3.383
image 15	14756	2	8.236
image 16	67784	9	5.477
image 17	17086	8	6.360
image 18	5330	1	7.081
image 19	5755	1	5.358
image 20	38357	8	5.609
		total cell number:	total mean:
		113	6.036

Table G. 3 FRET data of A_{2A}R-D₂R heterodimerization

Without agonist			
	Pixel count	Cell number on image	Mean of FRET efficiency
image 1	2898	8	10.003
image 2	1125	16	8.193
image 3	5071	9	9.544
image 4	4715	8	9.032
image 5	10639	7	16.771
image 6	6515	5	15.093
image 7	1465	2	9.350
image 8	351834	10	16.486
image 9	109262	4	22.143
image 10	272383	12	22.977
image 11	80905	2	19.090
image 12	168037	6	17.114
image 13	82157	8	12.464
image 14	83121	2	22.452
image 15	108640	4	24.148
image 16	167981	16	11.713
image 17	480619	20	13.800
image 18	319905	14	9.257
image 19	234139	6	11.269
image 20	479507	12	17.295
		total cell number:	total mean:
		171	14.910

Table G.3 cont'd FRET data of A_{2A}R-D₂R heterodimerization

With agonist			
	Pixel count	Cell number on image	Mean of FRET efficiency
image 1	3114	2	11.635
image 2	165434	13	21.822
image 3	661	15	9.104
image 4	6969	8	13.757
image 5	121627	6	21.748
image 6	80196	2	22.844
image 7	86830	3	22.112
image 8	265294	6	18.171
image 9	84726	8	19.985
image 10	227474	9	16.516
image 11	196647	5	17.909
image 12	140487	6	18.169
image 13	173231	11	13.535
image 14	226474	14	9.536
image 15	434641	22	11.804
image 16	274173	13	9.983
image 17	144487	12	24.327
image 18	396198	20	8.942
image 19	278409	17	15.440
image 20	401650	13	13.857
		total cell number:	total mean:
		205	16.060

Table G. 4 FRET data of A_{2A}R-NR1 heterodimerization

Without agonist			
	Pixel count	Cell number on image	Mean of FRET efficiency
image 1	36131	5	6.284
image 2	35433	6	7.972
image 3	24354	7	6.126
image 4	15454	5	7.919
image 5	48724	10	6.991
image 6	21634	7	9.346
image 7	15507	6	7.071
image 8	42802	13	6.698
image 9	27940	6	7.887
image 10	43921	5	6.616
image 11	14062	2	7.063
image 12	24772	6	7.134
image 13	32929	6	6.049
image 14	14417	4	6.459
image 15	123214	7	13.532
image 16	131974	8	9.557
image 17	30529	4	8.992
image 18	46425	2	8.044
image 19	41078	3	13.482
image 20	145075	2	12.683
		total cell number:	total mean:
		114	8.295